Aston University

Some parts of this thesis may have been removed for copyright restrictions.

If you have discovered material in AURA which is unlawful e.g. breaches copyright, (either yours or that of a third party) or any other law, including but not limited to those relating to patent, trademark, confidentiality, data protection, obscenity, defamation, libel, then please read our Takedown Policy and contact the service immediately

Upgrading of Fast Pyrolysis Oils by Hot Filtration

Doctor of Philosophy

JÜRGEN SITZMANN
ASTON UNIVERSITY

March 2009

This copy of the thesis has been supplied on condition that anyone who consults it is understood to recognise that its copyright rests with its author and that no quotation from the thesis and no information derived from it may be published without proper acknowledgement.

Aston University

Upgrading of Fast Pyrolysis Oils by Hot Filtration

Jürgen Sitzmann

Doctor of Philosophy, 2009

Summary

Fast pyrolysis converts biomass into high yields of pyrolysis oil with char and gases as by-products. The pyrolysis oil can be used as a fuel in boilers, engines and turbines. However the oil typically contains up to 0.5 % char fines which cause problems during combustion. Furthermore the char fines increase the inorganic compounds in the oil, as during fast pyrolysis the mineral matter concentrates in the char. In order to reduce char fines to lower levels, hot filtration of the pyrolysis vapours were commenced. Therefore, a hot filtration unit downstream of a 1kg/h fluidised bed fast pyrolysis reactor was designed and build. The filter unit operates at 450°C and consists of 1 exchangeable filter candle with reverse pulse cleaning system. The experimental set-up included different filter candle materials, different face velocities of the gas stream and pre-coating the filter candle prior to filtration.

Hot filtration experiments up to 7 hours were performed with beech wood as feedstock. It was possible to produce fast pyrolysis oils with a solid content below 0.01 wt%. The additional residence time of the pyrolysis vapours and secondary vapour cracking on the filter cake caused an increase of non-condensable gases at the expense of organic liquid yield. The oils produced with hot filtration showed superior quality properties regarding viscosity than standard pyrolysis oils. The oils were analysed by rotational viscosimetry and gel permeation chromatography before and after accelerated aging.

During filtration the separated particulates accumulate on the candle surface and build up the filter cake. The filter cake leads to an increase in pressure drop between the raw gas and the clean gas side of the filter candle. At a certain pressure drop the filter cake has to be removed by reverse pulse cleaning to regenerate the pressure drop. The experiments showed that successful pressure drop recovery was possible during the initial filtration cycles, thereafter further cycles showed minor pressure drop recovery and therefore a steady increase in differential pressure. Filtration with pre-coating the candle to form an additional layer between filter candle and cake resulted in total removal of the dust cake.

The filter cakes were analysed by visual inspection, optical microscopy and scanning electron microscopy. Furthermore the specific resistance to flow of the filter cakes was calculated using Darcy's law. The filter cakes showed different particle size distributions at different face velocities. It was found that a high face velocity (3.5 cm/s) causes larger char particles included in the cake and therefore creating a more porous filter cake with a high permeability. At a low face velocity (2.0 cm/s) the large particles separate already by gravity leading to a smaller average particle size and lower permeability of the filter cake.

Keywords: Biomass, Fast Pyrolysis, Hot filtration, Filter candles,

To

Frederico

Acknowledgements

I would like to acknowledge my supervisor Professor Tony Bridgwater for his guidance, patience and valuable support throughout the project.

I would like to thank the past and present members of the Bio-Energy-Research-Group. Special thanks go to Adisak Pattiya, Romani Fahmi, Mark Coulson, Clemens Hörweg, Dr. Courdner Peacocke, Dr. Elma Gyftopoulou and Dr. Heiko Gerhauser for the encouraging scientific discussions.

Thanks also to Emma Wylde for the administrative support and the well organised research meetings.

Last but not least, I would like to thank my families in Germany and Portugal for their patience and support on this long road.

List of Contents

List of Figures

List of Tables

1 Introduction

1.1 The fast pyrolysis process

Fast pyrolysis is a well established technology, which thermo-chemically converts biomass in high yields of around 70 wt% into a pyrolysis liquid (also referred to as pyrolysis oil, bio crude oil, bio-oil) with non-condensable gases and char as side products [1]. During the conversion the alkali metals and earth alkali metal remain in the char so that the bio-oil contains virtually no alkalis [2]. The bio-oil can be used as a fuel for boilers and engines and due to the low alkali content it is also suitable for the combustion in turbines [3]. Furthermore, it is considered to use fast pyrolysis units as decentralised pre-step to large scale gasification. As it is a liquid it is easier to store and to transport than biomass, especially as the energy density on a volume basis is higher than in the original biomass [4]. In addition, pyrolysis oil can act as a source for highly valuable speciality products like food flavours, additives and fertilisers or to recover fine chemicals like levoglucosan or hydroxyacetaldehyde.

However, the bio-oil contains char fines which are not removable by conventional cyclone separation and usually has an average solid content between 0.1-0.6 wt%. These char fines cause difficulties during injection in boilers and engines. Furthermore, the char fines contain the alkali metals of the oil which makes it unsuitable for turbines [5]. Additionally, the char can accumulate and sediment over time leading to a more viscous separated phase. It is also known that the alkali metals increase the storage instability by catalysing secondary polymerisation reactions during storage.[6]

1.2 High temperature filtration

Hot filtration using rigid filter candle technology has reached near industrial stage for advanced coal-fired power production facilities such as Integrated Gasification Combined Cycle (IGCC) or Pressurised Fluidised Bed Combustion (PFBC) [7]. Process development units have shown reliable filtration with filtration efficiencies higher than 99.99 % to make the gas suitable for gas turbines [8].

A filter candle resembles a cylinder with a permeable wall and a closed and an open end. During the filtration process the raw gas has to pass the wall of the filter candle

where the dust particles are removed and the clean gas flows inside the candle cavity through the open end of the candle and leaves the filtration unit. As the dust particles get separated a dust cake builds up on the outer surface of the candle. The emerging filter cake increases the pressure difference between clean and raw gas side of the candle. If this pressure drop reaches a certain value the filter is cleaned by the injection of a reverse jet pulse of pressurised gas in the opposite direction of the filtration flow which detaches the filter cake.

Intensive research has been carried out to develop new types of filter candles to withstand the high temperatures and corrosive environment. Different types of ceramic filters were developed of which the second generation of ceramic filter candles is now able to resist temperatures of up to 1100 °C [9, 10]. Other materials used in high temperature filtration are metal alloys such as Inconel which also withstands temperatures up to 900 °C [11].

1.3 Objective and methodology

The objective of this work is to remove the char fines of the pyrolysis oil in the vapour phase of the process by hot filtration. Rigid filter technology was chosen as the particle removal efficiency is superior to other particulate separation techniques i.e. granular bed filters, Electrostatic Precipitators (EPs) or multi-cyclones [12]. The aim is to reduce the solid content of the oil below 0.01 wt% to achieve turbine fuel standard. Furthermore, it is intended to improve the quality of the pyrolysis oil due to secondary cracking of the vapours as they pass the char filter cake. It is known that the char or the alkali metals inside the char are catalytically active and therefore shall crack the lignin derived high molecular weight compounds of the biomass which reduces the viscosity of the oil [13].

To achieve this objective a hot filtration test unit with a single filter candle was installed downstream of a 1kg per hour fast pyrolysis reactor. The operation temperature was set above 400°C to keep the oil in the vapour phase as condensation of the vapours would plug the filter candle. The additional residence time of the hot vapours in the filtration unit will increase the production of non-condensable gases. Therefore, to avoid extensive losses in the yield of pyrolysis oil the filtration temperature should not exceed 500°C.

In the first part the results in this thesis focus on the influence of the filtration system on the fast pyrolysis process. The changes in the mass balance and the impact on the pyrolysis oil between conventional fast pyrolysis and a fast pyrolysis system with filtration unit were examined. For this reason a detailed mass balance of the process was produced to compare the product yields of organic liquid, process water, non-condensable gases and char. Furthermore, the produced fast pyrolysis oils were analysed using various analytical methods to assess the quality of the oils regarding their solid content, viscosity, storage stability and energy content.

What is important for the durability of the filtration process is the filter cake removal by reverse pulse cleaning. Some dusts show very strong adhesive and cohesive forces between the particulates so that the forces generated during the reverse pulse are not enough to dispatch the filter cake. For that reason the second part of the work concentrates on the filtration process to assess the filtration characteristics. Therefore, the filter cakes, produced with different experimental set-ups like inclusion and exclusion of a primary cyclone, were analysed regarding their resistance to flow and particle size distribution. Additionally, the pressure drop development across the filter candle was monitored during the course of the experiment and after reverse pulse cleaning to investigate the cleaning behaviour of the filter cake. Furthermore, two different filter candles were used to examine the influence of the filter candle material.

2 Fast Pyrolysis Process

2.1 Introduction

Pyrolysis means the thermal decomposition of biomass in the absence of oxygen, resulting in the formation of liquid, gaseous and solid phase products. The aim of the fast pyrolysis process is to maximise the liquid yield, herein after referred as pyrolysis oil (PO) or just as oil. Other terms which are commonly used are Bio Crude Oil (BCO) or bio oil. Typical yields of the conversion of biomass are 75% Oil, 13% gas and 12% char on mass basis. To achieve this high liquid yield the fast pyrolysis process requires special process conditions, such as:

- high heating rates of the biomass (> 1000°C)
- short residence time of the hot vapours of below 2 s
- narrow temperature window between 400°C and 500°C
- rapid cooling of the vapours to condense the pyrolysis [14]

To achieve the high heating rates into the biomass particle various types of fast pyrolysis reactors were developed during the past 20 years. A number of extensive and excellent reviews, which describe the advantages of the specific systems, already exist [15-17]. Therefore it is not the intention to review the reactor configurations in detail but to give only a short overview. The reactor principles are:

- bubbling fluid bed reactor
- circulating fluid bed reactor
- ablative pyrolysis
- rotating cone reactor
- vacuum pyrolysis
- vortex reactor
- rotary and/or auger kiln reactors

2.2 Reaction kinetics

Figure 1 shows a simplified model of the reaction pathways of biomass during thermo-chemical decomposition. The intensity of the reaction pathways depends on the process parameters as described below. Reaction temperatures above 600°C promote pathway K3, whereas temperatures below 400°C promote K1. The optimum liquid yield is achieved with pathway K2 between 400 and 600°C. K4 illustrates further secondary cracking of vapours due to long residence time of the hot vapours.

Figure 1: Simple kinetic model of biomass pyrolysis by Radlein. [18]

As the reaction pathways have shown, fast pyrolysis is a moderate temperature process with reactor temperatures between 450-600°C. At lower temperatures the char yield increases and higher temperatures enhance production of non-condensable gases. The process requires high heating rates to minimise the exposure of the biomass to lower intermediate temperatures, which would promote pathway k1 (see Figure 1) and therefore increase the char yield [19, 20].In addition Lede and Mercadier [21] suggest that there is a molten intermediate state of the solid biomass before the further decomposition into gases, vapours and char.

Furthermore, the residence time influences the reaction pathways. It can be divided into the residence time of the biomass particle in the reactor and the residence time of the hot vapours. The residence time of particle means the time to decompose the volatile compounds and depends on the heating rate. It should be below 1s to avoid a large time dependent temperature gradient, which would promote pathway K1 of the reaction kinetic. Due to the low thermal conductivity of biomass this is requires finely ground biomass. The residence time of the pyrolysis vapours is defined as the time that the vapours remain in the hot environment. It includes the residence time of the vapours in the reactor and the residence time in the pipe-work and cyclones before the vapours

enter the condensation unit. In fast pyrolysis both residence times should be preferably below 2 s. An increase in residence time promotes secondary cracking of the vapours, which increase the amount of non-condensable gases, as indicated by pathway K4 in Figure 1. Consequently reaction temperature, heating rate and residence time of the hot vapours influence the yields in gaseous, liquid and solid product. [22]

In addition the feedstock composition influences the intensities of the reaction pathways. Beside the ratio of cellulose, hemi-cellulose and lignin it is mainly the mineral matter which affects the decomposition of a specific biomass. Especially the ash constituents potassium and calcium are known to be catalytically active [23]. Nowakowsky et al [24] made Thermo-Gravimetric Analysis (TGA) of potassium doped willow and found that potassium can lower the average first-order activation energy for pyrolysis by up to 50 KJ/mol. Additionally, they experienced that the presence of potassium promotes char production.

Scott et al [25] removed the mineral content of poplar wood by washing with deionised water prior to fast pyrolysis in a fluidising bed reactor. They found that in the absence of potassium and calcium cations the organic liquid yield increased and char as well as gas yield decreased. Furthermore, the analysis of the liquid yield showed that the presence of metal cations promotes the production of hydroxyacetaldehyde whereas the absence of cations conversely increases the amount of the anhydrosugar levoglucosan. It has been known for some time that these compounds are derived from the cleavage of the cellulose and hemicellulose chain [26, 27]. Radlein et al [28] suggest that the alkaline metal cations catalyse fragmentation of the sugar ring whereas in the absence of cations depolymerisation of the cellulose chain is the main reaction pathway (see Figure 2).

Aston University

Illustration removed for copyright restrictions

Figure 2: Mechanism of thermal decomposition of cellulose by fast pyrolysis in the presence and absence of alkaline cations. [28]

2.3 Fast pyrolysis oils

2.3.1 Physical and chemical characterisation

Fast pyrolysis oil is a highly oxygenated organic liquid with typical water content between 15 and 40 wt%. The oil has a dark-brown to reddish-brown appearance and a smoky smell. The amount of water depends on the moisture content of the feedstock and reaction water produced in the conversion process. The main components are carbon (ca. 55 %), hydrogen (ca. 6-7 %), oxygen (ca. 37 %) and nitrogen (ca. 0.1 %). The elemental composition results in a Higher Heating Value (HHV) of 16 – 18 MJ/kg which is less than half of the HHV of fossil fuel with 40 - 42 MJ/kg. Due to its polar character and high oxygen content it is not miscible with fossil fuels. The density of the oil is around 1.2 g/cm^3 and it contains organic acids which give it an acidic character with a pH between 2 and 3. [29]

The amount of inorganic ashes is below 0.1 % and is found in the remaining char fines, which are transported with the vapours in the condensation system. The pyrolysis liquid itself can be considered nearly ash free, as the minerals in the feedstock are accumulated in the char, because they remain in the solid phase due to their low vapour pressure at 500°C. The solid content of the pyrolysis oil depends on the particle size distribution of the feedstock, process characteristics like gas velocity and efficiency of the solids

recovery system. Typical solid contents achieved with cyclone separators vary between 0.5 and 1 wt%. [30]

The viscosity of the oil is strongly dependent on the content of water and light organics. The published data on viscosity ranges from as little as 13 cSt to 80 cSt at 50°C. Furthermore, the viscosity changes significantly with temperature. The oil is not as stable as fossil fuels but tends to polymerise during storage or thermal treatment which causes an increase of viscosity. [31]

Normally fast pyrolysis liquids are single phase but depending on water content and feedstock quality it can come to phase separation into a hydrophilic water phase and a hydrophobic organic phase. Fratini [32] found that large lignin derived high molecular weight compounds exist as micro-emulsion inside a water fraction. He explains the phase separation of the oil at water content above 40 wt% with the assumption, that at a certain water level, the acids required to keep the micro-emulsion in balance are removed around the large molecular weight compounds and the solubility of the pyrolysis liquid matrix changes.

2.3.2 Storage stability

During fast pyrolysis the rapid thermal decomposition of the biomass particle forms volatiles which include free radicals and other instable molecules. Afterwards the vapours are immediately cooled from the pyrolysis temperatures to produce the condensate. Therefore, pyrolysis oil is not a product of thermo-dynamic equilibrium at storage temperatures and chemically reacts with storage time. During storage, the chemical composition changes towards chemical equilibrium under storage conditions, resulting in mainly polymerisation reactions which increase viscosity, molecular weight and mutual solubility of its many compounds. [33]

Adding of low molecular weight solvents like methanol or ethanol has a remarkably stabilising effect on the storage stability of bio-oils [34-36]. The addition of solvents shifts the stoichiometry from polymers to oligomers which are stabilised by the reacted solvent group. Therefore, solvent addition reduces the viscosity of the oil and decreases the stability during aging immensely. Diebold [37] found that addition of 10 wt% of

methanol dissolved in bio-oil increases the viscosity only from 20 to 22 cP over a 4-month period when stored at 20°C.

2.3.3 Chemical composition

Fast pyrolysis oil is a complex mixture of water and organic compounds like organic acids, alcohols, ketones, phenols, furans and olefins. Some of the phenolic molecules like guaiacol and syringol exist as di-mers and tri-mers or as even larger molecules which are described as pyrolytic lignin. The large amount of more than 200 different chemical compounds and the extremely wide range in molecular weight of these compounds makes analysis of pyrolysis oil a very challenging task.[38, 39]

A common method for PO analysis is to fractionate it into a hydrophobic organic fraction and a hydrophilic water fraction by adding water until the oil phase separates and to treat these fractions separately [40]. Oasmaa [41] improved this method by partitioning the water fraction with ether and the organic fraction with dichloremethane further as it can be seen in Figure 3.

Figure 3: Fractionation of pyrolysis oil after Oasmaa. [41]

The ether soluble of the water fraction consists mainly of volatiles compounds and is comprised of acetic and formic acid, ketones, alcohols and aldehydes. Furthermore, it

contains lignin derived phenolic monomers like guaiacol and syringol. All the compounds are detectable by Gas Chromatography (GC).

The ether insoluble of water fraction consists mainly of levoglucosan and other degradation products of carbohydrates. In addition to these compounds mainly mono-saccarides and hydroxyl-acids are found. The evaporation residue is a dark brown syrup like substance which elutes only partially in the GC. Oasmaa and Meier [42] proposed HPLC for the analysis of the missing compounds. Analytical pyrolysis with subsequent GC analysis (Py-GC-MS) of this fraction resulted in decomposition products of poly-saccarides. Therefore Oasmaa [41] concludes that the missing compounds are anhydrosugar oligomers and carboxylic acids (C>10).

The water insoluble fraction consists of degraded lignin, extractives and solids. Analysis with Fourier Transformation Infrared (FTIR) resulted in a spectrum similar to that of lignin. Analysis with Py-GC-MS confirmed this result with the detection of only lignin derived pyrolytic decomposition products. Only a few poorly in water soluble phenolic monomers are eluted during GC analysis. [41]

Further fractionation results in the dichloromethane soluble of the water insoluble fraction. This fraction contains Low Molecular Mass lignin derived material (LMM–lignin) and extractives. LMM-lignin is a thick viscous liquid with Mean Molecular weight (MMW) of 400 g/mol. [43]

The water insoluble and dichloromethane insoluble fraction is a powder-like light brown material. None of the compounds are GC-detectable but the powder dissolves in organic solvents like methanol. Oasmaa describes it as High Molecular Mass (HMM) lignin with a molecular weight of ca. 1000 g/mol. Meier et al receives a similar fraction by dissolving droplets of oil in rigorously stirred water and describes it as Pyrolytic Lignin (PL). They have been analysing PL for years with various analytical methods[40, 44]. In the last work Bayerbach et al [45] were able to give a proposal for the structural formula of the lignin derived macro-molecule of this fraction.

2.4 Improving pyrolysis oil quality

2.4.1 Bio-oil solids content

The condensed pyrolysis liquid contains char fines of around 0.5 – 2 wt% which are transferred with the gas stream into the condensation unit. The amount of char fines depends on:

- Density and particle size distribution of the feedstock
- Process characteristics (gas velocity, abrasion of char inside the reactor)
- Particle removal technique (i.e. cyclone separators)

The remaining char fines are caused by the decreasing filtration efficiency of cyclones below 10 µm. The entrained char causes problems during production, storage, handling and in applications of pyrolysis oil. The reasons for these disadvantages are described below:

The char fines can cause problems during the production process by clogging downstream pipe-work and equipment. The char fines tend to deposit wherever gas turbulences occur and cause fouling in the pipe-work. Especially, if liquid condensates in the pipe-work due to heat sinks, the char particles agglomerate and can quickly plug the pipe-work. At the entrance of the condensation system this problem is inherent as a temperature gradient at this point is inevitable. Additionally, the condensation unit itself is prone to fouling due to the entrained solids.

In addition the char fines lower the quality of the produced oils. They decrease the suitability for storage because of their tendency to settle down slowly over time, leading to a sludge in the bottom of the vessel. Another disadvantage is that the char fines increase the viscosity of the oil, which is problematic during handling of the oil and increases the energy consumption for pumping. Furthermore, Agblevor [6] found that alkali and earth alkali metals present in the char promote catalytically carbonisation reactions of oil compounds. Therefore it can be expected that the removal of char will increase the storage stability as the minerals remain in the solid phase during the fast pyrolysis process.

In applications like boilers and engines the char could plug or abrade orifices of burners and lead to difficulties during atomisation. Additionally, the burning characteristics of char are different to those of the oil which can lead to incomplete combustion and development of soot. Because the ash of the feedstock gets accumulated in the char, the char mineral content is about 7 times higher in the char than in the parent material. The ash could damage boilers and turbines and would make a flu gas cleaning necessary. Especially turbine applications require a fuel quality with less than 1 ppm alkali. Therefore, Diebold concludes that due to the high potassium and calcium content of the char, pyrolysis oil from woody biomass would need a solid content below 0.02 wt% or 0.002 wt% from switchgrass to meet turbine fuel standards.[46]

2.4.2 Secondary vapour cracking

Very little information is available on the composition of the vapours phase of the pyrolysis products prior condensation. Lede et al [47] postulate the theory that, during decomposition, the biomass exists briefly in an intermediate liquid state and that during evaporation of that liquid some of material is ejected as high molecular weight aerosols. Due to the complexity of the vapour phase compounds with water vapours, organic vapours and high molecular weight compounds which can condense already at temperatures around 400°C, it is difficult to use analytical methods (i.e. GC). Evans and Milne et al [48] developed Molecular Beam Mass Spectroscopy (MBMS) as an analytical method and were able to apply it to the hot vapour stream. They found that the organic vapours have a molecular weight well below 200 g/mol but also report lignin derived dimmers with molecular weight of around 270 g/mol. Daugaard and Brown [49] made assumptions about the constitution of the transport phase by measurement of the differential pressure from which they derived the volume flow of organic vapours. They found that up to 90 wt% of the collected bio-oil can exist as liquid aerosols when leaving the reactor but that the aerosols will evaporate during the further course given enough residence time.

Various researchers investigated in catalytic secondary cracking of the hot vapours to improve the quality of the latter oil [50]. Intense work has been carried out on Zeolite catalysts with promising results regarding the production of aromatic hydrocarbons [51-53]. However, the catalyst showed a very short lifetime due to coking and possibly

poisoning. Metal oxide catalysts were also investigated as to their ability of quality improvement of the pyrolysis oil. Various sorts of metal catalysts were tried, but no significant quality improvement was achieved [54]. The most promising was ZnO which showed minor improvement of the viscosity of the produced oils[55, 56]. However, most of the researchers report rapid coking of the surface which can lead to a fast deactivation of the catalyst.

In the context of this work it is more important to gain information about secondary cracking of vapours due to prolonged residence time and vapour cracking on char and its compounds. Although it is known that the mineral matter in biomass influences the decomposition pathways, very little information is available on the influence of char, or the ash compounds, on secondary vapour cracking in fast pyrolysis. As the high molecular weight lignin derived compounds are known to decrease the quality of the oil (see 2.3.3), the additional secondary cracking of these compounds includes the option to produce less viscous and more stable oil.[16]

Diebold [57] found that the fraction of vapour losses to permanent gases increases exponentially above a temperature of 350°C. Furthermore, he found that an increase in residence time increases the amount of non-condensable gases further. Boroson et al [58] report cracking of vapours on char and on the ash with increasing formation of carbon. Pattiya [59] confirmed the catalytic impact of ashes using analytical pyrolysis gas chromatography (Py-GC-MS) with a micro secondary reactor.

2.5 Characterisation of solid pyrolysis products

The three solid products that are produced during the thermal degradation of biomass are usually termed as char, soot and coke. However, these terms are not clearly defined for the thermo-chemical conversion of biomass but are originated historically in the coal- and charcoal industry or derived from fuel-rich combustion. This causes some confusion during their application in thermo-chemical conversion of biomass and the following paragraph aims to specify these terms more clearly for their use in the context of this work.

Char is the solid residue which remains after the evaporation of the volatile matter of biomass. It evolves from kinetic primary reactions which decompose biomass into char, vapours and gases. Coking and soot are formed in secondary or tertiary reactions of the vapours and gases, possibly with char as catalytic active material. For this reason soot and cokeing are described as secondary char in some kinetic pathways on thermo-chemical decomposition of biomass.

2.5.1 Char

As char is the remainder after evaporation of the volatile matter, all the minerals of the biomass which does not go into the vapour phase remain in the char. In the case of fast pyrolysis with a process temperature of 500°C it can be assumed that nearly all of the minerals (K, Na, Ca and Si) remain in the solid phase and stay in the char. Therefore, the ash compounds get concentrated in the char and the ash content is approx. 7 times as high as in the original biomass, varying with the amount of volatiles and ash originally present in the biomass.

The appearance of biomass chars reflects the cell structure of the parent material. Figure 4A shows the solid residue of a pyrolysed beech wood particle recovered from an experiment on the 1kg/h fluidising bed reactor. It can be seen that the morphology of the particle resembles the original wood cell structure with the carbonised cell walls remaining and the volatile matter of the cell content evaporated. Even small particles of primary char still retain the cell structure of the original wood particle as can be seen in Figure 4B. Due to evaporation of the volatile matter it comes to shrinkage and fragmentation, which reduces the particle size. Additionally, char is very prone to physical abrasion and the actual particle size also depends on the abrasive forces applied during the process.

The morphology of char is related to its parent material, the heating rate and the maximum heat treatment temperature. Guerrero et al [60] found that at a low heating rate the natural porosity of the wood structure allows the gradual release of volatiles without significant changes is morphology. However, rapid heating causes a large release of volatiles in a very short time. The subsequent trapping of volatile matter results in swelled surfaces and produces vesicles and bubbles. In addition it was found that at temperatures above 600°C more roundness of the edges was developed.

Furthermore, high temperature can cause melting of inorganic compounds which can stick contacting surfaces of separate particles and create clusters. Biagnini et al [61] compared the behaviour of different parent materials. They found that size variation in samples of olive kernels is negligible but found a reduction of average particle length of 30% for wood. They explain the different behaviour of the feedstocks by stating that fibrous structures are more numerous in wood and that fibres are more likely to shrink than the compact structure of olive kernels.[62]

Due to this formation pathway char has a very high inner surface which depends on the conditions described above. Guerrero et al found the inner surface area increases with temperature up to a temperature of 800°C. At higher temperatures it comes to a decrease in the surface area which they believe is due to structural ordering and micropore coalescence. The influence of pressure on the surface area was investigated by Cetin et al [63] and was found to decrease the surface slightly with increasing pyrolysis pressure. Addtionally the H/C and the O/C ratios of the char decreased with increase in temperature [64].

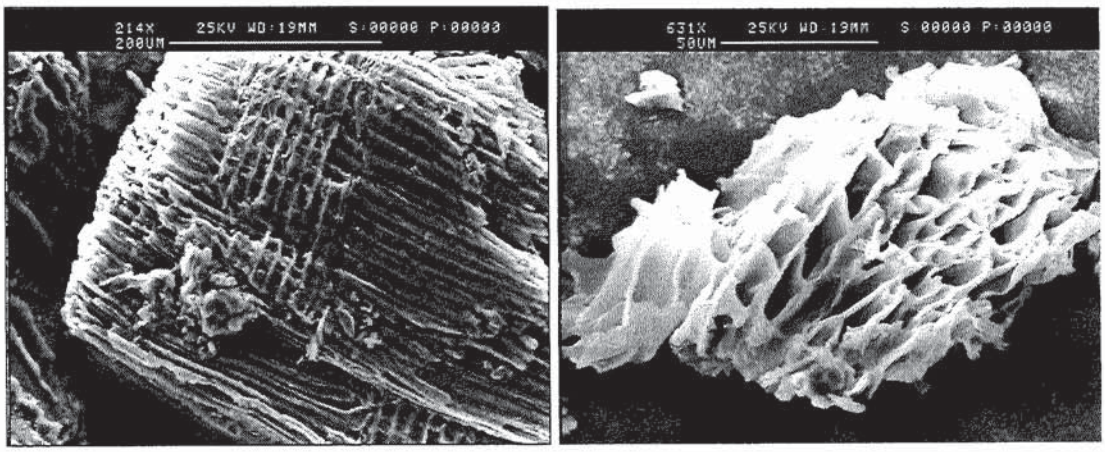

A B

Figure 4: SEM pictures of coarse char (A) and abraded smaller char particle (B)

Abrasion of char particles or the conversion of very dusty biomass creates char fines with a particle size of 5 µm and below. These char fines tend to accumulate, especially in areas with turbulences, in the pipe-work and form clusters with low density

Figure 5 and Figure 6 give an example of this phenomenon. Most of the char fines still resemble the cell structure and can be identified as primary char due to their morphology in comparison to coke and soot which will be described below.

Figure 5: Cluster of fine char with large char particle in the background.

Figure 6: High resolution of the char fines from Figure 5.

2.5.2 Coking

The term coking is commonly used for various types of carbon deposition during the thermal processing of carbonaceous solids, vapours and gases. However there is no clear definition as to which specific solid carbon product is described as coking. Coking found in the pyrolysis process can have quite different forms of appearances depending on the specific conditions during its evolution. In general, it can be distinguished between a graphite-like type of coking and an amorphous type of coking, as illustrated in Figure 7 and Figure 8.

The different types of coking can be explained by different formation routes. The first way of development is catalytic coking. This means carbon deposition on a catalytic active material caused by secondary cracking of vapours or aerosols on the surface of the catalyst. This is the case during coking of quartz sand inside the fluidised bed or on dolomite applied as catalyst in a secondary reactor. [65]

With time the deposition of elemental carbon grows and forms a graphite-like solid structure. Due to its evolution it has a very high fixed carbon content and less volatile matter. Characteristic for this type of coking is, that it very quickly forms a thin

carbonaceous coat that deactivates catalysts (i.e. Zeolites), but the growth decreases with deactivation of the catalytic surface.

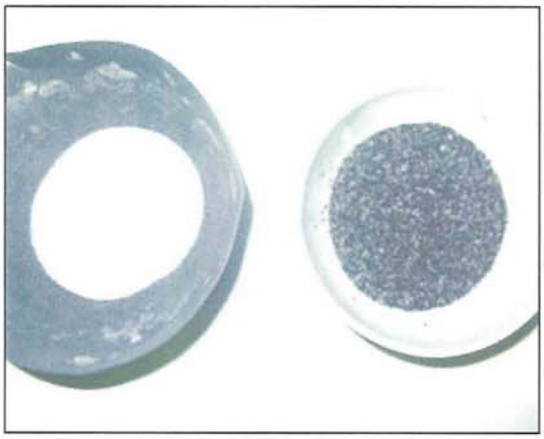

Figure 7: Dolomite before and after use in a fixed bed secondary reactor for catalytic cracking of pyrolysis vapours (Aston University)

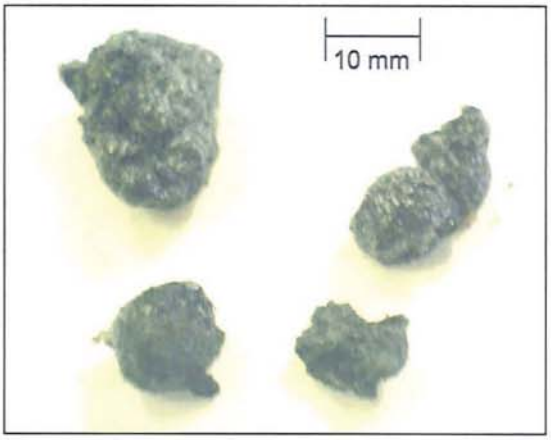

Figure 8: Amorphous coke found in the entrance of the condensation unit of 1kg/h fast pyrolysis reactor (Aston University)

The type of coking which causes frequent blockage of pipes and process units in fast pyrolysis is described herein as amorphous coking. Its formation can be explained by the condensation of vapours or deposition of aerosols on the inner surface of pipes due to cold spots. It is very commonly observed at the entrance of the condensation unit due to the temperature gradient at the point between vapour and liquid phase. A necessary prerequisite, which massively enhances the growth of this type of coking, is the presence of particulates in the gas stream. The particles get trapped where liquids are condensed and increase the viscosity of the liquid-particle emulsion. As the agglomerate is still in the hot gas stream, cracking reactions will increase the viscosity further. Finally the agglomeration of particles and cracking reactions will create a solid coke deposition. Typical for the amorphous coking are areas with high void fractions inside the agglomerate and a high content of volatile matter. Due to the enclosed condensates the density of this type of coking is higher than char.

2.5.3 Soot

The term soot originates from the incomplete fuel-rich combustion of carbonaceous fuels and there has been intense research to study the formation pathways of it. However, most of the studies are made on the kinetics of model compounds and are not suitable to describe in detail the numerous reactions during decomposition real biomass.

One of the findings of the work with model compounds is that soot can already derive during the decomposition of very small compounds via the formation of free radicals [66]. These radicals build benzenes and phenols and condense in time to Poly Aromatic Hydrocarbons (PAH's). The PAH's grow in molecular size and nucleate and further coagulate to form a nano-sized particle. Then the growth continues via surface mediated reactions and a solid spherical particle forms, typically in the size of ca. 5 µm. The particles fuse or agglomerate to form finally. dendritic structures and very porous clusters. A schematic drawing of this formation pathway can be seen in Figure 9. Liu et all [67] give information about the mechanisms of surface growth of soot. They were able to directly observe the carbon growth by scanning tunnelling microscope and found that reactions mainly take place at defective carbon sides and no reactions were found on smooth graphite surface planes.

Figure 9: Schematic drawing of soot formation during fuel rich combustion of natural gas. [66]

During the thermal decomposition of real biomass it is not just the synthesis of PAH's from small molecules but also a breakdown of large molecules [68]. The aromatic ring

structure already exists in the lignin macro-molecule and during its decomposition it comes to cleavage and the formation of primary, secondary and tertiary tars and finally soot. Primary tars contain no PAH's but phenols and phenolic di-mers and tri-mers, secondary tars are PAH's less than 5 aromatic rings and tertiary tars are PAH's with more than 5 aromatic rings. Experimental data have shown that the formation of tars is temperature dependent with secondary and tertiary tars produced at temperatures above 650°C whereas below 650°C mainly primary tars are produced [69]. Britt et all [70] found that the amount of PAH's directly derived from plant compounds like steroids is very low and that PAH's are mainly found during secondary pyro-synthesis reactions with initial cracking into fragments followed by radical addition and cyclisation reactions.

3 High temperature filtration

3.1 Filtration principles

Filtration means the removal of a substance/particle from a gaseous or liquid stream by passing the intermixture through a permeable filter medium which separates the substance/particles to be removed from the stream. It can be distinguished according to the type of filtration behaviour between 'depth' and 'barrier' filtration as described below. [71]

3.1.1 In-depth filtration

During in-depth filtration the particles penetrate into the porous filter media where they are collected and retain in the filter material. The mechanical mechanisms of particle collection are: diffusion, inertia, direct interception, gravity, electrostatic attraction. An illustration of the particle removal mechanisms can be seen in Figure 10.

Figure 10: Particle capture mechanism in fabric fibre [12]

For very small particles diffusion is the dominant force, whereas for larger particles inertial impaction dominates. All filters have a most penetrating particle size where the

collection efficiency is at the minimum, which is usually between 0.1 and 1.0 µm. It shifts slightly depending on the filter medium, temperature and flow velocity. Higher temperature increases Brownian diffusivity and therefore enhances collection of submicron particles but decreases inertial impaction due to decrease of the viscosity of the transport medium. With increasing flow velocity the minimum filtration efficiency shifts more to a larger particle size (>1 µm) because the filtration efficiency due to diffusion decreases whereas the inertial impaction increases. The collection efficiency of a mechanical filter for different particle sizes can be seen in Figure 11. Particles removed by in-depth filtration cannot be removed from a depth-filter without shutting down the filter and removing the filtration medium. [72-74]

Aston University

Illustration removed for copyright restrictions

Figure 11: Fractional collection efficiency versus particle diameter for a mechanical filter. The dip shows the most penetrating particle size. [75]

3.1.2 Barrier filtration

In barrier or surface filtration the particle or aerosol is collected on the surface of the filter medium without penetration into the filter medium. The separation mechanism can be due to simple sieving if the particle is larger than the pore size of the medium or more commonly due to bridging of the particles on the pores of the filter surface. Due to accumulation of the separated particles a filter cake on the filter surface builds up. The filter cake itself acts then as filter medium and removes oncoming particles. Pure surface filtration is rare as during the first period of filtration with an unused filter usually some of the particles penetrate into the filter. Figure 12 illustrates surface

filtration of fine dust particles. The large circles on the left represent the filter fibres. The fine dust particles are collected due to the mechanisms described in 3.1.1 and bridge the filter surface by forming dendritic structures with high porosity.

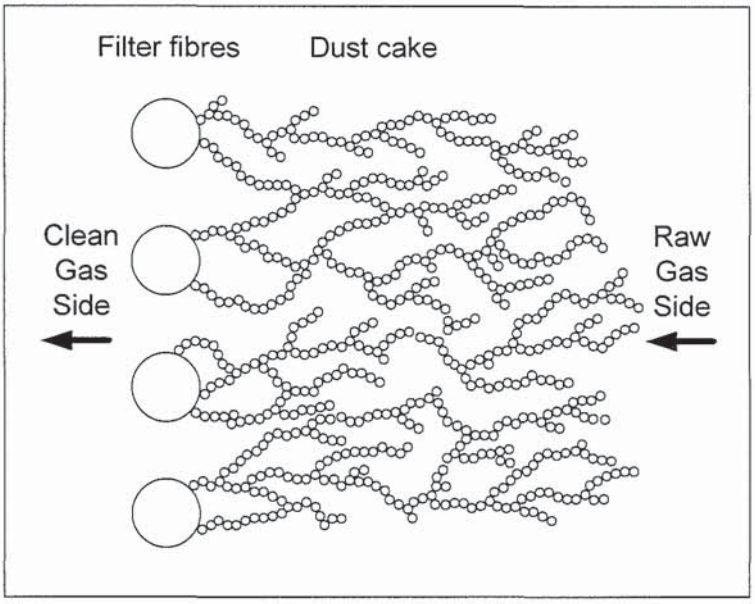

Figure 12: Filtration of fine particles due to bridging on the filter surface

3.2 High temperature filter candle technology

3.2.1 Introduction

During filtration the filter candle acts as a barrier filter which separates the particulates on the surface of the filter candle. The separated particulates bridge on the filter surface and develop a filter cake. The filter cake then acts as an additional filter medium where particulates are separated due to in-depth filtration. The filter cake increases the pressure drop between the raw and clean gas side of the candle with filtration time. Figure 13 describes the function of a filter candle with raw and clean gas side and developing filter cake. After a pre-described time or a certain amount of pressure drop the filter cake is removed by reverse pulse cleaning. During reverse pulse cleaning a high pressure gas stream with high momentum is injected via a nozzle on the clean gas side of the filter candle. This jet pulse creates a reverse flow in the filter medium and detaches the filter cake. In the early phase of filtration some small particles penetrate into the filter medium and are therefore not removable by reverse pulse cleaning. This phenomenon is described as conditioning of the filter candle. The conditioning causes a steady increase of residual pressure drop which can not be reduced by the cleaning

procedure. The pressure drop over the system is the limiting factor of the filtration process and therefore has to be kept as low as possible. Different types of filter candles have been developed, which are able to sustain high temperature and chemical corrosive environment as well as combining good filtration efficiency with high permeability of the filter media.

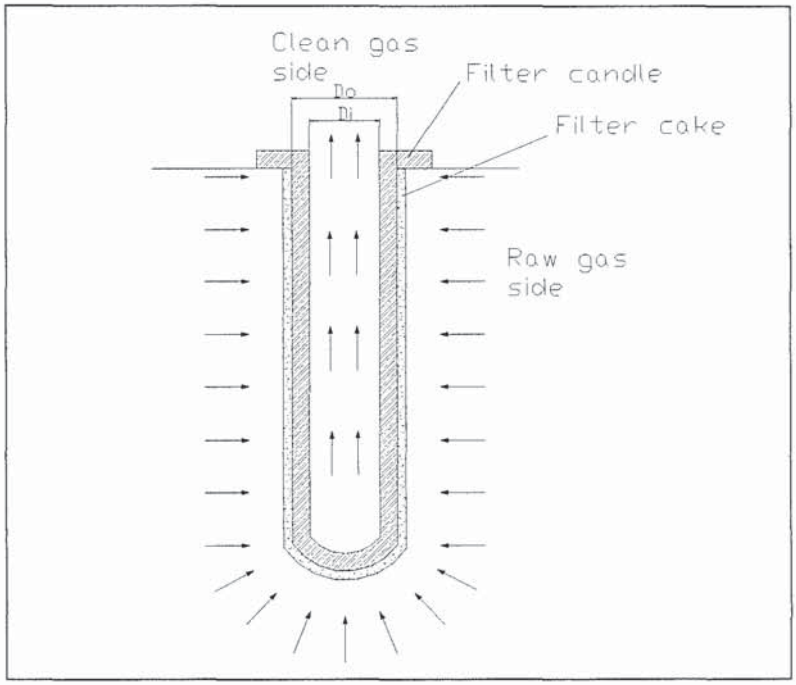

Figure 13: Schematic drawing of barrier filtration on candle surface with developing filter cake

3.2.2 Pressure drop, Resistance to flow, Permeability

The total pressure drop over the filter candle during filtration consists of the sum of the pressure drop over the filter medium and the pressure drop over the filter cake (see Equation 1). The flow of the gas through the filter medium and the distribution of the pressure drops are illustrated in Figure 14.

$$\Delta P_T = \Delta P_M + \Delta P_C \qquad \textbf{Equation 1}$$

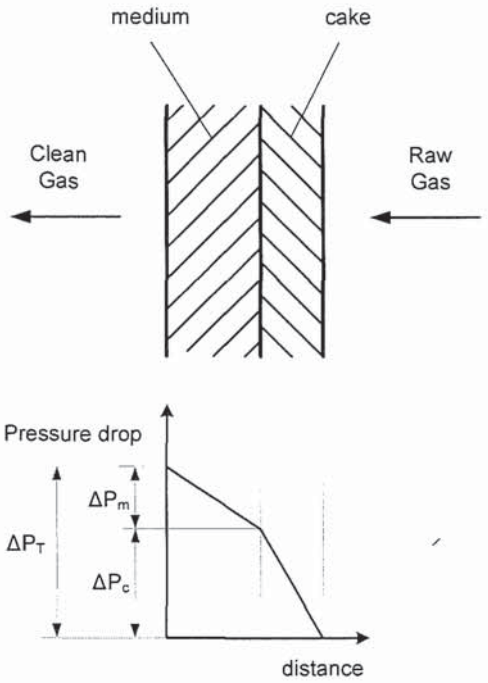

Figure 14: Pressure drop distribution across filter medium and filter cake

The pressure drop can be calculated using Darcy's law for a gas flow through a porous medium (see Equation 2**Fehler! Verweisquelle konnte nicht gefunden werden.**).

$$\Delta P = k * \mu * u * L \qquad \textbf{Equation 2}$$

k is the specific resistance to flow of the filter medium or the filter cake, μ is the viscosity of the gas; u is the face velocity of the gas and L the thickness of the filter medium or the filter cake.

More often than the resistance to flow, the permeability is used to describe the specific characteristics of a filter material. The permeability (b) is described as the reciprocal value as illustrated in Equation 3. Normally the permeability of a ceramic filter candle is in the order of magnitude of 10^{-11} m^3/m.

$$b = \frac{1}{k} \qquad \textbf{Equation 3}$$

3.2.3 Flow pattern on filter candle

Inside the candle cavity is a pressure difference with lower pressure on the open end compared to the closed end along the candle. The pressure difference is caused by higher gas momentum at the open end of the filter tube and friction losses on the inner tube walls. This results in a higher pressure drop across the filter candle on the open end which causes a higher velocity of the gases compared with the closed end [76]. The misdistribution of gas velocity over the length of the candle gradually decreases with filtration cycles as a higher gas flow leads to more deposition of particulates and increases the resistance to flow and therefore reduces the differences in gas velocities.

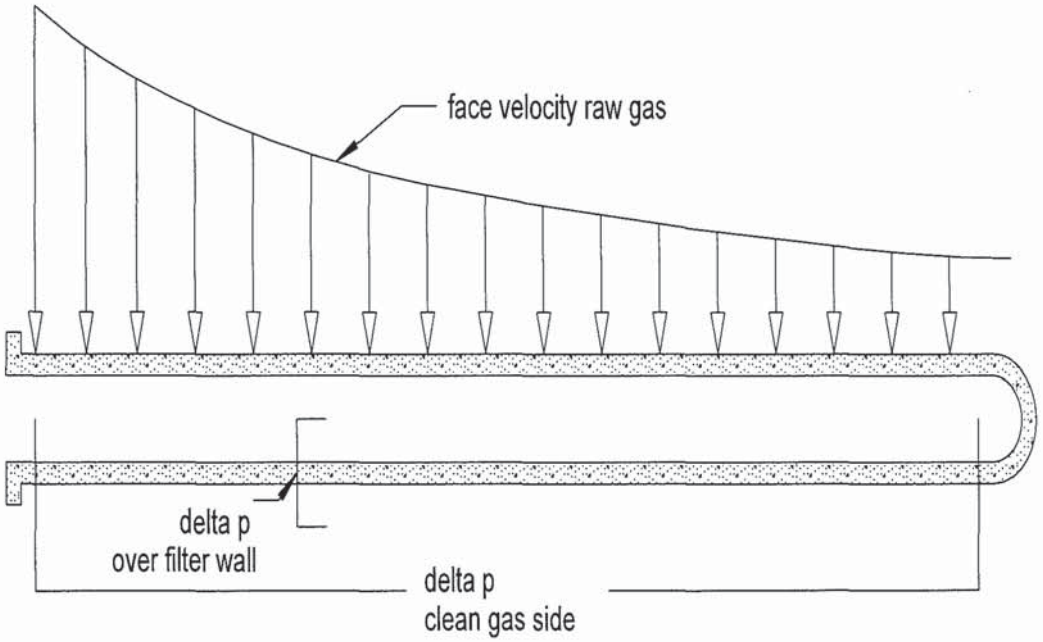

Figure 15: Face velocities at different length of the filter candle

3.2.4 Filter cake structure

The filtration mechanisms which lead to the formation of a filter cake were already described in 3.1.2. This paragraph concentrates on the structure of the filter cake and the process characteristics which influences it. The properties of the filter cake depend mainly on the separated dust particles and the face velocity of the gas which affects the kinetic energy of the particles [77]. The particle properties which influence the dust cake structure regarding porosity and permeability are:

- particle size and shape
- particle density
- adhesive and cohesive properties
- energy content

The collection of a particle at the first point of contact forms dendrite structures with a high void fraction and low density. Therefore, cohesive particles separated at low gas velocity create dendrite filter cakes whereas dense particles with low cohesive forces and high kinetic energy build dense filter cakes. The influences of particle properties on the porosity of the filter cake are listed in Table 1 below.

Table 1: Correlation of particle properties and filter cake porosity

	Particle property	Cake porosity
Particle size	Increase	Increase
Particle density	Increase	Decrease
Kinetic energy	Increase	Decrease
Cohesive forces	Increase	Increase

Various researchers [78-81] developed models to simulate the porosity and/or permeability of the developing filter cake. But up to now no quantitative prediction of the cake properties has been possible, so that real experiments are inevitable.

3.2.5 Reverse pulse cleaning

3.2.5.1 Introduction

It is essential to have a well designed reverse pulse cleaning system for a long term operation of the filtration unit at the lowest possible pressure drop. The regeneration efficiency of the pressure drop by removing the filter cake is dependent on the design of the reverse-pulse system, the properties of the filtered dust respectively filter cake and the interaction between dust layer and filter media.[82]

During jet pulse cleaning a gas stream from a pressurised reservoir vessel gets expanded via a quick acting valve. The jet pulse is introduced by an injection nozzle, situated above the open end of the filter vessel, into the filter candle cavity. As the gas leaves the

blowback nozzle some surrounding fluid will be entrained into the expanding gas and increases the actual gas stream. The resulting gas stream with high momentum generates an overpressure inside the filter cavity leading to a reverse gas flow in opposite direction of the filtration gas stream. The velocity of the reverse gas stream through the filter medium and filter cake depends on the differential pressure between clean gas side and raw gas side of the filter candle. The performance of the cleaning system can be characterised by the intensity of the differential pressure over the filter cake during the reverse pulse.

3.2.5.2 Differential pressure during reverse flow

Various researchers investigated into the differential pressure profile generated during reverse pulsing [72, 76, 82-85]. Some of the published data varied considerably regarding the signal form, the order of magnitude and the pressure drop behaviour along the filter candle. This can be explained with different reverse pulse design set up, candle geometries as well as differently applied evaluation methods.

Fast piezzo-resistive pressure transducers in connection with an oscilloscope are necessary to monitor the very fast changes in differential pressure. Figure 16 shows typical pressure profiles obtained by fast pressure transducers between the clean and the raw gas side of the filter candle at a certain position along the candle. The two graphs represent the pressure development on two different types of filter candles at the middle measurement position and a reservoir pressure of 600 kPa. The upper graph shows the pressure curve for a DIA Schumalith candle made of ceramic grain material and a porosity of ca. 37 % whereas the lower graph shows the curve of a fibrous ceramic material with a porosity of ca. 90 %. It can be seen that the gas stream is retained for a short while before the pressure inclines to a maximum peak. After the maximum peak the pressure reaches a quasi-steady flow profile. Berbner [72], Mai [86] and Schildermann [87] received this type of pressure profile especially at the middle and end position of the candle. Other researchers (Laux [84], Stephen [88]) found a more quasi-stationary type profile without the large superimposed peak.

Figure 16 shows that the candle material also influences the intensity of the differential pressure and the intensity of the reverse flow. It can be seen that the grain ceramic candle (Schumalith F40) with lower permeability generates a higher differential

pressure compared to the fibre ceramic candle KE85/60. This does not increase the detachment forces as it only reflects the permeability but actually reduces them as a smaller amount of the differential pressure is applied on the filter cake.

Figure 16: Course of differential pressure between clean gas and raw gas side of the filter candle. [73]

3.2.5.3 Variation of delta p along the filter candle

The differential pressure during reverse pulse varies along the filter candle with a lower delta p at the open and the maximum delta p at the closed end of the filter candle (see Figure 17). The pressure profile is in the section close to the open end strongly oscillating with even negative peaks. The negative differential pressure in this section is possible if the injection nozzle is too close to the candle which causes an entrainment flow from the raw gas side of the candle. In the middle and the end position the pressure profile is normally comparable to the one described in Figure 16. [85]

Figure 17: Pressure drop over the filter wall at various measurement points (top = open end, bottom = closed end) along the filter candle. [89]

3.2.5.4 Design parameters

To achieve an effective cleaning of the filter candle an optimum design of the reverse pulse system is essential. It is desirable to achieve a maximum of reverse flow velocity for good cleaning performance while minimising the consumption of pulse cleaning gas. The main design parameters which influence the quality of the reverse pulse are:

- Cleaning reservoir pressure ($P_{Reservoir}$)
- Nozzle diameter (D_{Nozzle})
- Distance between nozzle and filter opening ($H_{Nozzle\text{-}Filter}$)
- Opening time of the reverse pulse valve
- Use of a venturi
- Filter candle geometry

3.2.5.4.1 Reservoir pressure

The influence of the cleaning pressure was investigated by Laux [84] and Berbner [90]. They found a direct relation between reservoir pressure and differential pressure

between filter cavity and raw gas side. However, the advantage of increased reservoir pressure becomes less clear above 600 kPa because of the risk of secondary raw gas entrainment at the open end section of the filter. This can lead to re-deposition of particles on the candle at high velocities at this part of the candle. In general, 600 kPa is the maximum applied reservoir pressure for jet pulse.

3.2.5.4.2 Nozzle diameter

With a small nozzle diameter the entrainment of secondary gas is enhanced leading to less consumption of cleaning gas. On the other side a large nozzle diameter enables a higher volume flow of cleaning gas from the reservoir into the filter cavity. Mai et al found that the pressure inside the filter cavity increased with increasing nozzle diameter. The nozzle diameter in practical use varies usually between 6 mm and 16 mm.

3.2.5.4.3 Distance between nozzle and filter

The optimum distance between nozzle and filter depends on the filter medium, filter geometry, reservoir pressure and filtration face velocity. If the distance is too close the reverse flow pressure difference in the open end section of the filter cake is very low and can become even negative. In case of a too long distance not all of the cleaning gas enters the filter cavity which reduces the maximum peak at the closed end. The optimum distance lies between these two extremes and varies typically between 100 and 140 mm. [91]

3.2.5.4.4 Effect of a Venturi insert

A Venturi device at the candle inlet has the advantage to improve the entrainment of secondary gas from the filter head into the candle cavity. This enhances the gas stream and can improve the cleaning intensity. However studies from Granell and Seville [91] showed that the influence of the applied Venturi inserts was negligible regarding the maximum overpressure in the candle cavity. However some Venturi inserts showed a positive impact on the pressure difference in the section on the open end of the filter candle, therefore avoiding gas entrainment through the wall.

3.2.5.4.5 Effect of candle geometry

The filter geometry, especially the inner diameter and the length of the candle affects the flow dynamics of the pulse gas. A small inner diameter has a positive impact of the

delta p across the filter wall due to the increased velocity of gases in the candle cavity [86]. The effect of the length of the candle is already described in 3.2.5.3. To balance the misdistribution of differential pressure over the wall along the length of the filter, Chuah et al did research on tapered filters. They were able to distribute the cleaning pressure difference more equally by using candles which reduce the diameter conical towards the closed end. [85]

3.2.6 Conditioning of the filter candle

After cleaning of the filter candle via reverse pulse is the resulting pressure drop over the system higher than with the original unused filter candle. This is caused by the remaining dust on the filter candle and by particles having penetrated into the filter matrix. The pressure drop after the cleaning cycle is defined as residual pressure drop. The increase in residual pressure drop during the first filtration cycles is defined as the "conditioning" of the filter candle. If the cleaning procedure is successful the residual pressure drop reaches a steady equilibrium. In the case of an unsatisfactory cleaning behaviour the residual pressure drop continues to rise over many filtration cycles. In this case the reverse pulse cleaning is insufficient or the dust cake sinters/sticks so that the filter cake is not or only partially removed. Consequently, the pressure drop will continue to increase from cycle to cycle and will never reach stable conditions [87]. During the conditioning process a thin residual dust layer is established on the filter surface. There is evidence that this residual dust cake consists of a smaller mean particle size and a higher resistance to flow then the remainder of the filter cake [71].

3.2.7 Filter cake detachment

The filter cake detaches from the medium when it experiences a tensile stress sufficient to overcome the adhesion forces between the dust cake and the filter medium and/or residual dust layer or the internal adhesion forces between particles inside the filter cake. In conventional fabric filters it is assumed that the required tensile cleaning stress is produced by the movement which displaces the fabric outwards during the cleaning pulse Rigid filter candles show no displacement during cleaning and the tensile stress has therefore been entirely generated by the pressure drop across the filter cake [71].

Due to the maldistribution of the generated pressure drop during cleaning along the filter candle (see Chapter 3.2.5.3) the filter cake detaches better at the closed end of the

candle then on the candle inlet. Furthermore, it was found that thick and compact filter cakes generate a higher pressure drop across the filter cake during reverse pulsing and are therefore easier to remove. Berbner [92] compared the cleaning intensity of filter cakes with 110 g/m^2 and 270 g/m^2. He found that the filter cake with 270 g/m^2 areal load was completely removed whereas the filter cake with 110 g/m^2 showed just partial removal of the cake.

Very frequently "patchy" cleaning of the filter candle is observed. As neither the adhesive/cohesive strength of the cake nor the applied stress is entirely uniform across the filter surface the cake detached in some areas of the filters and is completely retained in others. Several researchers investigated into this phenomenon and the consequences for the filter cake and differential pressure development [79, 93, 94].

3.2.8 Filter candles

A wide range of commercial available filter candles is meanwhile available for high temperature application. In general they can be distinguished between metal candles and ceramic candles.

3.2.8.1 Metal filters

Metal candles consist of a sheet of sintered metal or metal alloy which is mounted on a support frame. The sintered metal material is produced either from metal powder, fibre, or with wire laminate technology. The support frame is usually designed as a cage welded from a suitable metal which fits the requirements for the specific application. The advantages of metal candles are their high strength and ductility. Furthermore, the high thermal conductivity makes them resistant to high temperature gradients. This also makes them suitable if they are exposed to unforeseen high temperatures due to accidental combustion. The metal media for high temperature application is capable of withstanding operation temperatures of 650°C to 900°C. Common alloys used in this high temperature range are Hastelloy, Inconel and FeCrAl-matrices. They can withstand a corrosive and oxidative environment but are not recommended in the presence of gas phase alkali above 850°C. The main disadvantage of metal filters at this time is their high cost. [8, 95]

3.2.8.2 Ceramic filters

Because of their thermal stability and good resistance against corrosion, rigid ceramic filter candles are widely used in high temperature filtration. In general ceramic candles can be subdivided into fibrous and granular ceramics. The latest developments in second generation filter candles include composite ceramics which combine different ceramic materials [96].

Common monolithic fibrous ceramic oxide candles are made of Alumino-silicate fibres (Al_2O_3 + SiO_2). These candles have a wall thickness of ca. 20 mm and are self-supporting. They have good particle separation characteristics but show little mechanical strength. They have a good permeability due to their porosity of ca. 60 %. Furthermore, they have a low density which makes them very light and reduces cost for the construction of the filter housing. Another advantage is their low acquisition cost. A disadvantage is the potential hazardous dust (carcinogenic) which can cause a health risks during handling of the candles.

More robust are granular ceramic filter candles. They consist of granular SiC which is bonded together by a clay binder. SiC-candles show high mechanic strength but have a higher density then the fibrous candles. The second generation of SiC candles are made of a highly porous support body with large granules and a very thin filtration membrane of small granular or fibrous material [97]. The filter membrane is very thinly (50-200 μm) coated on the support body and consists of particulates with a mean diameter of 0.1 μm. This creates a very smooth surface and prohibits dust particulates from entering the filter candle and therefore guarantees a true surface filtration. The latest developments are membranes, made out of nano-scaled grains which reduce the adhesion forces between membrane and cake [98]. The disadvantage of these candles is the high price and high weight compared with fibrous ceramic candles.

3.3 Hot filtration of fast pyrolysis vapours

3.3.1 National Renewable Energy Laboratory (NREL)

The main work on filtration of fast pyrolysis vapours was done from Diebold et al [46],[5] at the National Renewable Energy Laboratory (NREL) in Colorado. They used a filtration unit containing 4 filter candles. They tested 2 different types of filter candles,

a sintered Inconel candle made by MEMTEC and a flexible ceramic cloth filter made from Nextel by 3-M. The filtration unit was operated at temperatures between 440°C and 470°C with an additional residence time of the hot vapours in the filtration unit of about 3-6 s. The filtration unit was located downstream of a Vortex reactor and the cyclones removed from the system. Oven-dry switch grass and poplar wood was used as feedstock. They report 38 wt% organic liquid yield, 16 wt% water, 22 wt% char and 20 wt% gases for switch grass with the filtration unit operated at a temperature of ca. 400°C. They found that the organic yield is reduced from 38 wt% to 27 wt% when the temperature in the filter is increased from ca. 400°C to 470°C. Therefore, they recommend operating the filter at the lowest possible temperature and designing the filter vessel with the lowest possible residence time to reduce the decomposition of organic vapours.

They found that the rigid sintered Inconel filter candle showed better particulate removal characteristics compared to the Nextel woven ceramic fabric candle. Therefore, they suggest operating the Nextel candle with a permanent filter cake to increase the filtration efficiency due to particulate removal inside the filter cake. The data presented on alkali metal content showed potassium content of 1380 ppm for oils with cyclone separation, 7-30 ppm with Nextel filter and 1-15 ppm with Inconel candle.

They report a steady pressure drop increase across the sintered metal filter candle from ca. 1.0 kPa to 4.8 kPa after 160 min of operation with just very limited pressure drop recovery during the frequent reverse pulse cleaning operations. For the Nextel filter they achieved better cleaning behaviour and report pressure drop recovery from 3.2 kPa down to 1.2 kPa during the cleaning procedure. They concluded that they could allow a thick filter cake to build up and were still able to recover the same low pressure drop as with more frequent back flushing. However, there was no data presented which showed the differential pressure across the candle for a filter operation longer than 100 min.

Although Jim Diebold showed that is possible to produce pyrolysis oil in superior quality due to a reduced solid content, he was not able to demonstrate stable filter operation longer than 160 min. One disadvantage of his filtration system is the introduction of cold nitrogen during the reverse pulse. This can probably lead to

condensation of pyrolysis vapours inside the filter candle and might be a reason for the very short filtration time.

3.3.2 Technical Research Centre of Finland (VTT)

VTT reported work on hot filtration of pyrolysis vapours as part of the EU contract [99]. They carried out experiments on a 1kg/h fast pyrolysis reactor using a filter unit with one filter candle. They were able to perform filtration experiments for up to 6 hours before they had to shut down because of the increasing differential pressure over the filter. They did not report any results regarding mass balance and pyrolysis oil quality of the filtration experiments. Additionally, some preliminary experiments were carried out to evaluate the drop in temperature caused by the cold reverse pulse nitrogen stream. They measured a temperature reduction down to 380°C and considered this as acceptable to avoid condensation of pyrolysis vapours on the filter candle. However, although the preliminary experiments showed no reduction in temperature below 380°C it cannot be excluded that some temperature sinks occur during the expansion of the nitrogen reverse pulse. Furthermore, it is questionable whether the accuracy of the thermo-couple is able to record very short drops in temperature.

3.3.3 University of Twente

At the University of Twente a hot filter system was developed with the filter candles directly emerged in the fluidised bed. With this arrangement it is intended to clean the filter cake by means of abrasion through the fluidised sand. The downside of the system is that not all of the process gases can be cleaned as some of them have to pass through the reactor top to stabilise the fluidising bed. They were able to perform filtration experiments for up to 2.5 hours and reported a solid content of the filtered oils of 1.47 wt% compared with 2.68 wt% for non-filtered oils. The particle size in the filtered oil was below 25 μm and it seems that some particles must have slipped through the filter possibly due to the specific set-up causing abrasion of sand on the filter surface. [100]

It can be concluded that the University of Twente found a method to overcome the difficulties of removing the filter cake by emerging the filter candles in the fluidising bed. However, due to the low filtration efficiency it can not be considered as a successful approach as a solid content of 1.47 wt% can be even achieved with cyclones.

4 Experimental

4.1 Experimental set-up

4.1.1 Objective and methodology

The objective of the experiments is to demonstrate hot filtration of fast pyrolysis vapours to remove the solid content of the later oil. Furthermore, the hot filtration unit will cause additional secondary vapour cracking due to the extended residence time of the hot vapours and cracking reactions on the developing char filter cake. The additional secondary vapour cracking will reduce the organic liquid yield to some extent, but can improve the pyrolysis oil quality beyond the solid removal by cracking high molecular weight compounds.

Hence it is intended to examine the influence of the additional residence time and vapour cracking on char on the fast pyrolysis process. For this purpose preliminary experiments were carried out using a fixed bed secondary reactor with a packed bed of wood char to compare them with standard fast pyrolysis experiments.

Furthermore, a hot filtration test unit was developed to fit into the existing 1kg/h fast pyrolysis system to make hot filtration experiments with realistic conditions. The experiments were examined by calculating the mass balance of feedstock educts and the pyrolysis products to evaluate the losses of organic liquid. An online gas analysis was executed to determine the amount and composition of the non-condensable gases. Additionally, the oils were analysed regarding solid content, viscosity and mean molecular weight to evaluate the quality of the produced oils.

Two different types of filter candles were used to examine the influence of the candle material on the product quality. The Tenmat firefly candle represents a ceramic element and the Bekaert Inconel candle is made of sintered metal fibre.

In addition to the product yield and quality, the performance of the cleaning system is of interest to evaluate the stability of the filtration process. It is imperative to remove the filter cake regularly to avoid a constant increase of pressure over the system. To

decrease the adhesion of the filter cake on the filter cake, or the adhesion of the particles inside the filter cake itself, the full char load was presented to the filter candle to produce a less dense and easier removable filter cake. Furthermore, one experiment was carried out with injection of a Pre-coat material to form an additional layer between filter candle and filter cake to decrease the adhesion of the filter cake.

To examine the cleaning behaviour of the filter cake the pressure drop on the filter candle was monitored and the filter cake examined. The filter cake was analysed with SEM to get an impression of the particle size distribution of the char. Furthermore, the resistance of flow of the filter cakes was calculated to characterise the filter cake of the different set-ups.

4.1.2 Experimental programme

The filtration unit was either used as a replacement of the existing char separation system or was used in line after a primary cyclone. Figure 18 and
Figure 19 show the simplified flow diagrams of the two different set-ups. In the first set up the whole char produced enters the filtration unit. This results in a high particle load of the gas stream but due to the coarse char particles it is intended to produce a less dense filter cake which is easier to remove.

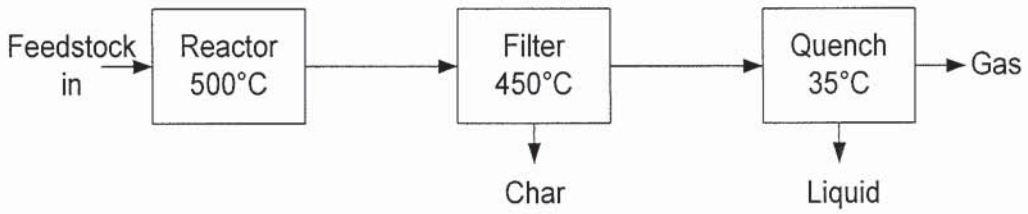

Figure 18: Flowsheet of experimental set-up with the filtration unit replacing the cyclone separator

The second set up includes a primary cyclone to remove the bulk of coarse char particles prior to the filtration unit. This reduces the amount of particles present in the gas stream by ca. 97 wt%. Therefore, the filtration time until the filter cake has to be removed will be longer than in the first set-up. In this set-up a pre-coat material is introduced prior the filtration and between each reverse pulse injection to produce a pre-coat layer between filter candle and filter cake. Aeroxide (fumed TiO_2, DEGUSSA) were chosen as pre-coat material because of its low density, nano-scale size and

spherical particle form. These parameters shall enable to establish a pre-coat layer with dendritic structures (see Figure 12) to achieve a high permeability beside small surface contact areas. The little surface contact between the pre-coat material and the candle surface is expected to reduce adhesion forces and to create a cake which is easy to remove.

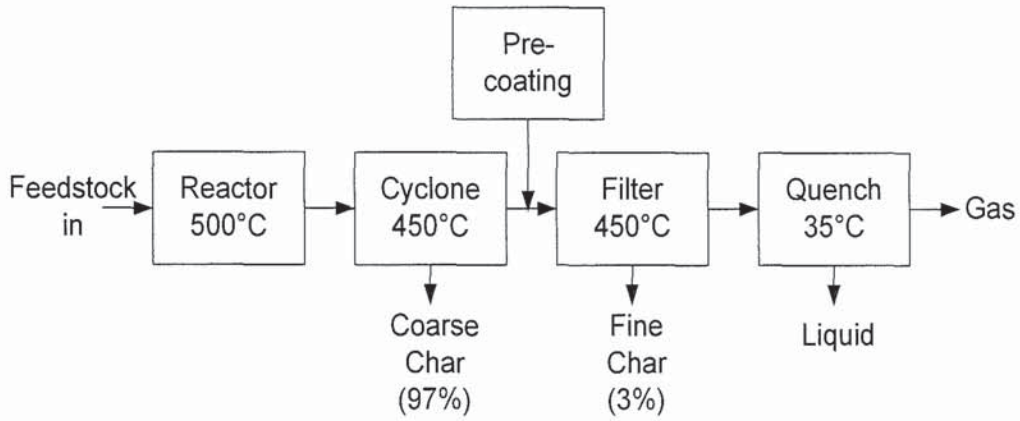

Figure 19: Flowsheet of experimental set-up with one primary cyclone prior the filtration unit and optional pre-coating.

4.2 Fast pyrolysis unit

4.2.1 General description

The flow sheet of the 1 kg/h fast pyrolysis unit at Aston University is shown in Figure 20. The pyrolysis rig consists of a fluidised bed reactor (2) at 500°C with nitrogen as the fluidising gas and silica sand as bed material. A nitrogen flow of ca. 40 l/min is preheated (1) before entering the reactor. The reactor temperature is maintained at 500°C. The biomass is fed from the hopper (3) via a metering screw followed by a fast conveying screw (4) into the reactor. An entrainment flow of ca. 7 l/min nitrogen supports the biomass transport and prevents the sand bed from flowing back into the screw feeder. The product stream of vapours, non-condensable gases and char particles leaves the reactor at the top and enters the char separation system (5). In the standard process the char separation consists of two cyclones in series. For the hot filtration experiments the filter unit replaced both cyclones. The separated char is collected in the char pot (6). After the char fines are separated the majority of the vapours are condensed in a disc and doughnut quench column (7) using Isopar V as a quench liquid. After the quench an Electrostatic Precipitator (EP) (8) traps the aerosols. The liquids captured by

the quench column and EP are collected together in the tank (7) and make up more then 90 % of the liquid yield. Residual water and light organics are then separated with a dry ice condenser (9) followed by a dry cotton wool filter (10). The volume of the remaining dry gas stream is then measured by a gas meter (11). Gas samples are taken at 3 minute intervals and analysed on-line using a Varian CP4900 Micro gas chromatograph with two separation columns and thermal conductivity detectors. The gases analysed are N_2, CO_2, CO, CH_4, H_2, C_2H_6 and alkanes/alkenes up to C4. Temperature readings are taken throughout the whole experimental run as well as differential pressure reading at the main components.

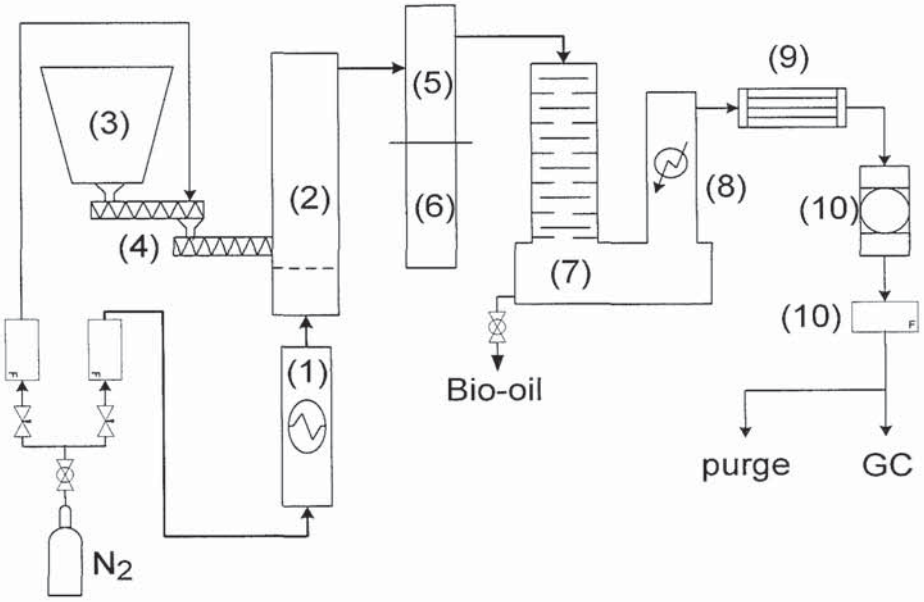

Figure 20: Flow sheet of 1kg/h fast pyrolysis unit with filtration system

4.2.2 Specification

4.2.2.1 Feeding system

The prepared feedstock (moisture content, particle size < 2mm) is filled in the feed hopper. The feedstock is delivered by means of contra-rotating twin screws (metering screw), which were calibrated for the specific feedstock in use. From there it falls into a high speed screw (fast screw) which feeds the feedstock into the reactor. The fast screw is cooled by a water jacket. An entrain flow of nitrogen (approx. 7 l/min STP) supports the feeding and creates a small positive pressure to avoid air entering the system. Furthermore, the entrained flow is important to suppress the fluidising sand entering the fast screw.

4.2.2.2 Reactor

The bubbling fluidising bed reactor is filled with ca. 1kg silica sand bed in a particle size distribution between 500 – 850 µm. The reactor is heated by external electrical band heaters and automatically controlled via thermocouples located inside the bed. The sand bed is fluidised by means of preheated nitrogen at 500°C and enters the reactor via a perforated distributor plate. The nitrogen flow rate is approx. 44 l/min STP which results in a ratio of superficial velocity to minimum fluidising velocity of approx. 2.5 cm/s. Above the sand bed the reactor diameter expands to reduce the gas velocity to avoid sand particles to entering the freeboard area and keeping the fluidizing bed in place. Alternatively, in the freeboard area a dummy cyclone increases the gas velocity to entrain char particles which float on top of the fluidizing bed into the gas stream and out of the reactor. The residence time of the hot vapours in the reactor depends on the gas velocity and is typically below 1 s.

4.2.2.3 Char removal

After the reactor the product stream of pyrolysis vapours, pyrolysis gases and char diluted in the nitrogen carrier gas enters the char removal system which consists of 2 hot cyclones in series for standard experiments. The cyclones and the pipe-work are heated electrically to 400 – 450°C to avoid condensation of the pyrolysis vapours whilst minimizing secondary cracking of vapours into non-condensable gases. The bulk of the char (ca. 95 wt%) is removed by the first cyclone and is collected in char pot 1. As all the larger char particles are already separated in the first cyclone the 2nd cyclone only removes char fines which tend to block the pipe between the cyclone and the char pot due to their cohesive character combined with their low density. To avoid this blockage the 2nd cyclone is equipped with a scrapper for manual cleaning in regular time intervals of approx. 30 min. Depending of the amount of char fines in the product char approx. 2.5 wt % of char is collected in char pot 2 and the remaining 2.5 wt% of char ending in the pyrolysis oil. In the course of this work the char removal system is altered by total or partial replacement of the cyclones by the filtration unit (details see Chapter 4.1).

4.2.2.4 Liquid collection

The liquid collection system consists of a quench column with disc and doughnut type of plates to increase the surface area. The vapours are condensed by contact with the quench liquid Isopar V. Isopar V is an Iso-paraffin with boiling point > 270°C. It is not miscible with the condensed pyrolysis oil and phase separates quickly in the liquid collection tank below the quench column. As Isopar V has a lower density than pyrolysis oil, it floats on top of the oil from where it is re-circulated. The quench column is cooled via an external water jacket to keep the temperature of the quench liquid at ca. 25°C when it enters the quench top.

After the quench column the gases, uncondensed vapours and aerosols enter the Electrostatic Precipitator (EP). The EP consists of a central wire electrode which charges the aerosols so that they migrate to the outer cylindrical electrode. The EP wall is flushed with Isopar which removes the captured aerosols and unites them with the condensed pyrolysis oil in the main collection tank. From the literature it is known that ca. 20 – 30 % of the pyrolysis oil is collected in form of aerosols by the EP.

The uncondensed vapours and gases pass then through a series of dry-ice/acetone condensers with the temperature in the dry-ice/Acetone mixture of ca. -70°C. After the condenser unit a Cotton Wool Filter (CWF) removes still uncondensed vapours.

4.2.2.5 Temperature and pressure measurement

K-Type thermocouples are used to measure the temperature at various points of the system and the data is recorded via a Data Acquisition System using Windmill software. The pressure difference over the reactor, pipe-work and cyclones, quench column and dry ice condenser are monitored by analogue pressure gauges. The location of the specific measurement points can be seen in the detailed flow sheet in Appendix 1.

4.2.3 Mass balance

The mass balance of the experiments was calculated on dry feedstock basis with the mass of water contained in the feedstock subtracted from the mass of educts as well as from the mass of products using Equation 4. The mass balance closure is the percentage of the feedstock recovered as products.

m (Educts) = m (Products) **Equation 4**

m (biomass dry) = m (organic liquid) + m (H_2O process) + m (char) + m (gas)

with:

m (biomass dry) = m (biomass) – m (H_2O biomass)

m (organics = m (total pyrolysis liquid) – m (H_2O biomass) – m(H_2O process)

m (H_2O process) = reaction water produced during fast pyrolysis

4.2.3.1 Pyrolysis liquid

There are two fractions of pyrolysis liquids condensed in the 1 kg/h fast pyrolysis test unit. The main part of the liquid yield is recovered at the quench column tank. It consists of a reddish-brown till dark-brown liquid which is herein referred to as Pyrolysis Oil (PO). A second liquid fraction is recovered at the Dry Ice Condenser (DIC). It consists of light organics and more then 50% water. It has a light-brown appearance and is referred to as DIC-liquid. A small amount of condensable vapours escape the DIC and are trapped in the Cotton Wool Filter (CWF). The vapours condensed in the CWF are calculated by difference. It is assumed that the condensate collected in the CWF has the same composition (i.e. water content) as the DIC-liquid and is added as DIC-liquid into the mass balance. The water content of the pyrolysis oil and the DIC-liquid is analysed by Karl-Fischer titration (see 4.2.5.1). The sum of pyrolysis oil fraction and DIC-liquid fraction are considered as total pyrolysis liquid. The mass of process water is calculated using the water contents of both fractions and the amount of water initially fed with the feedstock subtracted. Usually 90 wt% of the total pyrolysis liquid is recovered as pyrolysis oil in the quench column tank. However, the amount can vary between 95 wt% during the winter month when the water used to cool the quench column has approx. 8°C and approx. 88wt% during the summer period when the cooling water has approx. 16°C.

After draining the pyrolysis oil and the quench liquid from the quench column tank a part of the oil remains sticking on the tank walls. Therefore, the quench system is flushed with approx. 2 l ethanol. The ethanol dissolves the remaining oil/isopar from the quench column walls. From a representative proportion of the ethanol/pyrolysis-

oil/isopar mixture the ethanol and water is removed by rotational vacuum evaporation. The remaining oil and isopar phase separates after the evaporation of ethanol. The amount of oil which had remained in the quench column is then calculated from the proportional ratio of pyrolysis oil in the washing liquid. As the water evaporates as well it is assumed that the original oil that had stuck on the walls had a water content of 12%. Typically around 40 g of oil remain in the quench system

4.2.3.2 Gases

The amount of gases is calculated from the results of the online Gas-Chromatography (GC-MS) and the total volume of gases by the gas meter readings. A CP-4900 Micro Gas Chromatograph from Varian Chromatography Systems Inc. was used. The GC contains 2 columns. Column A (Molsieve 5A) measures hydrogen, oxygen, nitrogen, methane and carbon monoxide. Column B (Poraplot Q) measures nitrogen, methane, carbon monoxide, ethane, ethane, propene, propane and butane. The GC-MS is regularly calibrated using calibration gases with a dilution of 0.5%, 1% and 3% of each gas in nitrogen.

4.2.3.3 Char

The main part of the char is collected in the char-pot of the cyclones or in the char-pot of the filtration unit. Furthermore, the amount of char in the reactor was determined by the difference of the weight of the sand bed before and after the experiment. The char in the sand bed consists of remaining biomass char particles, which are not blown out of the reactor and coking of the surface of the sand particles. After an experiment the pipe work was carefully washed with solvent and the char collected by filtration of the washing solvent. Additionally, the amount of char in the oil was calculated from the char content of the oil and added to the char yield.

4.2.4 Feedstock analysis

4.2.4.1 Moisture content of the feedstock

The moisture content of the feedstock was determined according to ASTM-E 1756. 3g of the feedstock was weighed into a crucible and dried at 103 °C until weight constancy. The water content is then calculated from the weight loss during drying and the original weight of the biomass as percentage of the original biomass. Triplicates were made for all examinations. The scale used had an accuracy of +/- 0.1mg.

4.2.4.2 Ash content of the feedstock

The ash content of the feedstock was determined according to ASTM-E 1755. An amount of approx. 3g of the feedstock was dried until weight constancy at 103 °C and then heated in a muffle oven to 575 °C for at least 6 hours. The crucibles have to be closed with a lid to avoid losses of ashes during the combustion. After the "ashing" the crucibles are cooled in a desiccators before being weighed. The residuals remaining in the crucibles are considered as ash. The ash content is expressed in percentage of dry biomass. Triplicates were made for all examinations. The scale used had an accuracy of +/- 0.1mg.

4.2.5 Oil analysis

4.2.5.1 Water content of the pyrolysis liquid

The water content of the pyrolysis oil and the DIC-liquid was analysed by Karl-Fischer-Titration. A Metrohm 758 KFD Titrino was used for the volumetric water titration. Hydranal working medium K was used as solvent and Hydranal Composite 5K as corresponding titer reagens because of the specific ability of this titration agent to measure the water content in the presence of ketones and aldehydes. The solution for the titration consists of iodine, sulphur dioxide, pyridine and methanol. The determination is based on the oxidation of sulphurdioxid with iodine on the expense of water. Previously the determination the Titer was calibrated with pure water. Triplicates were made for all measurements.

4.2.5.2 Gel Permeation Chromatography

Gel Permeation Chromatography (GPC) was used to determine the molecular weight distribution of the pyrolysis oil. The integrated system PL-GPC 50 from Polymer Laboratories, UK, with Refractive Index (RI) detector was used. The equipment contained a PLgel 3 µm MIXED-E column, 300x1.5 mm which was heated to 40°C. The oil samples were prepared as a solution in HPLC-grade tetrahydrofurane (THF) in a concentration of 0.01 g/ml. Subsequently the solution was filtered through a Milipore Millex-GN filter with a pore size of 0.2 µm to separate solids or insoluble impurities. The Injection of the prepared samples was accomplished via a PL-AS RT autosampler. The GPC was calibrated with polystyrene calibration standards in a molecular weight range between 162 and 19880 g/mol. The molecular weight distribution was calculated

using Cirrus 3.0 software. The number average molecular weight (Mn), weight average molecular weight (Mw), molecular weight at highest peak (Mp) and the polydispersity (PD) were calculated from the area of the received signal curve.

4.2.5.3 Rotational Viscosimetry

The dynamic viscosity of the pyrolysis oil was determined by a rotational viscosimeter. The RotoVisco 1 from HAAKE GmbH, Germany was used in combination with a Phoenix P1 Circulator for temperature control and RheoWin Pro Software to process the data. The viscosity was measured at 25°C and 40°C by the use of a double gap cylinder sensor DG 42 in accordance with DIN 53544. The measurement was carried out with 4.2 ml oil sample. The whole system was then heated in a water bath to 25°C. After reaching the desired temperature the rotor applied the shear stress with a maximum velocity of 2000 r/min. The program allows including a degassing step prior the actual measurement to remove air bubbles from the oil. After the measurement at 25°C the whole system is heated to 40°C and the procedure repeated. Triplicates, accepted with a standard deviation of less than 1 %, were done for all measurements.

4.2.5.4 Stability

The stability of the oil was evaluated by comparing viscosity and mean molecular weight of the fresh oils (48 hours after production) and oils after accelerated aging. Oasmaa [33] found that heat treatment of the oils at 80°C for 24 hours correlates with 1 year storage at room temperature (20°C). Accelerated aging was done by heating approx. 200 ml oil sample at 80°C for 24 hours in the laboratory oven. The sample vials have to be closed tightly and the lids checked regularly to avoid losses of headspace gases.

4.2.5.5 Solid Content

The solid content was determined using the method proposed by Oasmaa and Peacocke [29]. The pyrolysis oil was dissolved in ethanol and filtered through a Micropore vacuum filtration system. Whatman GF/B Glass Micro Fiber Filters with a max. pore size of 1μm were used as filtration medium. The sample size of pyrolysis oil depends on the expected solid content with the aim to receive around 10 – 12 mg of solids on the filter. Therefore, the sample size for the oils with cyclone separation system was 5 g and

for the oils with hot filtration unit were 100 g. Triplicates were done for all measurements.

4.2.5.6 CHN-Analysis

The elemental analysis was executed by MEDAC Ltd., Surrey, using a CE-440 and Carlo Erba elemental analyser with an absolute accuracy of +/- 0.3 %. The water content of the oils and DIC-liquids was known and the carbon, hydrogen and nitrogen were calculated on a dry basis. The oxygen content was calculated by difference. All measurements were done in duplicates.

4.2.5.7 Heating Value

The heating value depends on the elemental composition and is reported as Higher Heating Value (HHV) or as Lower heating Value (LHV). The HHV refers to the heat released from the fuel during combustion with the original and generated water in a condensed state, whereas the LHV assumes the water in the gaseous state. The heating value can be measured by bomb calorimetry. In this work the HHV was calculated from the elemental analysis data using a formula proposed by Sheng and Azevedo [101], which was found to be the most accurate for biomass fuels.

$$HHV(MJ/kg) = -1.3675 + 0.3137C + 0.7009H + 0.0318O \qquad \textbf{Equation 5}$$

4.2.6 Particle analysis

The Scanning Electron Microscopy (SEM) pictures were accomplished with a Cambridge Stereoscan 60 analyser. The equipment included an Energy Disperse X-Ray analyser for elemental analysis with the designation EDXA 10000 Analyser from Cambridge. Optical microscope pictures were carried out with a Polyver 3-D light microscope from Reichert Jung. In addition CHN-analysis was done as described in 4.2.5.6.

5 Hot filtration test unit

5.1 Introduction

To achieve the aims described in Chapter 1.3, objectives and methodology, it was necessary to design and build a hot filtration test unit for the existing 1kg/h fast pyrolysis system. Based on the literature review on hot filtration the following design parameters were determined:

- Operation temperature of the filter above 420°C to avoid condensation of vapours in the system
- Face velocity of the gas/vapour stream on the candle surface of 1-5 cm/s to represent industrial conditions
- Exchangeable filter candle
- Pressurised reverse jet pulse cleaning system with inert gas (nitrogen) at 600 kPa
- Pre-heating of reverse pulse gas to around 400°C to avoid condensation of vapours during reverse pulse injection
- Mobile system which can be easily connected

With these design parameters a hot filtration system was developed together with CALDO Environmental Engineering, Worcester, which manufactured the filtration unit. A detailed description of the system is given below.

5.2 General description of filtration system

The filtration test unit consists of a filter vessel with 100 mm internal diameter, which is suitable for 1 exchangeable filter candle with 60 mm diameter and up to 600 mm length. The separated char is collected in the char pot below the filter. The filter vessel is heated electrically with temperatures recorded at various measurement points. The differential pressure betweens the raw gas and clean gas side is recorded. The reverse pulse system consists of an Atkomatic 4000 high temperature and quick acting valve which can operate at temperatures up to 400°C. Preheated nitrogen is used as a reverse pulse gas and discharged from a pressurised storage vessel at 400 °C and ca. 600 kPa. The storage vessel and the pipe work to the nozzle are electrically heated and the temperatures monitored. A schematic drawing of the filtration unit is shown in Figure 21 and a picture of the assembled unit in Figure 22.

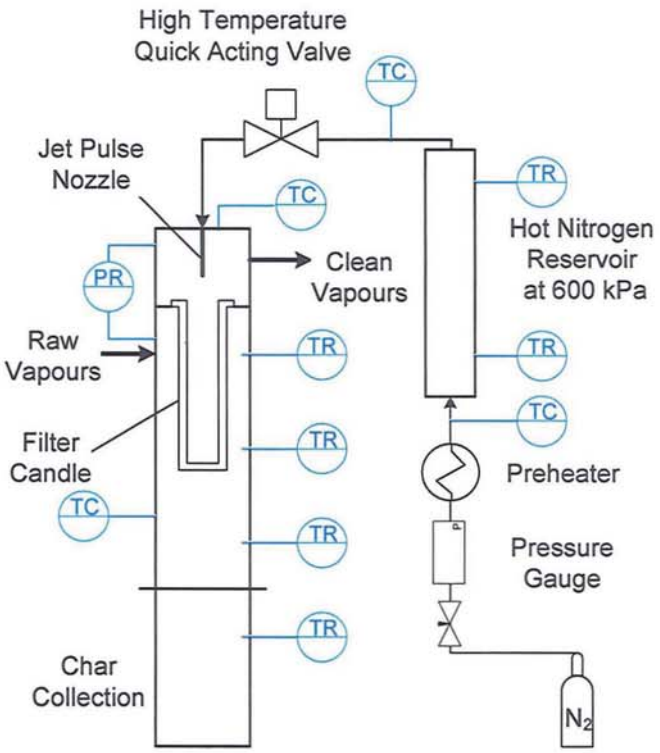

Figure 21: Flow sheet of filtration unit with reverse pulse system

Figure 22: Picture of assembled filtration unit

5.3 Specification

5.3.1 Filter vessel

The filter vessel is made out of a 4 inch i.d. seamless stainless steel 316 pipe with a wall thickness of 3 mm. The vessel is divided into three parts: filter head, filter main body, and char pot. The 3 parts are mounted together with flanges. A detailed technical drawing of the whole filtration system can be found in the attachment. The raw vapours enter at the upper part of the filter main body through a ½ inch pipe. They then have to pass the wall of the filter candle and exit the filter vessel at the filter head. The filter vessel is heated with three Watlow Ceramic band heaters (2x600W, 1x300W) located at the filter main body and the char pot. The upper part of the main body and the filter head is heated by 2 trace heating tapes (2x240W).

Figure 23: Drawing of filter vessel (Drawing: CALDO Eng., modified J. Sitzmann)

5.3.2 Reverse pulse system

The reverse pulse system consists of a pressurised nitrogen reservoir made out of a 2 inch seamless s/steel 316 pipe and a length of 500 mm. It contains a volume of 4 l and is electrically heated by means of 2 Watlow ceramic band heaters (2x300W). The reservoir tank is filled with pressurised nitrogen which can be heated to 500°C with the pre-heater to enable short reverse pulse intervals. The pipe work between the pre-heater, the reservoir tank, the fast acting valve and the filter head is heated with trace heating tapes. The reverse pulse gas is discharged from the reservoir tank via a high temperature quick acting valve (see specifications in Table 2) to the injection nozzle at the filter head.

Table 2: Specifications for high temperature quick acting valve

Manufacturer	Atkomatic
Series No.	4000
Type	Pilot-Piston Solenoid Valve
Pressure	500 psig
Temperature	< 400°C
Position	normally closed
Valve opening time	ca.100 ms
Pipe size	1 inch
Pipe material	s/steel 316

5.3.2.1 Reverse pulse injection

The pressurised nitrogen jet pulse is introduced into the filter candle via the injection nozzle. The jet pulse injection is illustrated in Figure 24. The nozzle has an inner diameter of 10 mm and a length of 100 mm. The distance between nozzle tip and candle inlet is 170 mm.

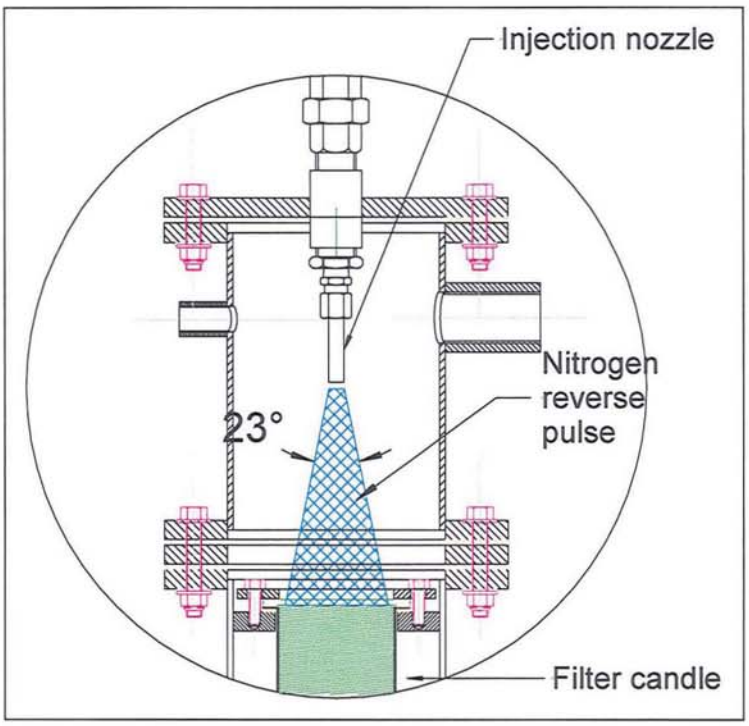

Figure 24: Drawing of reverse pulse injection showing the correlation between angle of discharged flow and distance to nozzle (Drawing CALDO Eng, modified J.Sitzmann)

5.3.2.2 Pressure and temperature control

The location of the thermo-couples (K-Type) and pressure measurement points can be seen in Appendix 1. The mean average temperature of the measurement positions Filter 1, Filter 2, Filter 3 and Filter Head is considered as average filter temperature. The main temperatures were recorded by a Windmill data acquisition system.

The differential pressure drop was measured and recorded manually by an analogue pressure gauge and after Experiment 193 additionally by differential pressure transducer which recorded to the data acquisition system.

5.3.2.3 Volume flow on filter candle

The hot gas stream which passes the filter candle consists of the nitrogen fluidising gas and the pyrolysis product gases and vapours. The amount of nitrogen and non-condensable pyrolysis gases are calculated using the gas meter reading and online GC-Analysis (see 4.2.3.2). The amount of vapours was estimated from the amount of water vapours and organic phase vapours. The water vapours were calculated from the water original in the feedstock and the reaction water. For the amount of organic vapours an

average molecular weight of 80 g/mol was assumed to calculate the volumetric flow rate from the mass of organics produced and throughput. A typical distribution of the gas/vapour stream can be seen in Table 3.

Table 3: Constitution of the gases/vapours product stream leaving the 1 kg/h fast pyolysis unit.

5.3.3 Filter candles

To evaluate the influence of the filter candle materials experiments were carried out using two different types of candles. A Tenmat firefly filter element was used to represent a ceramic candle and a Bekaert Inconel element was used to represent a sintered metal candle. The two types of filter candles are described below.

5.3.3.1 Tenmat firefly ceramic filter candle

The Tenmat Firefly CS1155 is a monolithic ceramic filter candle, produced by Tenmat Ltd, Manchester. CS1155 is a ceramic material which is made of extruded mineral fibre blended with Calcium Silicate (72 wt%), Silica (10 wt%) and starch as organic binder (<10 wt%) [102].The material withstands temperatures up to 1000°C. It is totally incombustible and highly resistant to thermal shock and corrosive environments. The density is 450 kg/m3 and the porosity varies from 85 % to 95 %. The producer claims that the filter elements possess three times the strength of its equivalent ceramic or mineral fibre competitors. The filtration efficiency is higher than 99.9 % (wt/wt).[103] The unused filter candle has a white appearance but the colour changes during heating to a grey-brownish appearance due to the combustion of the organic binder. A picture of the unused candle and a SEM picture of the fibre can be seen in can be seen in Figure 25. The technical data is listed in Table 4. [104]

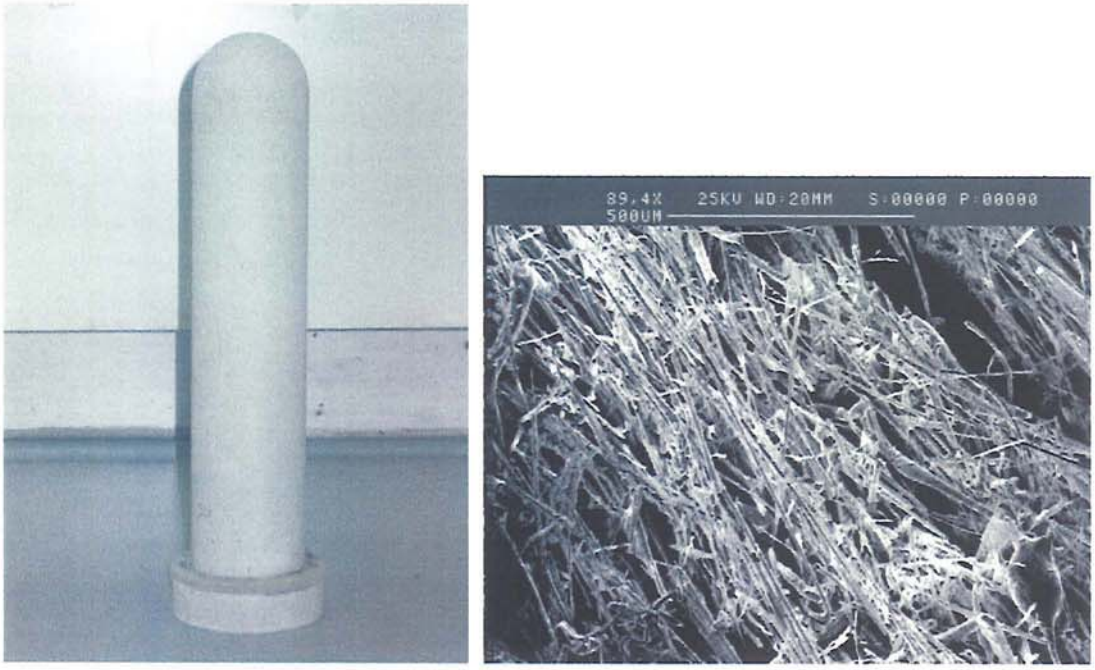

Figure 25: Picture of unused Tenmat firefly candle and SEM-analysis of the fibre structure

5.3.3.2 Inconel filter candle

The metal candle used in this work is made by Bekaert out of a Sintered Metal Fibre (SMF) fleece which is made out of 8 and 22 µm fibres and welded on a support body. The SMF membrane fleece has a high porosity of 87 % which makes it suitable for high gas flow rates. The membrane has a thickness of 0.4 mm and is cleanable with solvents respectively ultrasonic. As it is a very thin membrane with a very low pressure drop it shows good backpulse characteristics. It has a low thermal expansion and is therefore not prone to thermal shock. Additionally, it shows good resistance to mechanical shock. Inconel 601 consists of 58-63% nickel, 21-25 % chrome, 1.4% alumina and the balance to 100% filled with iron. The alloy fibre has a maximum operational temperature of 560°C but can withstand higher temperatures for short time.[82]

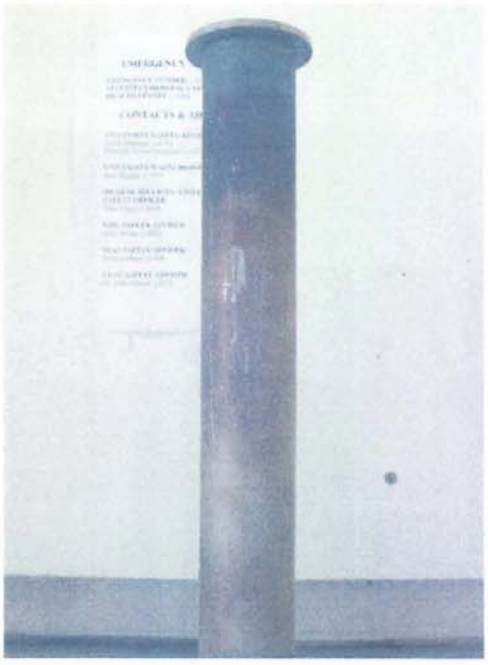

Figure 26: Unused Bekaert Inconel candle

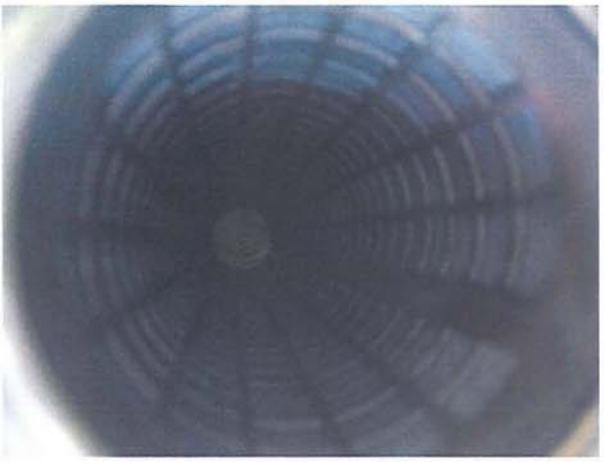

Figure 27: View into the unused Inconel filter candle showing the support cage

Table 4: Properties of the filter candles

Type	Unit	Tenmat Firefly	Bekaert Bekipor SMF
Material		CS 1150	Inconel
Length	mm	305/600	500
Outer diameter	mm	60	60
Inner diameter	mm	40	59.2
Porosity	m^3/m^3	85 - 95	76 - 82
Filter-rating	µm	n.m.	25

6 Preliminary experiments

6.1 Introduction

The experiments were carried out on the 1kg/h fluidized bed fast pyrolysis rig as described in Chapter 4. The experiments are presented with laboratory code numbers which are introduced to identify all the oils produced in laboratory 307. The numbers do not represent the actual amount of experiments carried out for this project.

Beech was used as feedstock for all the experiments. The particle size distribution of the feedstock is given in Chapter 0. The feedstock was oven dried to achieve equal moisture content and to avoid phase separation of the condensates due to high water content. For the Experiments 193 and 227 the feedstock was used as received with a moisture content of around 10 wt% to produce oils with realistic industrial conditions. The temperature in the fluidised bed reactor was set at around 500°C. Quartz sand was used as a fluidising medium with a particle size of 500-850 µm for the first experiments and was later increased to 600-850 µm to reduce the entrainment of the sand into the product stream. The feedrate of the metering screw was calibrated to feed approx. 1kg/h of feedstock (including moisture content). The flowrate of fluidising Nitrogen was set at ca. 40l/min which means around 3 times the minimum fluidising velocity of the sand bed. The entrainment flow of nitrogen was set at approx. 6 l/min, which resulted of a total nitrogen flow of approx. 46 l/min (STP). The minimum run duration was 1 hour to achieve a reliable mass balance. The residence time of the vapours in the hot environment was approx. 1.1 s for experiments with Standard set up and increased to approx. 4.4 s for the filtration experiments. An overview of the experimental parameters can be seen in Table 5.

Table 5: Overview of process parameters of preliminary experiments

Experiment No.		88	190	85	101	160
Description		Standard Rep1	Standard Rep2	Empty sec. reactor	Sec. reactor with char	Empty filter vessel
Date		03.02.05	22.09.06	25.01.05	03.03.05	18.05.06
Test duration	hh:mm	01:09	01:40	00:58	01:00	01:06
Feedstock		beech	beech	beech	beech	beech
FS converted	g	1156	1589	1097	1245	1575
Feedrate	g/h	1005	954	1135	1266	1432
Moisture content	wt%	0.91	2.86	1.23	0.54	1.07
Ash content	wt%	0.88	1.00	0.88	0.88	0.88
Particle size	µm	<2000	<2000	<2000	<2000	<2000
Reactor sand bed	µm	500-850	600-850	500-850	500-850	600-850
Temperature	°C	480	500	500	500	500
Flowrate gases	l/min (STP)	46.6	47.4	47.4	41.4	49.6
Residence time vapours	s	1.1	1.0	1.6	1.4	3.6

6.2 Feedstock characteristics

Beech wood (lignocell – Grade HBK 750-200) supplied by J Rettenmaier & Söhne GmbH, Germany was used as feedstock. The feedstock is commercially available as raw material for food smoking and was already used by a number of researchers which enables comparison of experimental results. The CHN-Analysis and higher heating value is given in Table 6.

Table 6: Elemental analysis on dry basis and Higher Heating Value (HHV) of beech feedstock. (Oxygen was calculated by difference)

	C	H	N	Ash	O		HHV
wt %	48.4	6.0	<0.1	1.0	45.5	MJ/kg	19.2

The particle size distribution was declared by the manufacturer to be between 720–2000 µm. However due to the fibrous character of wood the particles do not represent a spherical or even cubic form but have a needle like tubular shape. A picture of a fraction of the beech particles can be seen in

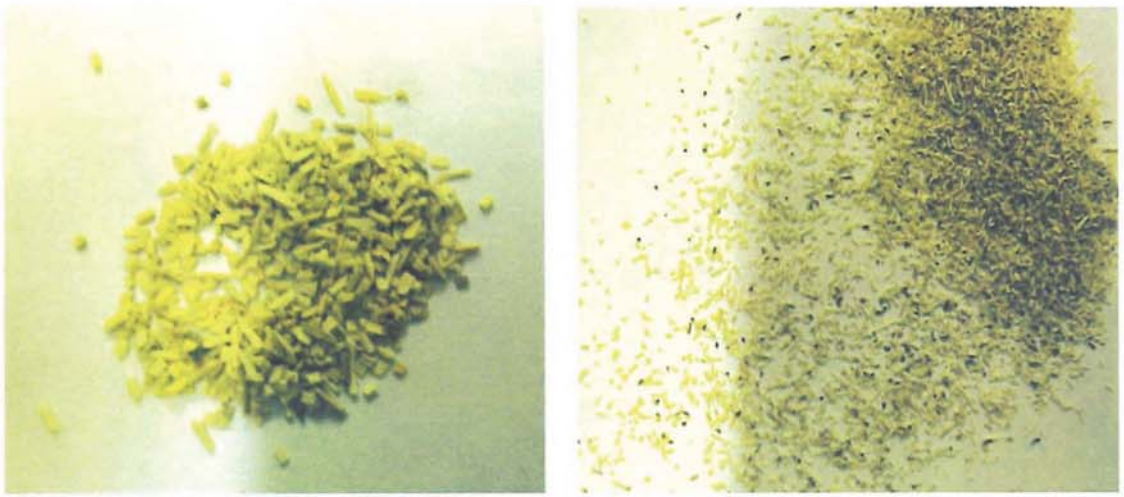

Figure 28: Pictures of the beech feedstock to illustrate the shape of the particles

6.3 Standard experiments

6.3.1 Experiment 88: Standard run, 1st replicate

Experiment 88 was the first conventional fast pyrolysis run on the 1kg/h fast pyrolysis unit carried out with two cyclones in series for char separation followed by the condensation system. The experiments with cyclone separators and no additional secondary reactor or filtration system are referred to as standard experiments. The specific parameters for the experiment were listed in Table 5. The experiment lasted for 1h 9 min without difficulties. 1156 g of beech-wood with a moisture content of 0.91 wt% and an ash content of 0.88 wt% were thermo-chemically converted. The fluidising bed reactor was operated with quartz sand with a particle size between 500-850 µm and an average temperature of approx. 480°C. The flowrate of fluidising gas and product vapour/gas was calculated as 46.6 l/min (STP) which resulted in a residence time of the vapours/gases in the hot environment of approx. 1.1 s. A simplified flow sheet of the experimental set-up can be seen in Figure 29.

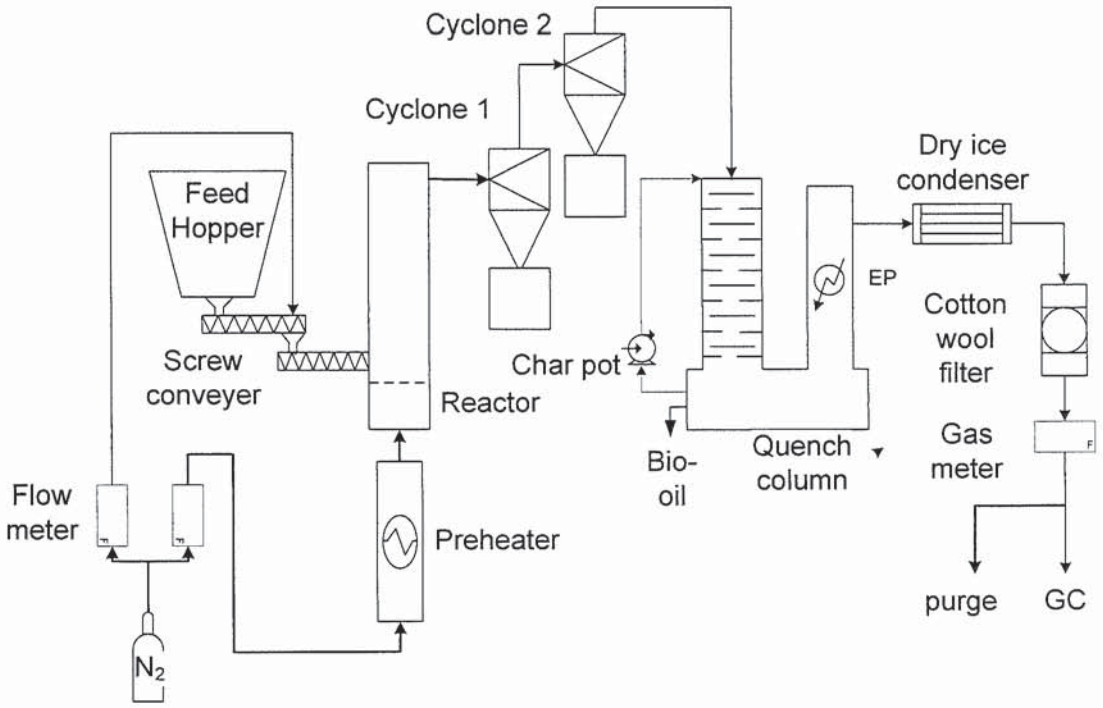

Figure 29: Flowsheet of 1kg/h pyrolysis rig with standard set-up with 2 cyclones

The results of the mass balance can be seen in Table 8. The total liquid yield on a dry basis was 66.4 wt% of which 95.7 % was recovered as bio-oil in the quench column and 4.3 % was recovered in dry ice condenser and cotton wool filter. The bio-oil was a single phase dark brown liquid with a water content of 17.1 wt%. The Dry-Ice-Condenser (DIC) fraction consisted of a yellow watery fraction with 68.8 wt% water and some light organics.

Figure 30 shows the gas analysis during the course of the experiment. It can be seen that the gas produced achieves stable values after approx. 15 min. The reduction in the end was caused by a reduction in feed-rate.

Figure 30: Gas analysis of experiment 88, standard run

The overall char yield resulted in 14.5 wt% of which 96.7 % was found in char pot 1, 0.6 % in char pot 2 and 2.7 % as char fines in the pyrolysis oil. The solid content of the pyrolysis oil was 0.56 wt%. Examination of the second cyclone revealed that the pipe transporting the char into the char pot was blocked. This blockage was caused by the tendency of the char fines to agglomerate and form clusters with extremely low bulk density. In the absence of coarse char particles, which would push the agglomerates down, these char fines clog the pipe tube.

6.3.2 Experiment 190: Standard run 2nd replicate

An additional experiment with a standard set up of the 1kg fast pyrolysis rig was done in September 2006. The purpose of the experiment was to have a replicate standard run and to produce fresh oil for the newly developed analytical methods like GPC and rotational viscosimetry which were not operating at the time of the first experiment.

The experiment lasted 1h 40 min and 1589 g beech wood was processed, resulting in a feed-rate of 954 g/h. Rettenmayer beech in a particle size between 750-2000 µm was used. The moisture content of the feedstock was 2.86 wt% and the ash content 1.00 wt%. The average reactor temperature was 500°C with quartz sand in a particle size between 600-850 µm as fluidising medium. The flow-rate of the product stream was 47.7 l/min (STP) which resulted in a residence time of the vapours in the hot environment of 1.0 s. A summary of the test parameters of the experiment is given in Table 5.

Due to the blockage of the transport pipe between the 2nd cyclone and the char pot, the 2nd cyclone was modified with a grater stick to remove the blockage manually. During the experiments the feeding was interrupted every 20 min. to allow the cyclone to be cleaned.

The total liquid yield resulted in 64.7 wt% with 88.6 % recovered as pyrolysis oil in the quench column and 11.4 % recovered in the dry ice condenser part. The pyrolysis oil had a water content of 15.5 wt%. The reduction of water in the pyrolysis oil can be explained by a reduction of condensation efficiency of the quench column. The cooling jacket of the quench tower is cooled with water which is taken from a water reservoir on the roof of the building. For the 2nd replicate of the standard experiment the water temperature was higher (12°C compared with 6°C at the first one) and therefore the cooling efficiency in the quench column decreased. This resulted in more of the water and light organics being transferred into the DIC-fraction, leading to an increase of the DIC-fraction and a decrease of water in the pyrolysis oil fraction.

The total char yield resulted in 14.6 wt%. The char was distributed in char pot 1 (97.0 %), char pot 2 (1.3 %) and in the oil (1.8 %). The solid (char) content of the pyrolysis

oil was analysed with 0.44 wt%. It can be seen that the cleaning of the 2nd cyclone had some effect by increasing the char collected in char pot 2 and decreasing the solid content of the oil.

6.3.3 Char characterisation

The particle size distribution of the char particles found in charpot 1 and from the beech particles were analysed by sieving. A comparison of the cumulative particle size distribution of the feedstock and the char from charpot 1 can be seen in .The graph gives the weight % of particles which were not passing the mesh.

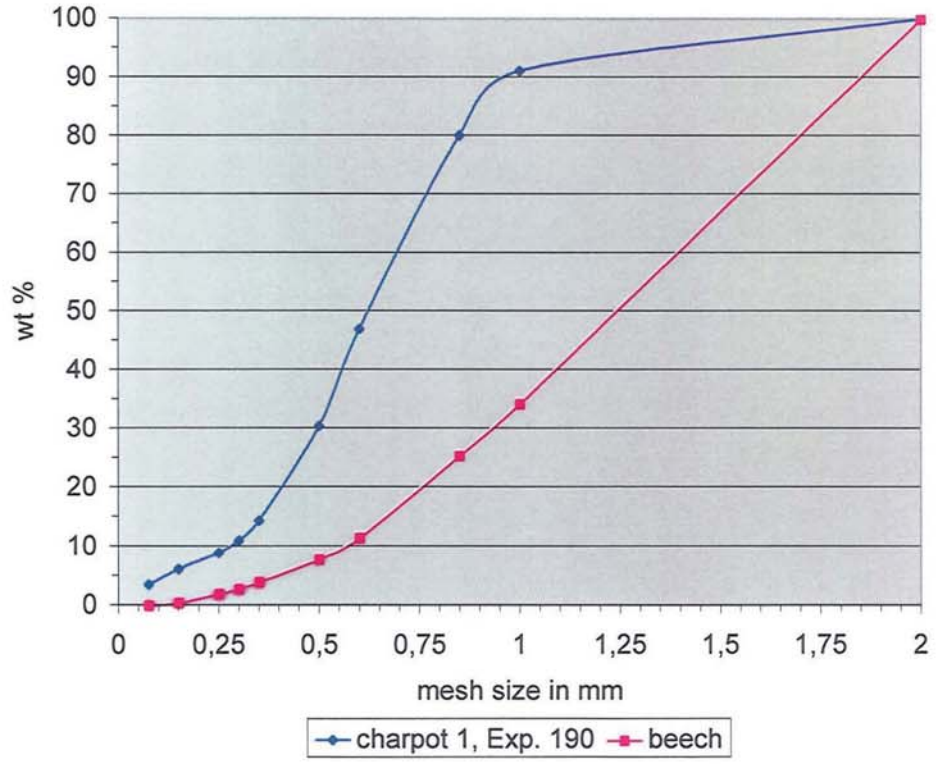

Figure 31: Comparison of the cumulative particle size distribution of char and beech

Ash analysis of the char sample turned out to be difficult due to sand particles which were entrained from the fluidising bed. It was not possible to remove the sand particles from the char sample with 100 % reliability and a couple of sand particles were spoiling the gravitational ash determination due to their high density. However it was possible to gain elemental analysis of coarse char particles (> 500 µm) of char pot 1 with calcium, potassium, magnesium and natrium analysed as representative minerals (see Table 7).

Table 7: Elemental analysis of char particles found in char pot 1

ELEMENT	C	H	N	Ca	K	Mg	Na
Exp. 85 (wt%)	72.09	3.22	0.32	1.83	0.26	0.25	0.01
Exp. 88 (wt%)	69.38	3.80	0.10	1.44	1.02	0.23	0.06

All of the char fines found in char pot 2 were below 100 μm, which made analysis by sieving impossible. Figure 32 shows a SEM picture of these char fines to give an impression of the particle size distribution. It can be seen that the bulk of particles are below 20 μm and that the particles still show the morphology of wood tissue. EDAX-Analysis was made of the areas specified in the picture to determine the nature of the particles. It was found that particle 1 contained a large amount of nickel and chrome and was therefore identified as carbonised metal impurity. All the other areas contained more than 90 % carbon and minerals original present in the parent material like silicate, potassium, chlorine, magnesium and sodium.

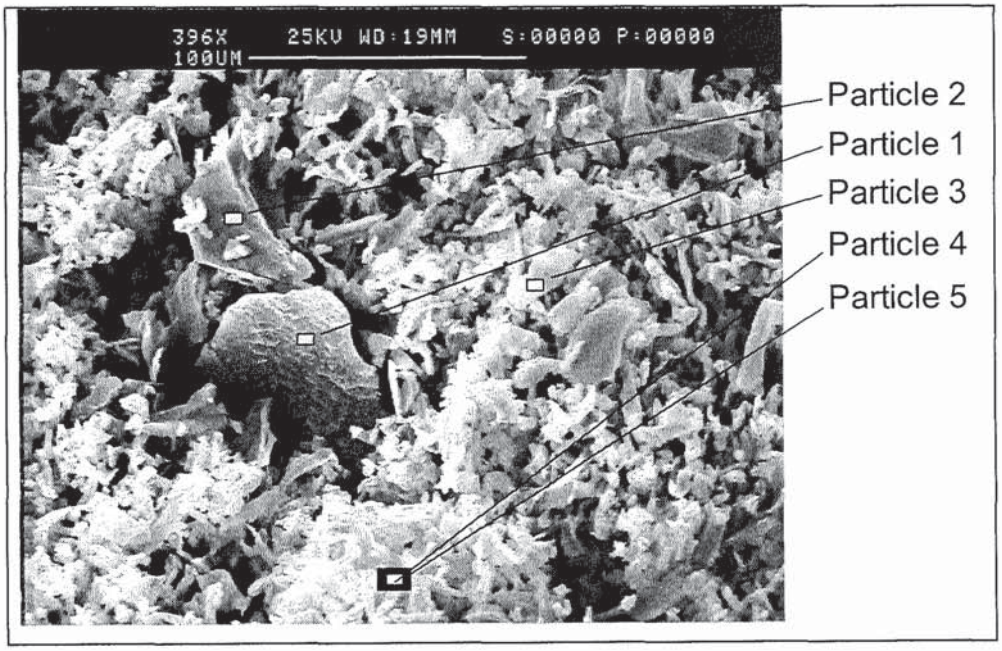

Figure 32: SEM picture of char/solids recovered in char pot 2

6.3.4 Discussion of char collection and characteristics

The 2nd serial cyclone is prone to blockage due to low density clusters of char fines which do not fall into the char pot by gravity. Even with a modified cyclone, with a manual fettling tool to remove the blockage, a reduction of solid content in the oil below 0.4 wt% is not possible.

97 % of the char is collected with the first cyclone. The escaping 3 % is either collected in the second char pot or ends up in the oil. The analysis of the particle size distribution shows a reduction of particle size of more than 30 % compared with the particle size of the parent material. Especially the particle size below 70 micron increases 5 times which cannot only be attributed to shrinkage but means some particle size reduction by abrasion inside the reactor. Additionally, the char fines found in the 2nd charpot and in the oil, show sharp edges, so that it can be assumed that their origin is due to abrasion rather than aerosols or soot derived from secondary vapour reactions. Chemical analysis of the char particles by EDAX show that beside one metal particle (Particle 1) all the other particles analysed contain more than 90 % carbon beside oxygen and mineral matter.

6.4 Experiments with secondary reactor

Figure 33 shows the flow sheet of the experimental set up with secondary reactor. The fixed bed secondary reactor was placed above the primary cyclone. After the secondary reactor the product stream was directed to the quench system. The secondary reactor was heated using trace heating tape to 500°C. The secondary reactor contained two stainless steel meshes to keep the fixed bed in place. A technical drawing of the fixed bed reactor can be found in the Appendix.

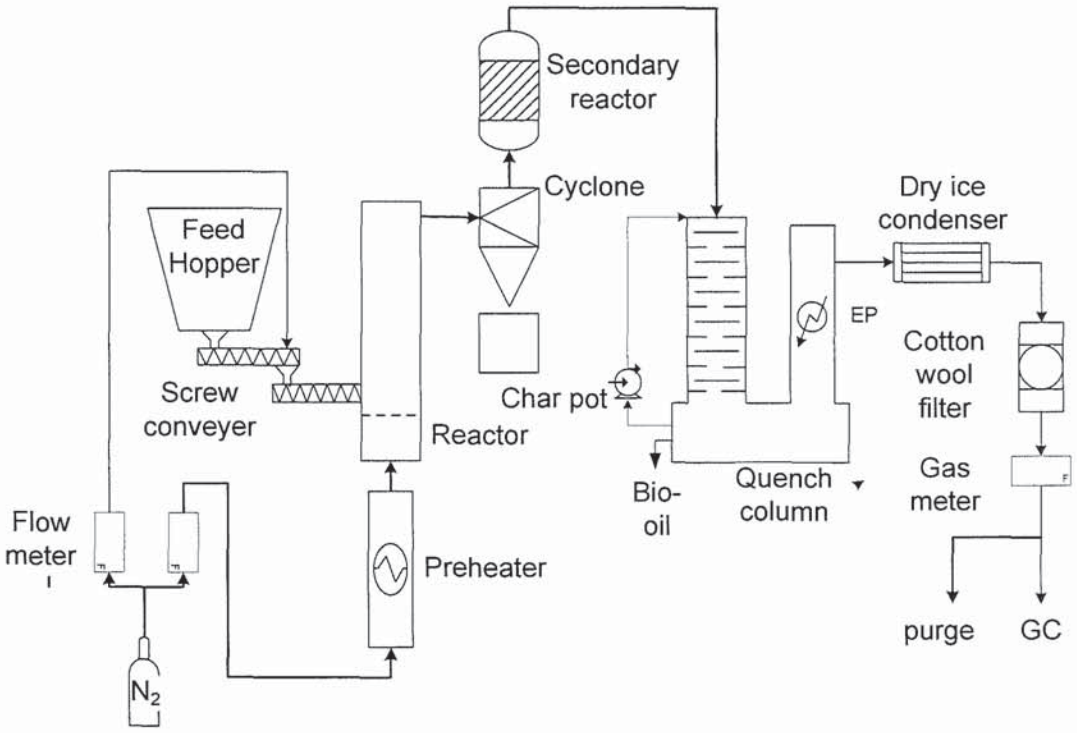

Figure 33: Flow sheet of experimental set up with secondary reactor

6.4.1 Experiment 85: Run with empty secondary reactor

To evaluate the influence of secondary vapour cracking of fast pyrolysis vapours on char a fixed bed secondary reactor was designed as described above. This experiment was carried out with empty secondary reactor for comparison with the char filled secondary reactor (Experiment 101). However, the secondary reactor was not fully empty as it contained two stainless steel meshes (see Appendix) to hold the fixed secondary bed in place. The experiment lasted 58 min in which 1097 g of beech was converted. The test parameters of the experiment can be seen in Table 5. The temperature in the fluidising bed reactor as well as in the secondary reactor was 500°C. The diameter of the secondary reactor resulted in a gas velocity of 26.9 cm/s inside the reactor, which resulted in an additional residence time of the hot vapours of 0.6 s.

6.4.2 Experiment 101: Run with fixed char bed in secondary reactor

Run 101 was carried out to investigate in the influence of secondary cracking of fast pyrolysis vapours on char. Therefore, a fixed secondary reactor was placed downstream of the cyclone (see Figure 33). The secondary reactor was filled with a fixed bed of beech char (taken from Experiment 88) in a particle size between 500 and 1000 µm. The fixed bed had a diameter of 100 mm and a height of 30 mm. The face velocity in the

secondary reactor was 22.0 cm/s, which makes the contact time of the vapours comparable with a filter cake of 3 mm at an expected face velocity of 2.2 cm/s in the filtration unit. The temperature in the fluidised bed reactor and the secondary reactor was set at 500°C. The duration of the experiment lasted 60 min in which 1245 g of beech was converted. A summary of the test parameters can be seen in Table 5. The additional residence time of the gases/vapours in the secondary reactor was 0.7 s which resulted in a total residence time of the gases/vapours in hot environment of 1.7 s.

It can be seen in Figure 34 that the pressure difference over the secondary reactor increased constantly up to 20 kPa after 60 min of experiment duration. This can be explained by the separation of char fines in the fixed bed which acts as granular filter. The char fines fill the gaps between the coarse char and increase the pressure difference. The result also shows that the system is able to handle a significant pressure increase without affecting the performance of the fluidised bed.

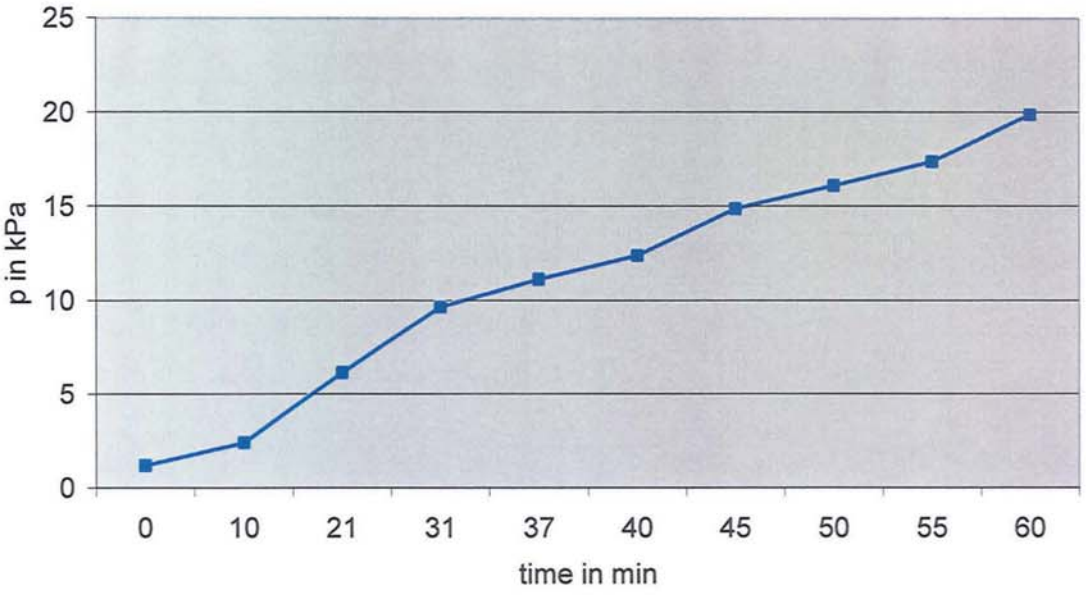

Figure 34: Change in differential pressure over fixed char bed in secondary reactor (Run 101)

The graph of the online gas analysis of experiment 101 is shown in Figure 35. It can be seen that the amount of produced gases increases for all of the detected gases. The increase of gas production can be attributed to an increase of contact intensity due to pressure increase over the secondary reactor.

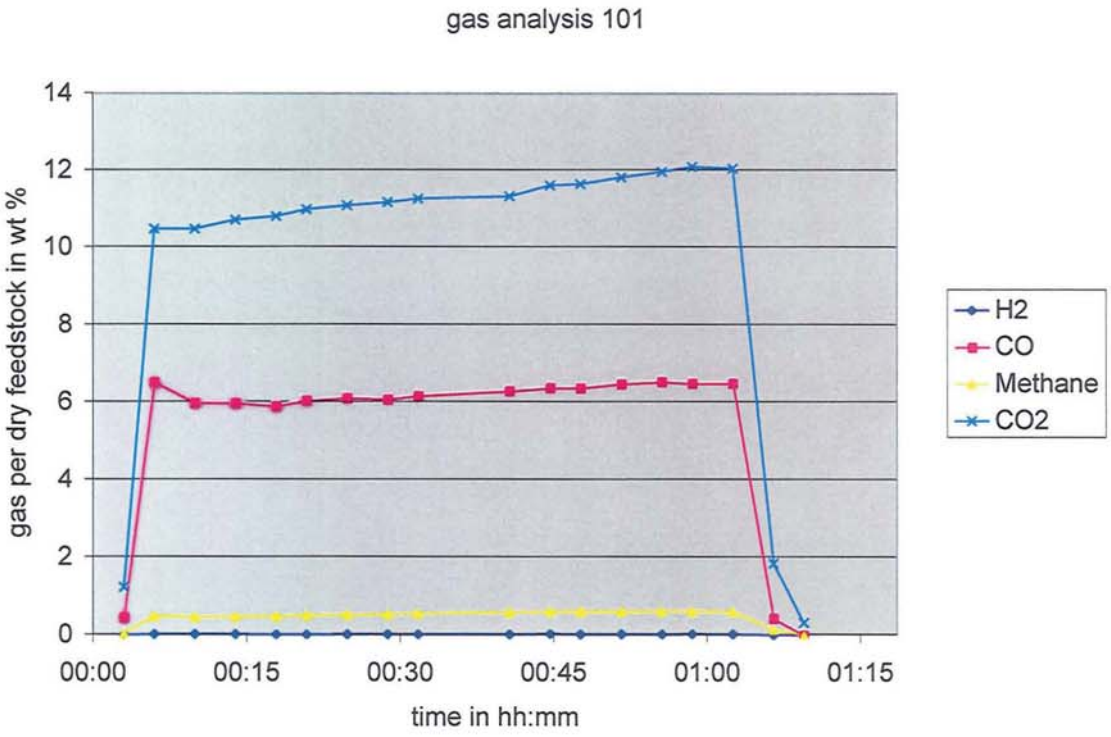

Figure 35: Online gas analysis for experiment 101

6.5 Experiment 160: Run with filtration unit without filter candle

In experiment 160 the filtration unit was installed without filter candle to investigate in secondary vapour cracking due to extended residence time but without vapour cracking on the filter cake. A cyclone was put upstream of the filtration unit to remove the bulk of entrained char. The experiment lasted 1h 6 min during which time 1575 g of beech feedstock was converted. The pyrolysis reactor temperature was set at 500°C and the temperature of the filter unit was on average 450°C. The filtration unit increased the residence time of the hot vapours about 3.0 s to a total residence time of inside the reactor, pipework and filter unit of 3.9 s.

6.6 Results and discussion of preliminary experiments

6.6.1 Mass balance

Table 1 shows the mass balances of the standard experiments with cyclone separators as well as the preliminary experiments which were made to evaluate the influence of the extended residence time and the additional vapour cracking over a fixed char bed.

Subsequently the results are discussed regarding the development of the different product fractions organic liquid yield, reaction water, char and non-condensable gases.

Table 8: Mass balances from the Standard experiments, experiments with secondary reactor and the experiment with empty filtration vessel. Calculations in wt% based on dry feedstock

Experiment No.		88	190	85	101	160
Description		Standard Rep1	Standard Rep2	Empty sec. reactor	Sec. reactor with char	Empty filter vessel
Yield in wt%	Organics	55.6	53.4	53.7	46.8	53.3
	Water	10.8	11.3	10.8	13.2	11.3
	Char	14.5	14.6	15.4	16.8	14.2
	Gas	14.6	16.0	15.9	18.6	15.7
	Closure	95.4	95.3	95.8	95.4	94.6

6.6.1.1 Mass balance closure

The mass balance closure for the preliminary experiments varies between 94.6 wt% and 95.8 wt%. The low mass balance closure can be attributed to the very high dilution of vapours in the fluidising nitrogen and non-condensable product gases which reduces the efficiency of the condensation system. Therefore, it can be assumed that around 4 wt% of light organics and water vapours are lost with the gases and 96 wt% can be seen as an acceptable mass balance closure.

6.6.1.2 Organic liquid yield

The average standard run, calculated as the mean average of the 2 replicates, has an organic yield of ca. 54.5%. The results in organic liquid yield are comparable with mass balances from the literature[45] [65], where organic yields between 55 and 59 wt% are reported. The slightly lower yields can be explained by the smaller particle size (350-500 µm) of the feedstock which is used in small scale laboratory experiments. Due to the small particle size the heat transfer into the biomass particle is better and therefore more of the volatiles can evaporate (see 2.2). Additionally, remaining char particles inside the reactor which are not entrained in the gas flow due to their particle geometry cause a layer of char floating on top of the fluid bed. This char layer can cause secondary cracking of the pyrolysis vapours and increase the amount of non-condensable gases.

The experiment with empty secondary reactor at 500°C showed with 53.7 wt% organic yield no significant reduction and the experiment with empty filter vessel at 450°C only a slight decrease to 53.3 wt%. It can be concluded that an extended residence time at 500°C will not cause significantly more decomposition of the molecules. Especially if there is a proper heat transfer inside the reactor, so that all of the particles and primary vapours have experienced that temperature, it can be expected that there will be no more significant additional thermal cracking of chemical bondages.

However, the presence of a catalytic active material like char decreases the organic liquid yield substantially. This can be seen in the experiment with char inside the secondary reactor which decreased the organic yield around by 15 % from 54 wt% to 47 wt%. An explanation for this additional secondary vapour cracking is that some alkali metals like potassium, which can be found in char, reduces the activation energy for the decomposition of biomass derived primary tars (see 2.4.2).

6.6.1.3 Reaction water

The water yield showed constant values in the range of 10.8 and 11.3 wt% for the standard experiments and the experiments with extended residence time. In comparison the yield of reaction water showed an increase to 13.2 wt% for the experiment with char in the secondary reactor. It can be concluded that secondary vapour cracking over char caused the formation of additional water.

6.6.1.4 Char

The amount of char showed constant values between 14.2 and 14.6 wt% for the standard runs and the run with empty filter vessel but showed a slight increase to 15.4 wt% at the experiment with empty secondary reactor and a further increase to 16.8 wt% with the char filled fixed bed secondary reactor. As the amount of char recovered in the secondary reactor was around 0.1 wt% the increase of char yield in that order of magnitude cannot be attributed to additional secondary char formation in the secondary reactor. It is possible that an increase in pressure causes more vapours to get pushed down into the char pot where some of them condense and increase the amount of volatiles in the char.

6.6.1.5 Gas yield

The gas analysis showed no significant increase of the production of non-condensable gases due to the extended residence time in comparison with the standard experiments. The values for these experiments range from between 14.6 and 16.0 wt%. The experiment with the fixed char bed in the secondary reactor shows an increase of incondensable gases to 18.6 wt% which can be attributed to catalytic cracking of the gases on the char surface and/or on the alkali metals on the char.

6.6.2 Solid content

The solid content of the pyrolysis oil recovered at the Quench vessel was analysed by dissolving the oil in ethanol and subsequently filtering it (see Chapter 4). The results of the solid content of the standard experiments, experiments with secondary reactor and the experiment with empty filter vessel are presented in Table 9.

Table 9: Solid content of pyrolysis oil produced with cyclone separation system

Experiment No.	88	190	85	101	160
Description	Standard Rep1	Standard Rep2	Empty sec. Reactor	Sec. reactor with char	Empty filter vessel
Solid content [wt %]	0.56	0.44	0.27	0.12	0.28

It can be seen that the solid content for oil produced by the standard set up with two cyclone separators in line is 0.56 wt% respectively 0.44 wt%. With the empty secondary reactor after the primary cyclone it was already possible to reduce the solid content to 0.27 wt%. The unfilled secondary reactor contains two stainless steel meshes to hold the fixed bed in place. These meshes acted as a filter and were able to remove already some char fines from the gas stream. The experiment with the char filled secondary reactor resulted in 0.12 wt% solid content of the produced oil. This shows that the fixed char bed additionally improved the filtration behaviour of the secondary reactor which can be attributed to in-depth filtration of the fixed char bed and surface filtration on the lower mesh. In addition, during the experiment with the empty filtration vessel the solid content was reduced to 0.28 wt% compared with the standard experiments. This can be explained by the abrupt expansion of the pipe diameter and therefore decrease of gas velocity during entering the filtration vessel which leads to some separation by gravity.

7 Filtration Experiments

7.1 Introduction

In total 5 experiments with the filtration system were carried out. An overview of the process parameters and experimental set-up of the filtration experiments is given in Table 10. For three experiments the filtration system replaced the cyclone separators and the full char load was brought to the filter candle. In these experiments a Baekert Inconel candle (Exp. 157) and a Tenmat Firefly Ceramic candle (Exp.161 and 193) were used. Furthermore, one experiment was executed with precoating the filter candle (Baekert Inconel) with Aeroxide (Exp. 191) and one experiment was commenced with one cyclone separator prior a Tenmat firefly candle (Exp. 227).

With the exception of experiment 227 the process parameters in the fast pyrolysis unit were kept equal for all experiments. Rettenmayer beech was used as feedstock and the target for the reactor temperature was 500°C with sand as fluidising medium. Experiment 227 was commenced in the framework of another project which made it necessary to use mixed softwood as feedstock and lower temperatures. A description of the experiments can be found in the following paragraphs.

Table 10: Overview of process parameters of the filtration experiment with jet pulse regeneration system

Experiment No.	157	161	193	191	227
Description (Candle type + Set-up)	Inconel candle	Tenmat candle Rep1	Tenmat candle Rep2	Inconel candle + pre-coat	Tenmat candle + cyclone
Date	06.04.06	31.05.06	23.11.06	03.10.06	24.08.07
Test duration [hh:mm]	02:20	03:03	06:44	01:35	02:45
Feedstock	beech	beech	beech	beech	softwood
Feedstock conv. [g]	2287	3312	6155	1509	2251
Feed-rate [g/h]	980	1086	914	953	818
Moisture content [wt%]	1.07	2.68	10.30	3.09	10.13
Ash content [wt%]	0.88	1.00	1.00	1.00	0.29
Particle size [µm]	<2000	<2000	<2000	<2000	<2000
Particle size bed [µm]	500-850	600-850	600-850	600-850	600-850
Temperature [°C]	500	500	500	500	450-470
Flowrate [dm^3/min]	45.6	44.3	44.6	41.4	47.9

Figure 36: Picture of the experimental set-up showing the 1kg/h fast pyrolysis reactor with filtration unit

7.2 Experiment 157: Filtration run with Inconel filter candle

7.2.1 Test parameters

Experiment 157 was the commissioning run of the hot filtration test unit using a sintered Inconel filter candle (O.D: 60mm, length: 500 mm, Pore size: 20 µm). The filtration unit was placed between the reactor and the quench system of the 1kg/h pyrolysis test rig as described in 4.1. A detailed flow sheet of the process is given in Figure 37. An overview of the test parameters gives Table 10. The experiment lasted 2h 20 min in which 2287 g of feedstock was converted. The pyrolysis reactor was set at 500°C and the average temperature in the filtration unit was 450°C. The surface area of the filter candle was 943 cm^2 which resulted in a face velocity of the gases of 2.02 cm/s. During the experiment 2263 g dry beech feedstock was converted which means 2.40 g/cm^2 feedstock per filter area.

The mass balance resulted in 62.2 wt% of liquid yield, of which 92 % or 1315g was recovered in the quench column as Pyrolysis oil and 8 % was collected as DIC-liquid.

The Pyrolysis oil was single phase with a water content of 17.1 wt% and the solid content was analysed with 0.15 wt%.

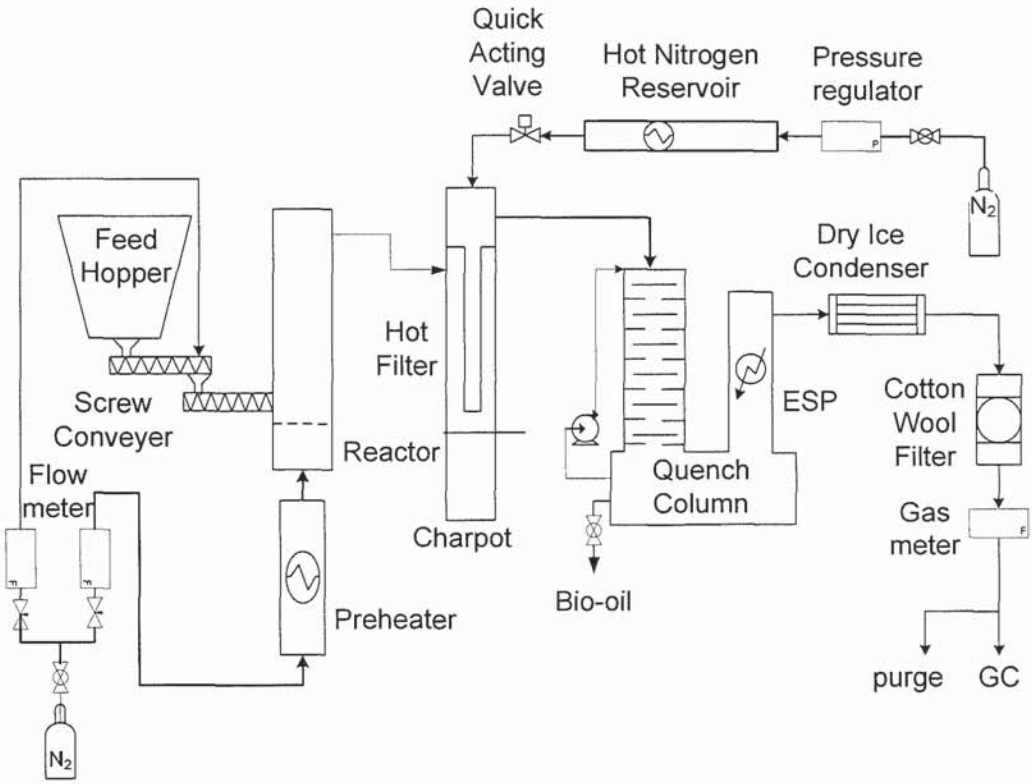

Figure 37: Flow sheet of 1 kg/h fast pyrolysis rig with filtration test unit

7.2.2 Differential pressure over filter candle

The progress of the pressure course is summarised in Figure 38. It can be seen that the initial pressure drop of the Inconel candle is 0.6 kPa. As fast pyrolysis begins the pressure increases to 0.8 kPa due to the development of product gases and vapours. There is then a continuous slow increase of pressure for 40 min. to 1.1 kPa. The pressure drop increased to a pressure difference of 1.45 kPa after 1 hour when the reverse jet pulse was initiated. The reverse pulse resulted in a reduction of pressure drop to 0.97 kPa indicating a successful filter cake detachment. The filtration time reduced to 35 min when the pressure drop reached again 1.45 kPa and the second reverse pulse was introduced. The second reverse pulse achieved a good pressure drop recovery resulting in a differential pressure of 0.8 kPa. After further 35 min the pressure drop again reached 1.45 kPa and the 3rd reverse pulse was initiated. This time only a small pressure reduction was achieved and the following 2 additional reverse pulses had no effect.

Afterward the experiment was stopped, the rig dismantled and the filter candle inspected.

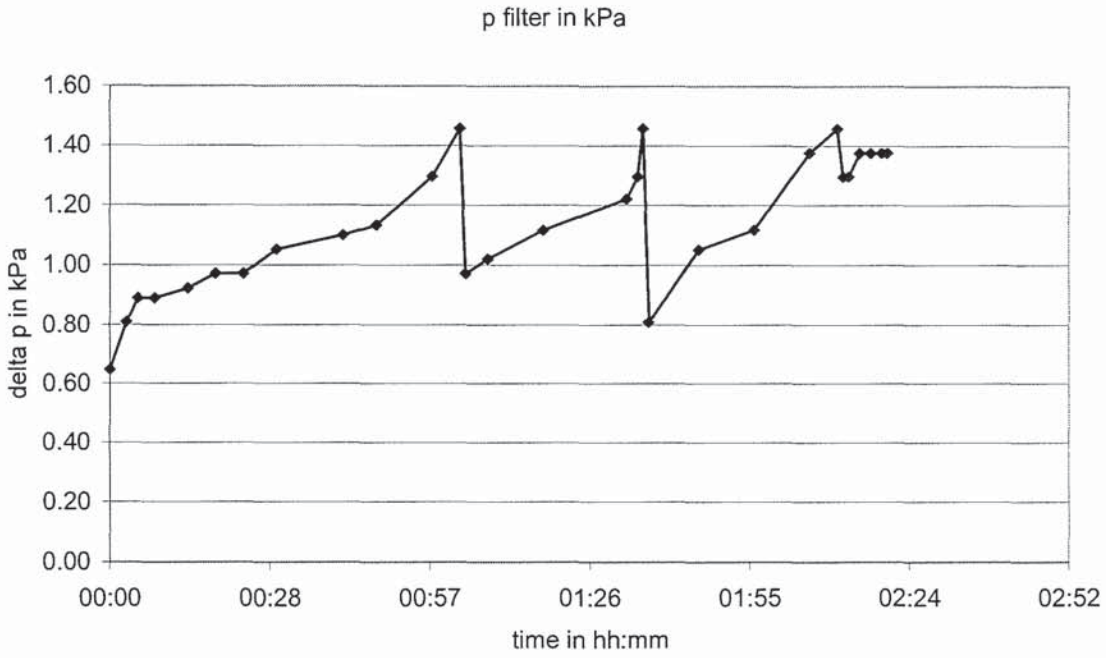

Figure 38: Course of differential pressure over the filter candle

7.2.3 Filter candle examination

A picture of the used filter candle is shown in Figure 39. The examination of the filter candle revealed that a permanent filter cake of about 2 mm thickness remained on the candle. The weight of the filter cake was 16.53g, which results in an area load of char of 0.018 g/cm^2 at the filter candle. The filter cake showed round areas of around 3-8 mm diameter of patchy cleaning distributed over the whole candle but with higher frequency on the closed filter end where also a larger patch was removed. The filter cake contained fine char with a particle size below 200 µm (see 9.2.1). The coarse char particles were not adhering to the filter candle but had fallen into the char pot as a result of gravity. The filter cake could easily be removed by brushing the char off.

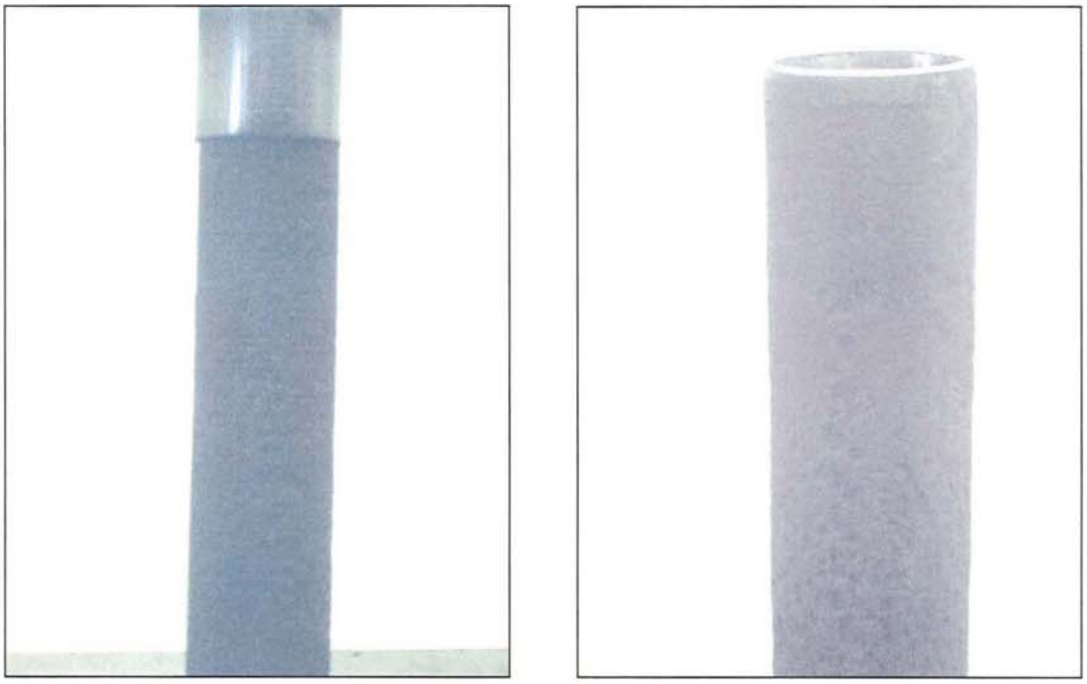

Figure 39: Pictures of used Baekert Inconel filter candle (experiment 157)

7.3 Experiment 161: 1st Filtration run with Tenmat firefly candle

7.3.1 Test parameters

For the second Filter experimented with a Tenmat firefly ceramic candle. The outer diameter was 60 mm and the length of the candle was 355 mm. A description of the filter candle can be found in Chapter 5.3.3. The filtration unit replaced the cyclone separators, as in the experiment before (see Figure 37), with the full char load in the gas stream. The experiment lasted for 03 h 03 min during which 3312 g of feedstock was converted. The reactor temperature of 500 +/- 5 was kept continuously constant for the whole duration of the experiment. The temperature in the filtration unit was set at around 450°C and varied between 420°C and 450°C at the different heights of the filter vessel. The face velocity of the gases was calculated with 44.3 l/min (STP), which resulted in a face velocity on the filter candle of 3.26 cm/s.

The reverse pulse was injected online with nitrogen at 400°C and 550 kPa in the pressure reservoir. During the course of the experiment three reverse pulses were injected. The course of the differential pressure on the filter candle can be seen in Figure 38

The mass balance resulted in 61.3 wt% of liquid yield, of which 92 % or 1892 g was recovered as pyrolysis oil in the quench column and 8 % was collected as DIC-liquid. The pyrolysis oil was single phase with a water content of 15.8 wt% and the solid content was analysed with 0.008 wt%.

7.3.2 Differential pressure on filter candle

The initial pressure drop of the Tenmat candle at a flowrate of nitrogen and product gases of 44.3 l/min (STP) was 1.25 kPa. To avoid the patchy cleaning of very small patches as experienced in Exp. 157, it was decided to allow a thick and dense filter cake to build up, before introducing the first cleaning pulse. The aim of this decision was to have a higher resistance to flow on the filter cake and therefore create higher cleaning forces and detach the cake in large patches. After 2 hours and at a differential pressure of 2.8 kPa the first reverse pulse was injected. The reverse pulse was injected online against the gas flow with 550 kPa reservoir pressure. The cleaning pulse resulted in a reduction of pressure drop to 2.5 kPa. After another 50 min of filtration time and at a differential pressure of 3.1 kPa a second and a third reverse pulse was injected but without monitoring a reduction of differential pressure. The experiment was stopped after 3 hours and the filter candle inspected.

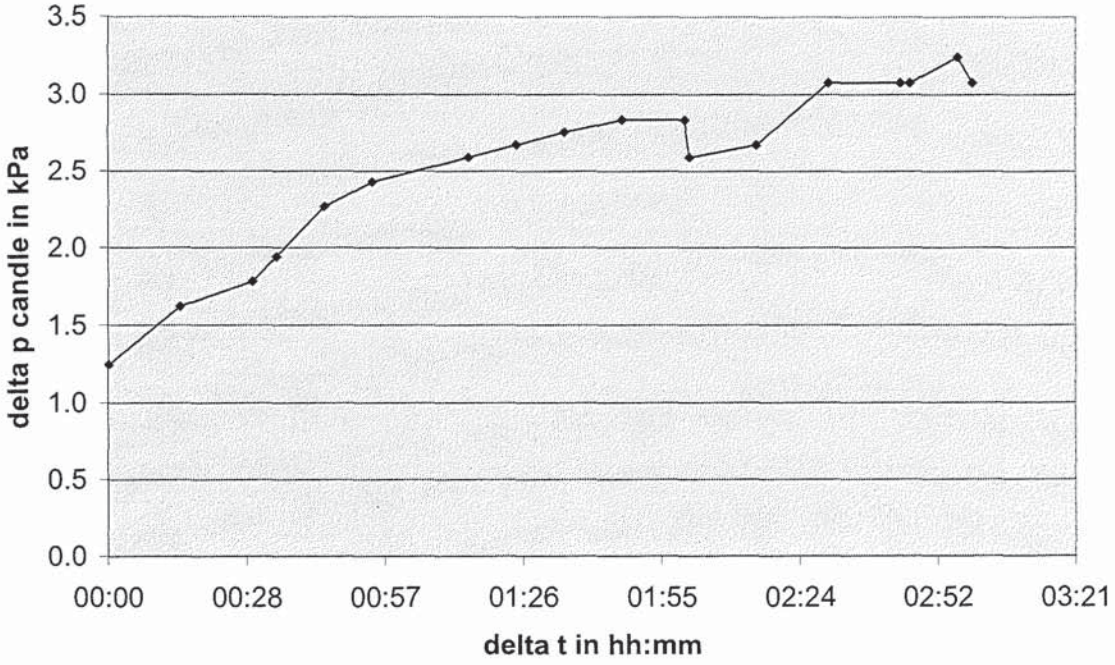

Figure 40: Course of differential pressure on Tenmat filter candle during experiment 161

7.3.3 Filter candle examination

The examination of the filter candle showed partial removal of the filter cake in large patches of around 20 % of the candle area. A picture of the filter candle and removed cake parts found in the char pot can be seen in Figure 41. The remaining filter cake had a thickness of 3-4 mm.

Figure 41: Picture of used Tenmat filter candle (left) and removed patches of filter cake found in the char pot (right) after experiment 161

7.4 Experiment 193: 2nd Filtration run with Tenmat firefly candle

7.4.1 Test parameters

The aim of experiment 193 was to evaluate the pressure drop development over an extended period of time. Furthermore the pressure measurement was improved by a differential pressure transducer with digital data recording to upgrade the data acquisition. The thoroughly cleaned Tenmat filter candle from experiment 161 was used as filter medium. By using the same candle it is intended to get more filtration time on the filter candle to evaluate whether there is some deposition inside the candle structure. The overall duration of the experiment was 08:00 h in which 6 h 44 min feeding of woody biomass was achieved. Feeding was interrupted due to refilling of the feed hopper as well as shutting down biomass feeding before injection of the reverse

cleaning pulses. During the experiment 6155 g beech wood with a moisture content of 10.3% was converted. This resulted in a feedrate of 914 g/h biomass. The feedstock was used as received without additional drying. This was done to find out whether it is possible to produce single phase oil under industrial conditions. The temperature of the filter unit was in between 400°C and 450°C and the face velocity of gases and vapours on the filter element was 3.29 cm/s.

7.4.2 Differential pressure over filter candle

The initial pressure drop with fluidising nitrogen was 1.2 kPa. The pressure drop increased to 1.5 kPa with the product gases and vapours entering the system. With increasing filtration time the pressure drop increased to 2.3 kPa after 1 hour when the first cleaning of the filter candle was conducted. This time it was intended to stop the gas stream to increase the reverse pulse intensity. Therefore, the feeding of the biomass was stopped. As after approx. 2 min the vapours in the EP disappeared the fluidising and entrained flow of Nitrogen was stopped. Then the cleaning system was activated introducing a reverse jet pulse of hot nitrogen at 550 kPa. After reverse pulsing the fluidising and entrained flow were opened again and thereafter the metering screw for biomass feeding was started. There was no pressure drop recovery monitored after this first cleaning cycle. In the further course of the experiment the pressure difference continued to increase steadily till it reached 3.0 kPa after approx. 30 min of continuous feeding. At this point the second cleaning cycle was injected with the same procedure as before. This time the cleaning was successful by decreasing the pressure difference from 3.0 kPa down to 2.0 kPa. In the further course of the experiment it was possible 2 times more to reduce the pressure difference from approx. 2.7 kPa to 2.1 kPa after continuous pyrolysis of 50 min each time. Then the feed hopper had to be refilled causing an interruption of the experiment of ca. 40 min. The next reverse pulse was induced after 30 min pyrolysis as the pressure drop reached 2.8 kPa. This time just a slight reduction of differential pressure down 2.7 kPa was achieved, and after another 30 min pyrolysis the differential pressure reached 2.9 kPa. This time the injected reverse pulse showed no effect and the pressure difference reached 3.1 kPa. After further 30 min the pressure difference reached 3.5 kPa and the subsequently injected reverse pulse was able to reduce the differential pressure down to 3.3 kPa. In the further course it was possible 2 more times to reduce the pressure, but it was not possible to reduce the pressure drop drastically, indicating that just patchy cleaning without full removal of

filter cake occurs. After 7 hours and 30 min experiment respectively 6 hours and 20 min continuous feeding the pressure difference was 4.0 kPa. The injected reverse cleaning pulse after 6 hours 30 min was unsuccessful and the pressure difference increase up to 4.5 kPa before stopping the experiment after 6 hours and 44 min pyrolysis. The course of the pressure difference at the filter candle is shown in Figure 42.

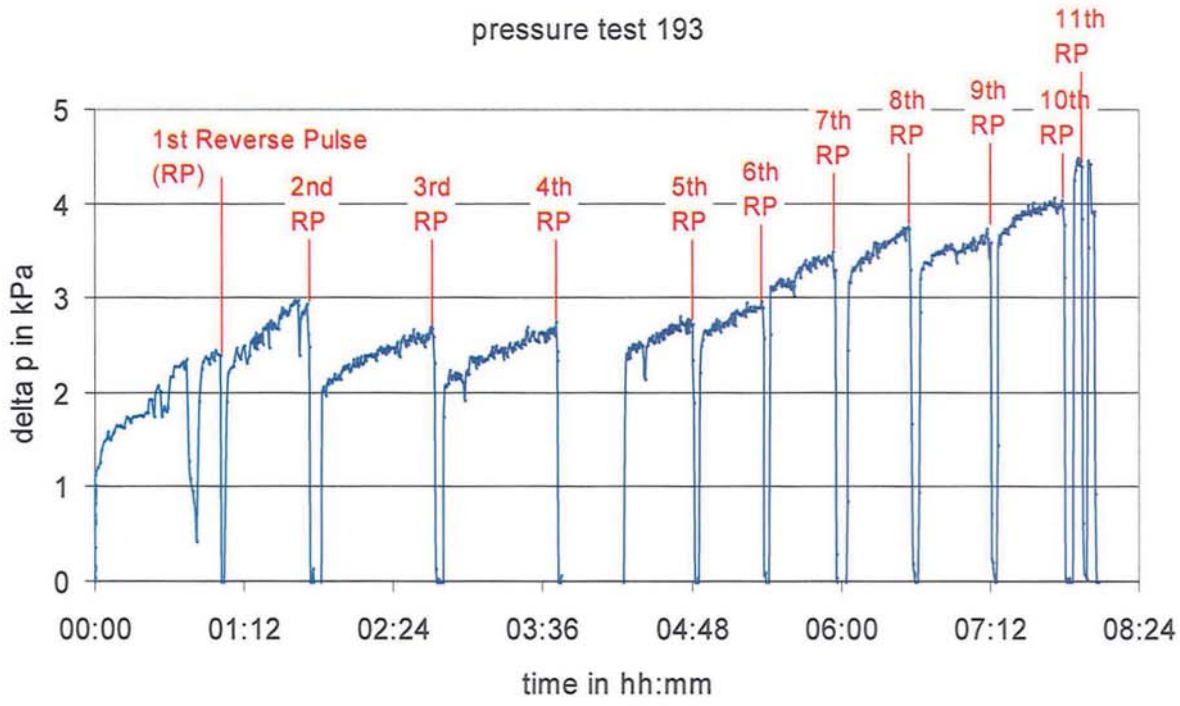

Figure 42: pressure course experiment 193, showing pressure drop recovery after each reverse pulse

7.4.3 Filter candle examination

Examination of the used filter candle after the experiment showed patchy cleaning of the attached filter cake. In it can be seen that the char cake was not totally removed but showed round areas of patchy cleaning on the cake surface. The filter cake consists in generally of char fines in a micro scale size (<100µm) with just occasionally coarser char particles, as SEM analysis of filter cake from experiment 157 has shown. Further investigation into the cake structure regarding particle size distribution is planned. It is intended to soak a sample of the filter cake in epoxy resin and perform SEM analysis in different depth layers of the cake.

Figure 43: Used filter candle before experiment 193

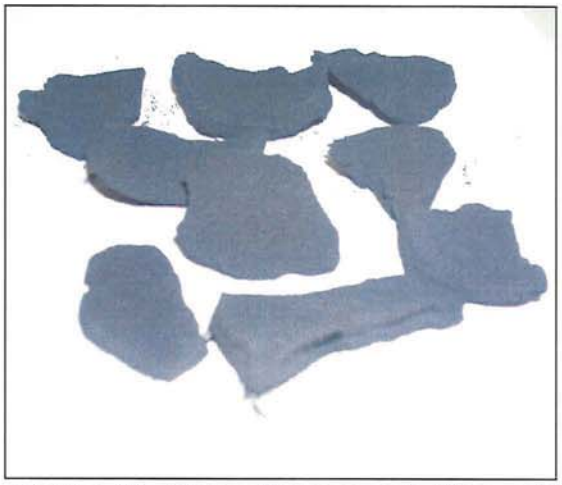

Figure 44: Manually removed filter cake patches after experiment 193

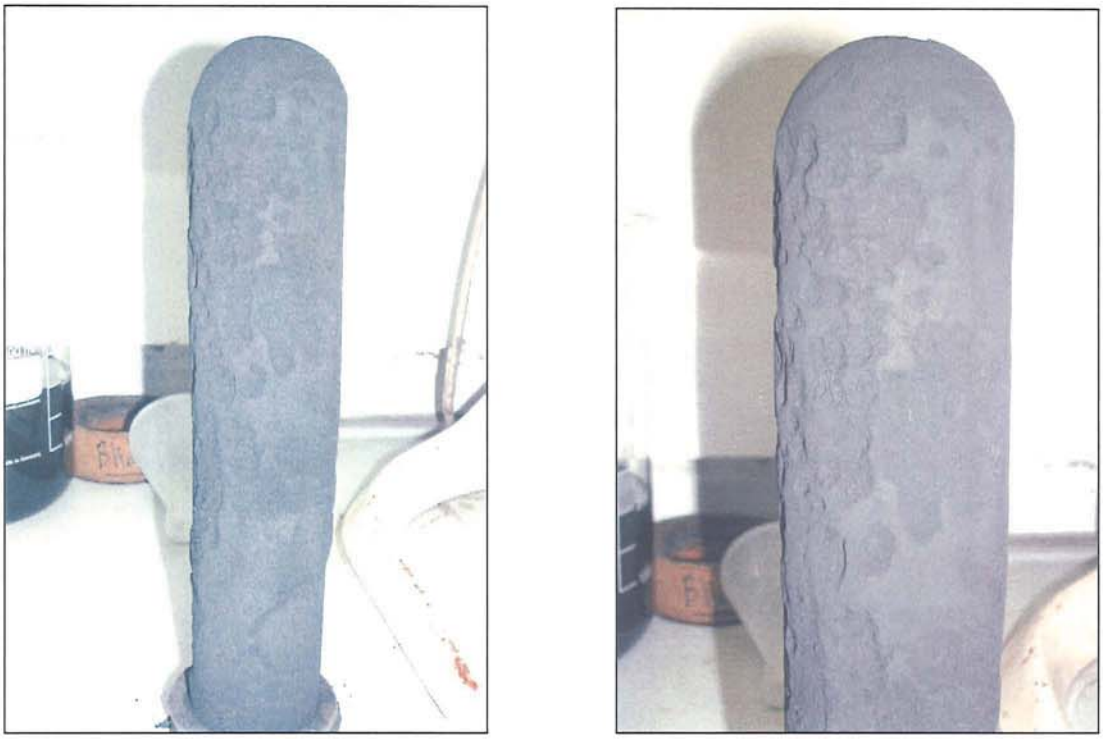

A **B**

Figure 45: Filter candle with developed char cake after experiment 193

If the filter cake is manually removed it comes off easily in large sections. Figure 44 shows a picture of the removed filter cake parts, illustrating that the filter cake removes in large sections in the shape of the filter candle.

7.5 Experiment 191: Filtration run with Inconel candle and pre-coating

7.5.1 Test parameters

Experiment 191 was carried out to investigate the effects of pre-coating the filter candle prior to filtration. This was done by introducing an additional non cohesive layer between the candle surface and the emerging char cake. It is expected to reduce the adhesion of the filter cake and make it easier to remove. The cleaned Inconel candle from Experiment 157 was used as filter. As the Inconel candle consists of a relatively large pore size (20μm) and showed low filtration efficiency (solid content Esp. 157 was 0.15) it is also intended to evaluate whether the pre-coat increases the filtration efficiency. Aeroxide (TiO_2) was used as a pre-coat material and 50g were introduced before filtration. The pre-coating was repeated after each reverse pulse. Because the procedure to introduce the pre-coat material increases the complexity of the process, the filtration time between the cleaning cycles should be long to reduce the amount of reverse pulses. In practical applications a cyclone would be applied to reduce the particle load of the gas stream and consequently the cleaning cycles. Therefore, the pre-coat experiment was commenced with one cyclone separator to have similar process condition regarding particle load and particle size distribution. The flow sheet of the experimental set-up can be found in Figure 46.

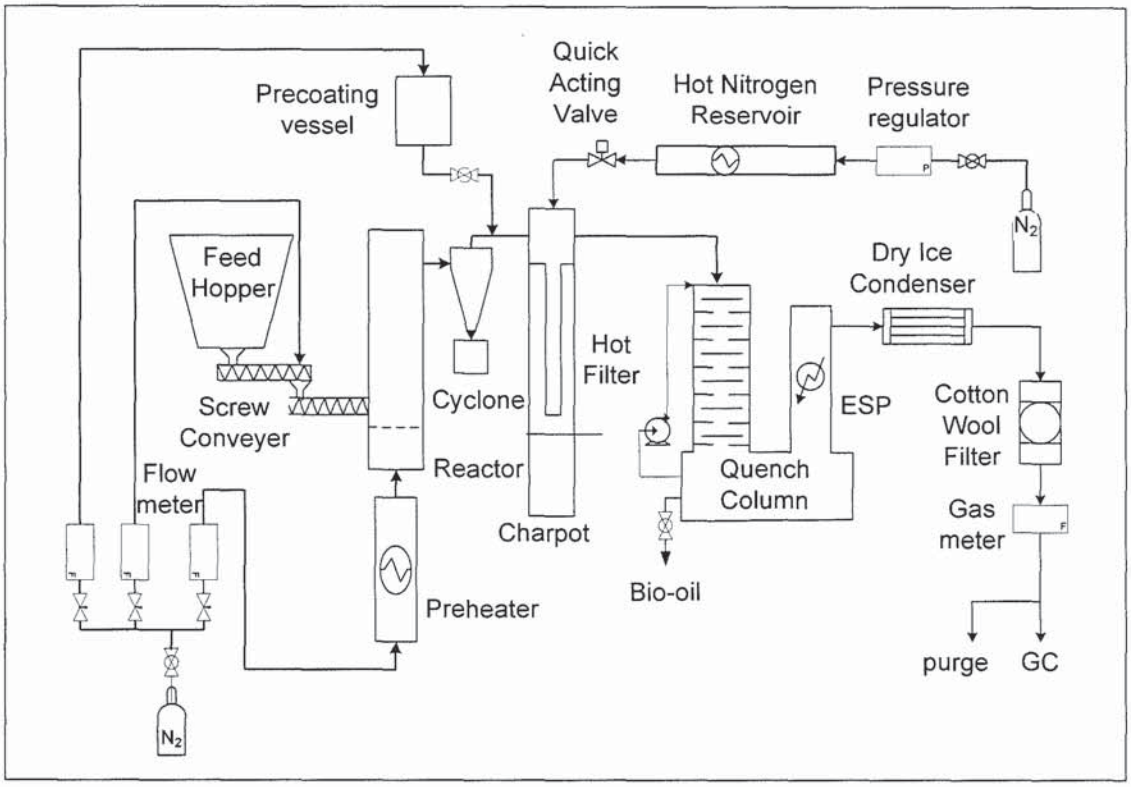

Figure 46: Flow sheet of experimental set-up with Pre-coating of the filter candle

The experiment lasted 1 h 35 min of feeding time with interruption to prepare the pre-coat. It was possible to accomplish two cleaning cycles. The process conditions were the same as in the experiments before with 500°C in the pyrolysis reactor and 400-450°C in the filtration unit. The gas flow resulted in a face velocity of 1.83 cm/s in the candle and a residence time of the vapours of 4.7 s in the hot environment.

7.5.2 Differential pressure over filter candle

The pre-coat increases the pressure difference on the filter candle from initially 0.49 kPa to 0.97 kPa. As biomass is introduced and pyrolysis vapours are produced the pressure difference increases further to 1.13kPa and continues to rise steadily till 1.46 kPa. Before introducing the reverse pulse the biomass feed and afterwards the nitrogen flow was stopped. Then the reverse pulse was injected. After injection of the reverse pulse it was paused for 5 min to let potential removed filter cake material settle down. Afterwards the nitrogen flow was opened and the bed re-fluidised. The pressure reading after the reverse pulse cleaning showed 0.81 kPa, which indicated that the char cake had been removed. As next another batch of Aeroxide was put into the system to pre-coat the filter candle. This caused the pressure to rise to 1.13 kPa. Thereafter, biomass

feeding was started again leading to a continuous increase in pressure due to char separation. After further 40 min of fast pyrolysis the pressure difference reached 1.62 kPa. At this point the cleaning procedure was started by stopping the biomass feed, closing the nitrogen flow and injection of the reverse pulse. After re-fluidising the reactor the pressure difference was reduced down to 0.81 kPa, which indicated successful cleaning of the candle and the experiment stopped.

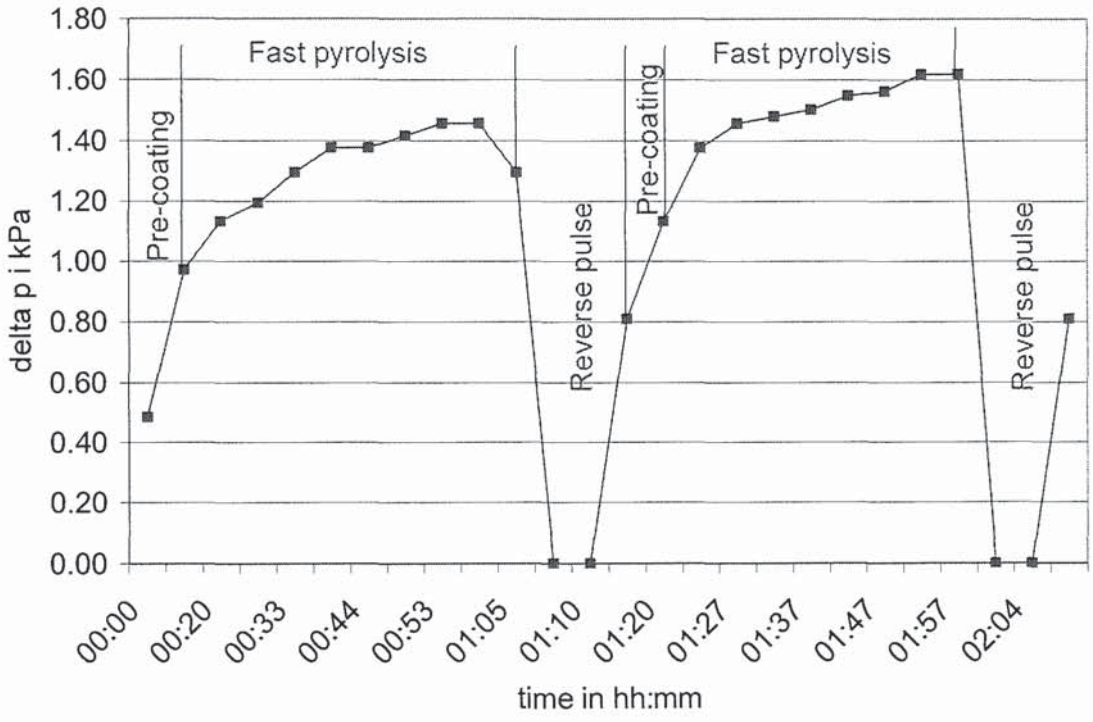

Figure 47: Differential pressure on filter candle versus time, experiment 191

7.5.3 Filter candle examination

Post examination of the filter candle showed total removal of the filter cake. Only a very small fluff of particles was distributed on the candle but no continuous layer.

Figure 48: Inconel candle after experiment 191 with precoating prior filtration. The dust cake was removed totally with reverse pulse. Only a thin residual dust layer remained on the candle surface.

7.6 Experiment 227: Tenmat candle (600 mm) with primary cyclone

7.6.1 Test parameters

The aim of the experiment was to investigate into the composition and pressure drop development of a filter cake made up of only fine char particles which are not removable by cyclones. A cyclone separator was placed upstream of the filtration unit to remove the coarse char particles, which represent ca. 97 wt% of the produced char. The filter candle used in this experiment was a Tenmat firefly with a length of 600mm. Due to increased surface area the face velocity of the vapours passing through the candle was reduced to 1.77 cm/s. The low face velocity was chosen to reduce the density of filter cake which is known to increase with the velocity of the filtration stream. Mixed softwood was used as feedstock with a moisture content of 10.13 wt% and an ash content of 0.29 wt% on wet basis. The feedstock was used as received and had a maximum particle size of 2 mm. The reactor temperature was between 450°C and 470°C with quartz sand as bed material. The average temperature in the filter unit was 450°C. The residence time of the hot vapours in the filter unit was 3.1 s and the total residence time of the vapours in the hot environment prior condensation resulted in 4.1

s. The experiment lasted for 2 h 45 min in which 2251 g of biomass was converted. Because the experiment was only done to evaluate the filtration performance and filter cake composition no mass balance or bio-oil analysis was conducted.

7.6.2 Differential pressure over filter candle

The pressure difference over the Tenmat firefly filter candle can be seen in Figure 49. It shows that the virgin pressure drop of the candle is ca. 0.3 kPa at 40 l/min STP and 450 °C in the filtration unit. The filter candle was then conditioned by introducing ca. 50g of Aeroxide into the gas flow. After a few minutes the candle was cleaned by reverse pulse. The introduction of Aeroxide was repeated twice. The conditioning of the candle resulted in a pressure drop of ca 0.35 kPa at 40 l/min STP. After the conditioning the flow-rate was increased to the fluidising velocity of 44 l/min STP which led to an increase of pressure drop to 0.42 kPa. As the feedstock was introduced the pressure drop increased further due to additional gases/vapours and an increase of the viscosity of the gas stream. A steady increase in pressure drop during the course of the fast pyrolysis experiment can be observed, resulting in a final pressure drop of ca. 0.8 kPa after 2h 45min continuous biomass conversion.

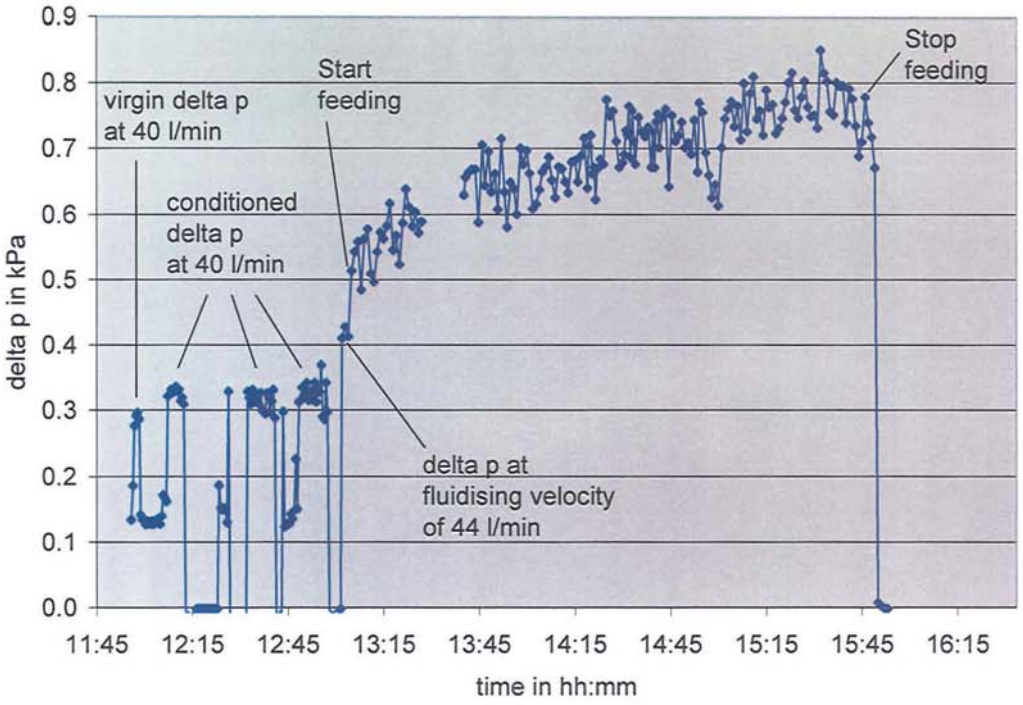

Figure 49: Pressure difference over Tenmat firefly candle in experiment 227

7.6.3 Filter candle examination

Post examination of the filter candle revealed a very thin but dense filter cake on the filter cake. The reverse pulse which was introduced after the experiment showed just tiny and superficial removal of filter cake. The mass of the filter cake was 14.7g and 0.8g of removed filter cake was recovered. The filter cake showed a very unequal distribution with thicker patches of char accumulations beside areas where the filter candle surface could be seen through. This can possibly be attributed to an unequal permeability of the candle material.

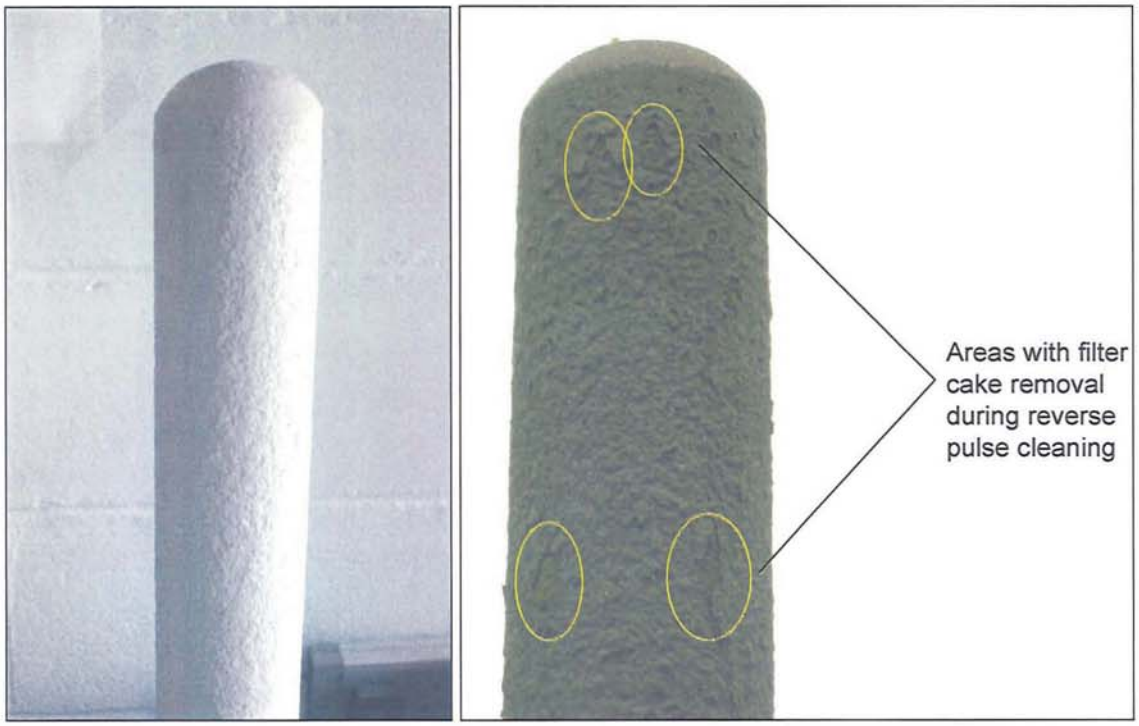

Figure 50: Tenmat filter candle before and after experiment 227

7.7 Mass balances of filtration experiments

Table 11 gives the mass balances of the filtration experiments followed by the discussion of the results.

Table 11: Mass balances attained from filtration experiments. Calculations in wt% based on dry feedstock

Experiment No.		157	161	193	191	227
Description (Candle type + Set-up)		Inconel candle	Tenmat candle Rep1	Tenmat candle Rep2	Inconel candle with pre-coat	Tenmat candle and cyclone
Yield in wt%	Organics	50.0	50.7	45.0	47.7	48.2
	Water	12.2	10.6	11.0	13.2	11.1
	Char	14.2	15.5	18.3	17.2	17.2
	Gas	18.5	16.3	20.3	n.m.	16.9
	Closure	95.0	92.6	94.6	78.1	93.4

7.7.1 Organic liquid yield

The amount of organic liquid yield resulted in 50.0 wt% with the Inconel candle. It showed 50.7 wt% for the first replicate experiment with the Tenmat candle and 45.0 wt% for the 2nd replicate experiment. The only difference between the two replicates was the duration of the experiments resulting in more biomass processed and hence a larger char cake on the filter candle in the 2nd replicate. Therefore, it can be concluded that the reduction of organic yield increases with increasing filtration time due to increased secondary cracking with developing filter cake. Furthermore, the increasing pressure possibly intensifies the catalytic impact of the mineral matter in the char additionally.

The organic yield for the experiment with the Inconel candle and pre-coating of the candle with TiO_2 particles resulted in 47.7 wt% and showed 48.2 wt% with the Tenmat candle and primary cyclone. In general the amount of organic liquid yield decreases from 54.5 wt% for the average standard run to 45 – 50 wt% for the experiments with filtration system, which means a reduction of 10 to 20 %.

7.7.2 Reaction water

The amount of reaction water showed no significant changes for the experiments with the Tenmat filter candle with water yield between 10.6 wt% and 11.1 wt% compared

with a water yield of 11.0 wt% for the average standard run. Whereas the amount of water produced during the experiment with the Inconel filter candle increased to 12.2 wt% and even further to 13.2 wt% in the experiment with the Inconel candle and TiO_2 precoating. This indicates that possibly the nickel present in the Inconel alloy, or the TiO_2 pre-coat, catalyses specific cracking reactions which promote the production of process water.

7.7.3 Char

The char yield increased for most of the filtration experiments. Only for the Inconel candle experiment (Run 157) it showed, with 14.2 wt%, a small decrease compared with the average standard run of 14.6 wt%. All the other filtration experiments showed an increase in char yield varying from 15.5 wt% for the first replicate with Tenmat candle and 18.2 wt% for the second replicate experiment with Tenmat candle. But as already discussed earlier (see 6.6.1.4) this cannot be attributed to an increase of secondary char production as the amount of char found on the filter candle is of negligible magnitude compared to the overall amount of char. As proposed earlier, the increase of char yield is likely to be due to condensation of volatiles in the char pot.

7.7.4 Gas yield

The amount of non-condensable gases increased for all of the filtration experiments. The first replicate of the Tenmat candle experiments shows, with 15.7 wt%, only a small increase compared to the average standard experiment with 15.4 wt%. However, it has to be considered that this experiment also shows a very low closure of just 92.6 wt% so it can be assumed that some of the gases might have been lost due to inaccuracies of the gas analysis. The other experiments showed a more significant increase of gas yield of 18.5 wt% with the Inconel candle (Experiment 157), 16.9 wt% with the Tenmat candle and cyclone (Experiment 227) and 20.3 wt% with the second replicate of the Tenmat candle experiment (Experiment 193). It can be concluded that the reduction of liquid yield is caused by an increase in non-condensable gases.

7.7.5 Gas composition

7.7.5.1 Results

Figure 51 shows the amount of the non-condensable gases obtained by the online GC-Analysis. The gases specified were CO_2, CO, CH4, H2, propane, propene, ethane and ethene. Propane, propene, ethane and ethene were summarised as C2-C3 compounds.

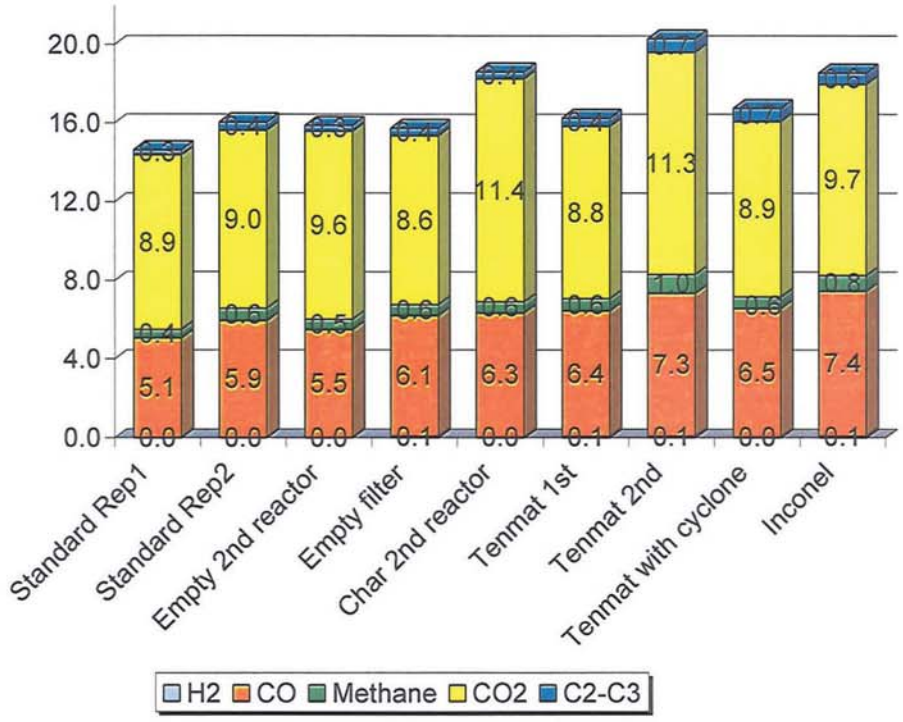

Figure 51: Results of the online gas analysis of the main gas components in wt% based on processed dry feedstock

It can be seen that CO_2 is the largest fraction with ca. 9.0 wt% at standard conditions and increases to around 11 wt% during filtration experiments. CO is the second largest fraction with between 5.1 and 5.9 wt% in the standard experiments and increases to 6.4 and 7.4 wt% in the filtration experiments. The values of methane vary between 0.4 and 0.6 wt% for the standard experiments and increase slightly and range between 0.6 – 1.0 wt% for the filtration experiments. The C2-C3 compounds vary between 0.3 and 0.4 wt% and show a slight tendency to increase and range between 0.4 and 0.7 wt% for the filtration experiments. The amount of hydrogen varies around 0.1 wt%. Due to the low molecular weight of nitrogen it is difficult to monitor it on a wt% basis.

Furthermore, the gas composition was calculated to evaluate whether the catalytic cracking of vapours on the char cake promote the production of specific gas compounds. The distribution of the gas compounds in percentage of the total non-condensable gases can be seen in Figure 52.

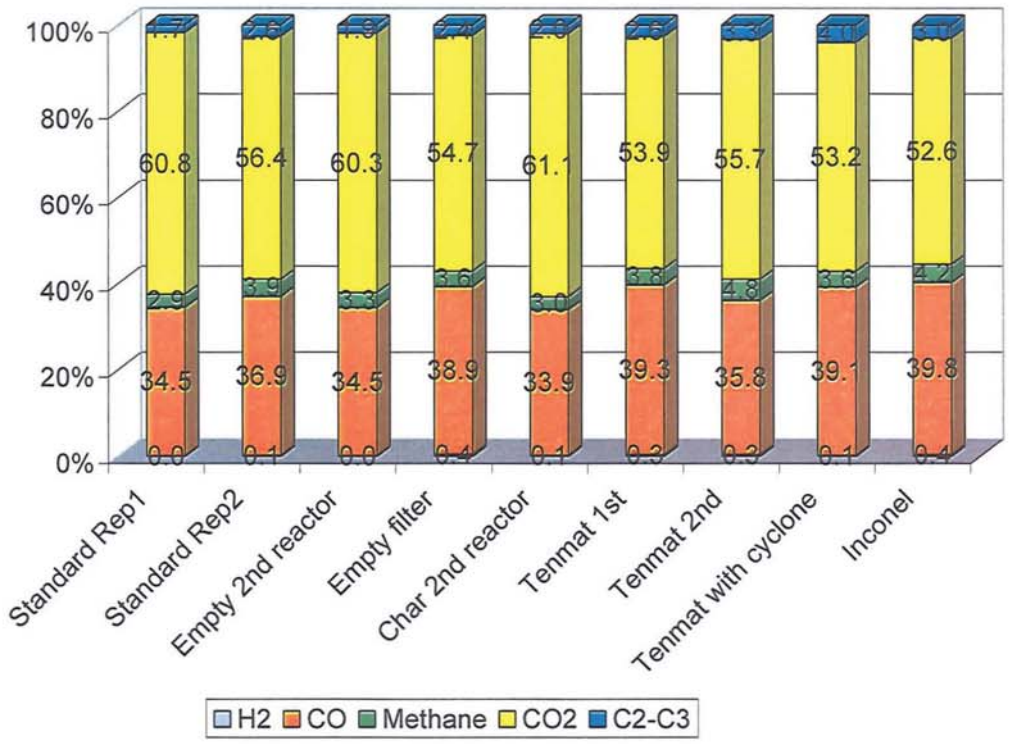

Figure 52: Composition of the gas fraction in wt% of the total gas yield for all the analysed experiments

It can be seen that there are small changes in the gas composition. The amount of CO_2 varies between 56.4 and 60.8 wt% for the standard runs and shows a tendency to decrease slightly to range between 52.6 and 55.7 wt% for the filtration experiments. The opposite trend can be seen with the CO where the amount ranges between 34.5 and 36.9 wt% for the standard runs and increases slightly to range between 35.8 and 39.8 wt% for the filtration experiments. The C2-C3 compounds show a slight tendency to increase from the range between 1.7 and 2.6 wt% for the standard experiments to the range between 2.6 and 4.0 wt% for the filtration experiments. Methane does not show a clear tendency ranging from 2.9 and 3.9 wt% for the standard experiments and varying between 3.8 and 4.8 wt% for the filtration experiments. Hydrogen shows an increase from around 0.1 wt% for the standard runs to range between 0.3 and 0.4 wt% for the filtration experiments.

As summary it can be said that the gas composition changes due to secondary vapour cracking on the char filter cake. To make the changes more visible the average of the produced gas compounds of the standard experiments and the average of the produced gas compounds during the filtration experiments were calculated. The results can be seen in Table 12. It was found that the amount of hydrogen changes from 0.01 % to 0.03 % which is an increase of around 3 times. Furthermore, there is an increase in CO and methane and a decrease of CO_2 whereas the preliminary experiment with char in the fixed bed secondary reactor shows an increase of CO_2 and a decrease of CO.

Table 12: Composition of the gas fraction of the avarage standard experiment compared with the average filtration experiment in percentage of the total gas yield

	H2	CO	Methane	CO2	C2-C3
Average standard (Exp. 88, 190)	0.1	35.7	3.4	58.6	2.2
Average filter (Exp.: 157, 161, 193, 227	0.3	38.5	4.1	53.8	3.2
Difference	0.2	2.8	0.7	-4.8	1.1
percentage change	267.7	7.8	20.7	-8.1	49.1

7.7.5.2 Discussion

Possible gas phase reactions during the extended residence time in the filtration unit are the homogenous water gas shift reaction, steam and dry reforming of carbon hydrates and thermal cracking reactions (see Equation 6 – 9).

Homogenous water gas shift

$$CO + H_2O \leftrightarrow CO_2 + H_2$$ **Equation 6**

Steam reforming

$$C_nH_x + nH_2O \leftrightarrow \left(n + \frac{x}{2}\right)H_2 + nCO$$ **Equation 7**

Dry reforming

$$C_nH_x + nCO_2 \leftrightarrow \left(\frac{x}{2}\right)H_2 + 2nCO$$ **Equation 8**

Thermal cracking

$$pC_nH_x \leftrightarrow qC_mH_y + rH_2$$ **Equation 9**

Furthermore, it is possible that heterogeneous gas phase reactions like the Boudouard reaction and the heterogeneous water shift reaction on the carbon of the filter cake occur (see Equation 10 and 11).

Boudouard reaction

$$C + CO_2 \leftrightarrow 2CO$$ **Equation 10**

Heterogenous water shift

$$H_2O + C \leftrightarrow CO + H_2$$ **Equation 11**

In general it has to be kept in mind that due to the sheer amount of organic vapours in addition with radical molecules, so many different reforming reactions happening simultaneously, it is difficult to promote specific reaction pathways. It can be said, that steam reforming and dry reforming are highly endothermic reactions. These reactions occur only at more elevated temperatures, which reflect in the general low content of hydrogen. The increase of hydrogen at process temperatures around 450°C is more likely due to the exothermic homogenous water shift reaction.

It can be concluded that the presence of alkali metals in the char filter cake will catalyse thermal cracking, which increases the overall gas yield. The increase of methane and C2-C3 hydrocarbons can probably be attributed to the scissoring of larger molecules. The additional thermal cracking is possibly also the reason for the increase in process water due to additional OH^- and H^+-Ions formation.

An explanation for the relative decrease of CO_2 in the gas composition of the filtration experiments can be found in the Boudouard reaction, which reduces CO_2 in the presence of carbon to CO. The Boudouard equilibrium can also explain the contrary results achieved in the experiment with char in the secondary reactor. During this experiment the pressure increases 10 times more than in the filtration experiments which shifts the equilibrium more to the left side with CO_2. Additionally the micro char fines of the filter cake have a higher surface area than the coarse char used in the secondary reactor, which leads to higher activity of the carbon.

8 Analytical results

8.1 Oil analysis

8.1.1 Solid content

Table 13 shows the solid content of the experiments with filtration unit in place. It can be seen that the filtration experiment 157 with the virgin Inconel candle resulted in 0.15 wt% solid content. This is still a high amount of solid which was able to pass the filter candle. It can be explained by the comparable large filter rating of 20 μm of the Inconel fibre fleece membrane. As it was an unused candle without preconditioning some amount of char was able to pass the candle prior to conditioning of the candle surface and the development of a filter cake. It can be expected that the filtration efficiency would increase with filtration time. However, it also shows that the pore size chosen is too large to filter particles below 5 μm efficiently.

The same Inconel candle was used after thorough cleaning with ethanol in experiment 191. In this experiment the candle was pre-coated with TiO_2 as described in Chapter 7.5. The solid content for the experiment with the pre-coated Inconel candle resulted in 0.03 wt%. This shows that the conditioning and/or pre-coating of the candle improve the filtration efficiency 5 times. It proves, therefore, that the filter cake is able to act as filter and removes particles before they reach the actual candle body.

In experiment 161 with the Tenmat filter candle the solid content was reduced to 0.008 wt%. This experiment represents a successful filtration and reaches the objective of a solid content below 0.01 wt%. The repetition of the experimental set up in experiment 193 resulted in a solid content of 0.006 wt% and confirmed the good cleaning performance of the filter candle. It showed that already the virgin filter candle was able to achieve the target of a solid content below 0.01 wt% and as the filtration efficiency improves with filtration time it can be said that it is possible to remove the solid content of fast pyrolysis oils below 0.01 wt%.

Table 13: Solid content of pyrolysis oils produced with filtration unit

Experiment No.	157	161	193	191
Description (Candle type + Set-up)	Inconel candle	Tenmat candle Rep1	Tenmat candle Rep2	Inconel candle with pre-coat
Solid content [%]	0.15	0.008	0.006	0.03

8.1.2 CHN – Analysis, Higher Heating Value

Table 14 shows the CHN-analysis of the produced oils. Nitrogen was for all of the oils below 0.1 wt% and oxygen was calculated by difference. Higher Heating Value (HHV) and Lower Heating Value (LHV) were calculated according the method described in 4.2.5.7. It can be seen that, with exception of the Inconel experiment, all of the filtration experiments have lower HHV and LHV due to the increase of process water. The 2nd Tenmat experiment which used feedstock with a moisture content of 10 % has with 14.4 MJ/kg a very low LHV. In general it can be said, that the feedstock has to be pre-dried to produce a fuel with reasonable fuel quality. However, as explained in chapter 6, it was found that it is possible to remove some of the water from the pyrolysis oil fraction to the DIC-fraction by increasing the cooling water temperature of the quench column. With this method it is possible to produce a reasonable fuel without pre-drying the feedstocks to an unrealistic extend.

Table 14: Elemental analysis of produced pyrolysis oils with HHV and LHV

Candle type + Set-up	Standard Rep1	Standard Rep2	Sec. reactor with char	Filter vessel empty	Inconel	Inconel pre-coat	Tenmat candle Rep1	Tenmat candle Rep2
C [%]	46.8	47.6	44.3	46.1	47.6	46.4	46.6	40.9
H [%]	7.3	7.1	7.3	7.1	7.6	7.2	7.2	8.0
O [%]	45.9	45.4	48.4	46.8	44.8	46.4	46.2	51.1
HHV [MJ/kg]	18.1	18.1	16.7	17.3	19.0	17.7	17.8	16.2
LHV [MJ/kg]	16.5	16.6	15.1	15.8	17.3	16.1	16.2	14.4
H_2O [%]	12.8	15.5	19.6	15.8	17.9	18.5	15.9	30.3

8.1.3 Mean molecular weight

The mean molecular weight of the fast pyrolysis oils were measured by GPC (see 4.2.5.2). Samples were taken 6 days after production (fresh oil) and after accelerated aging via heat treatment (see 4.2.5.4). Figure 53 shows the MMW of the analysed pyrolysis oils of different experiments before and after aging. It can be seen that the oil from the experiment with the empty filtration vessel has the highest molecular weight with 370 g/mol for the fresh and 607 g/mol for the aged oil. The second highest values shows the oil from the filtration experiment 161 using the Tenmat candle with 351 g/mol for the fresh oil and 559 g/mol for the aged oil. The oil from the 2nd standard experiment (Run 190), has with 322 g/mol for the fresh oil and 533 g/mol for the aged oil, shows lower values than the oil from the filtration experiment with Tenmat candle. The oil from the filtration experiment with the precoated Inconel candle shows the lowest values with 314 g/mol for the fresh oil and 526 g/mol for the aged oil. For the discussion of the results it has to be beard in mind, that the GPC only analyses the compounds with molecular weight above 105 Da, which excludes water and some low molecular organic acids, aldehydes and alcohols. It indicates therefore only the MMW of the molecular weight compounds above 105 Da rather than the MMW of the whole oil.

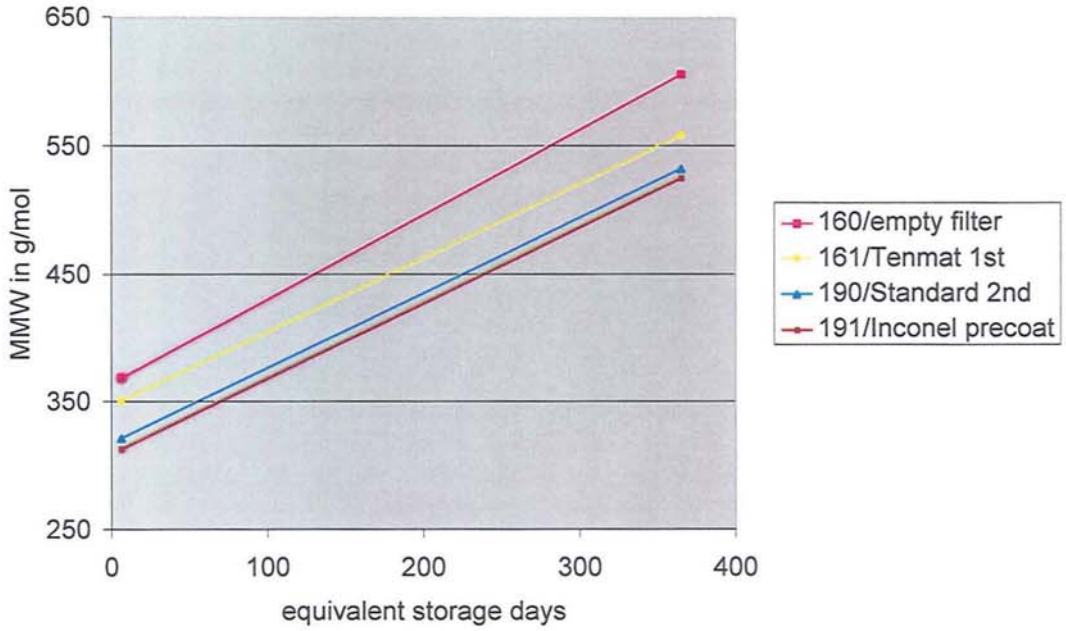

Figure 53: Mean molecular weight of pyrolysis oils from different experiments before and after accelerated aging

The inclination of the line between fresh and aged oils indicates the storage stability of the oil. A steep inclination refers to more unstable oil and a flat inclination shows oil with fewer changes in molecular weight during storage. It can be seen that there is no significant difference in the stability of the produced oils with or without filter system or due to the different filter candles.

The results show that there is no clear difference in MMW between filtered oils and unfiltered oils. The oil produced with extended residence time of the hot vapours but empty filter vessel (Exp. 160) has the highest MMW of the fresh oil and after accelerated aging, followed by the oil from the filtration experiment with Tenmat candle. The oil from the Standard experiment and the Filter experiment with Inconel candle have the lowest and nearly equal values.

It can be concluded, that the assumption that additional secondary vapour cracking, and/or reforming reactions due to extended residence time, can decrease the molecular weight of the condensed liquid, has to be refused. The results promote the assumption, that the high molecular weight compounds are formed during condensation from the vapour phase, rather than being primary decomposition products. This assumption is confirmed by Hanser, who analysed pyrolytic lignin from different pyrolysis oils with the result that the MMW is independent of process characteristics and similar for all the analysed oils. Furthermore, experimental work in Aston University on catalytic secondary vapour cracking using nickel-doped Olivines found, that it was possible to produce initially low molecular weight oils, but that the oils altered very fast during the first days of storage to the same or higher values than standard pyrolysis oils. Therefore it can be said, that increased secondary cracking produces more radical molecules, which will recombine during condensation respectively immediately after condensation, to create high molecular weight compounds.

8.1.4 Viscosity

8.1.4.1 Results

The viscosity of fast pyrolysis oils is strongly influenced by the water content of the pyrolysis oil, which lowers the viscosity significantly but reduces the heating value (see Chapter 2.3). Therefore, it is important to be aware of the water content of the oil for

comparison of the viscosity of different oils. The water content of the analysed oils is given in Table 15. It shows that it is possible to compare the presented experiments 160, 161 and 190 directly, because the oils have with 15.5 wt%, 15.8 wt% and 15.9 wt% similar water content. Only the oil from experiment 191 has with 18.5 wt% higher values than the other oils. Figure 54 shows the results of the viscosity measurements of the experiments 160, 161, 190 and 191. The oils were measured shortly after production and after accelerated aging (see chapter 4.2.5.4) indicated as 365 days on the time scale at the x-axes. It can be seen that the oil produced under standard conditions shows the highest viscosity. It has with 42.7 Pa.s for the fresh oil and 99.3 Pa.s significant higher values before and after aging than the filtered oils. The experiment with empty filter vessel has 33.4 Pa.s for the fresh oil and increases to 81.84 Pa.s for the aged oil. The oil from the filtration experiment with the Tenmat candle has with 21.8 Pa.s just half the viscosity at nearly the same water content as the one from the Standard experiment. Also the aged oil from that experiment is with 62.7 Pa.s significantly lower then the one from the standard run or the empty filter experiment. The fresh oil from the experiment with the precoated Inconel candle showed with 20.8 Pa.s nearly the same viscosity as the fresh oil from the Tenmat experiment. But as it has ca. 3 wt% more water content than the other 3 experiments, the actual viscosity of the pure organic liquid would be higher than the one from the Tenmat experiment. The increase in viscosity due to aging is with 51.4 Pa.s significant lower than in the oil from the Tenmat experiment.

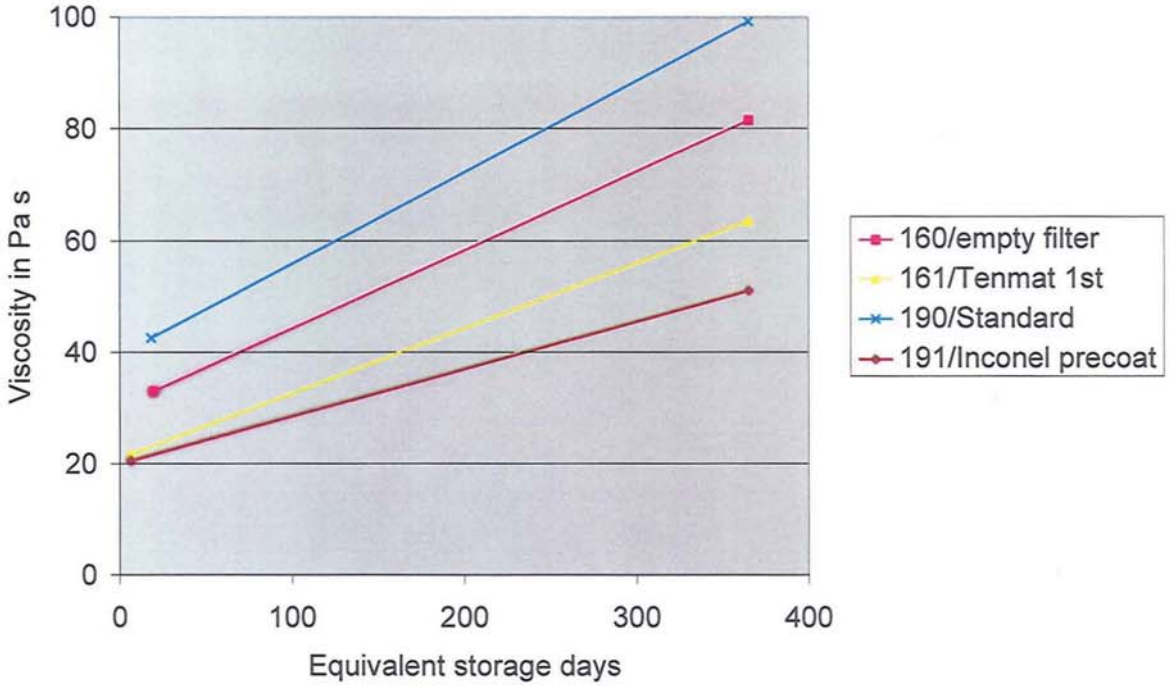

Figure 54: Dynamic viscosity of pyrolysis oils from different experiments before and after aging measured at 25°C.

Table 15: Water content of the pyrolysis oil which were analysed for viscosity

Experiment No.	190	160	161	191
Description	Standard Rep2	Empty filter vessel	Tenmat candle Rep1	Inconel candle pre-coat
Water content [%]	15.5	15.8	15.9	18.5

8.1.4.2 Discussion

It can be seen in Figure 54 that the quality of the filtered oils significantly improved by reducing the viscosity by around 50 % compared with the non-filtered oil. In terms of storage stability the filtered oil using the Inconel candle with pre-coat material showed the lowest inclination and also has the lowest final viscosity. The filtered oil with Tenmat candle has slightly worse stability characteristics but has a lower inclination than the non-filtered oils.

One explanation for the decrease in viscosity is the decrease of char fines of the filtered oils. This is confirmed by the fact that the standard oil with the highest viscosity also has with 0.5 wt% the highest solid content compared with the oil from the empty filter experiment, which has a lower solid content and lower viscosity. The filtration

experiments have with 0.008 wt% (Tenmat) and 0.03 (Inconel with pre-coat) beside the lowest viscosity also the lowest solid content.

Therefore, the increase in oil quality due to reduction of viscosity is most likely to be caused by physical reasons (reduction of solid content) rather the chemical reasons (reduction of high molecular weight compounds). However, another reason for the decrease of viscosity would be an increase of the solubility of the high molecular weight pyrolytic lignin. Although the GPC-analysis showed that there were no changes in the MMW of the pyrolysis oils it is possible that an increase of organic acids and/or alcohols increase the mutual solubility of the oil compounds and hence decrease the viscosity.

9 Results and discussion of filtration characteristics

9.1 Introduction

The methodology for the filtration experiments was described in 4.1 in Chapter 7. The experimental set-up included different filter materials, different candle sizes resulting in different face velocities, and inclusion or exclusion of a cyclone upstream of the filter.

The inclusion or exclusion of a primary cyclone as well as face velocity of the gas stream and surface area of the filter candle are influencing the filter cake characteristics such as particle size distribution and resistance to flow. Therefore, the particle size distribution of the filter cake was evaluated by Scanning Electron Microscopy (SEM). Additionally the resistance to flow of the filter cake (k_C) and the resistance to flow of the filter candle (k_F) were calculated (see Chapter 3).

Due to different amounts of char particles filtered and different surface areas of the filter candles k_C of the different experiments the resistance to flow was set into relation to the area load of char on the candle to make them comparable. To evaluate the overall performance of the experimental set-ups the final k_C of the experiment was set in relation of the total amount of char particles separated. A total of five experiments with filter candles were carried out with the summarised test parameters shown in Table 16.

Table 16: Test parameters of filtration experiments

Filter material	Tenmat	Tenmat	Tenmat	Inconel	Inconel
Run no.	161	193	227	157	191
Cyclone	No	No	Yes	No	Yes
Face velocity cm/s	3.41	3.25	1.77	2.02	1.90
Filter length mm	305	305	600	500	500
Filter surface area cm^2	575	575	1131	942	942
Biomass processed g	3271	5521	2023	2263	1462
Filter cake in g	33.0	63.6	14.7	16.5	4.37
Biomass per area [g/cm^2]	5.69	9.60	1.79	2.40	1.55
Char area load [g/cm^2]	0.0574	0.1107	0.013	0.0175	0.0046
k_F [1/m]	7.16E+08	8.56E+08	7.45E+08	9.53E+08	8.17E+08
k_C [1/m]	9.19E+08	1.67E+09	3.20E+08	6.10E+08	5.07E+08
K_{C+F} [1/m]	1.64E+09	2.53E+09	1.07E+09	1.56E+09	1.32E+09
Filter cake thickness [mm]	4	5	0.5	2	0.5
k_C/Areal load char [m/g]	1.60E+14	1.51E+14	2.47E+14	3.48E+14	1.09E+15
k_C/feedstock per filter area	1.62E+12	1.74E+12	1.79E+12	2.54E+12	3.27E+12

9.2 Filter cake analysis

9.2.1 Particle size distribution of filter cake

It was found that some of the coarse char separate due to gravity before reaching the filter candle with the amount of separated particles depending on the face velocity of the gases in the filter unit. SEM pictures of filter cakes produced at different face velocities can be seen in Figure 55. The picture on the left shows the filter cake of experiment 157 using the Inconel candle resulting in a face velocity of 2.0 cm/s The picture on the right shows the filter cake of experiment 161 with the shorter Tenmat candle resulting in a face velocity of 3.4 cm/s. Both of the experiments were carried out without primary cyclone. Although the order of magnitude of the pictures is different, it can be seen that filter cake at 2.0 cm/s consists mainly of char fines below 20 µm and only a few particles around 200 µm. Whereas the filter cake produced at a face velocity of 3.4 cm/s consists of a mesh of particles above 200 µm and the smaller particles agglomerated at the large particles. The larger particle size also results in a larger void fraction of the filter cake produced at 3.4 cm compared to the more dense cake at lower velocities. Hence it can be concluded that in the case of filtration experiments without primary

cyclone and the used process parameters a higher face velocity produces a less dense filter cake than at low face velocity. This is contrary to filtration experiments in the literature, where normally particles below 10 µm are used with the result that high face velocities produce denser filter cakes.

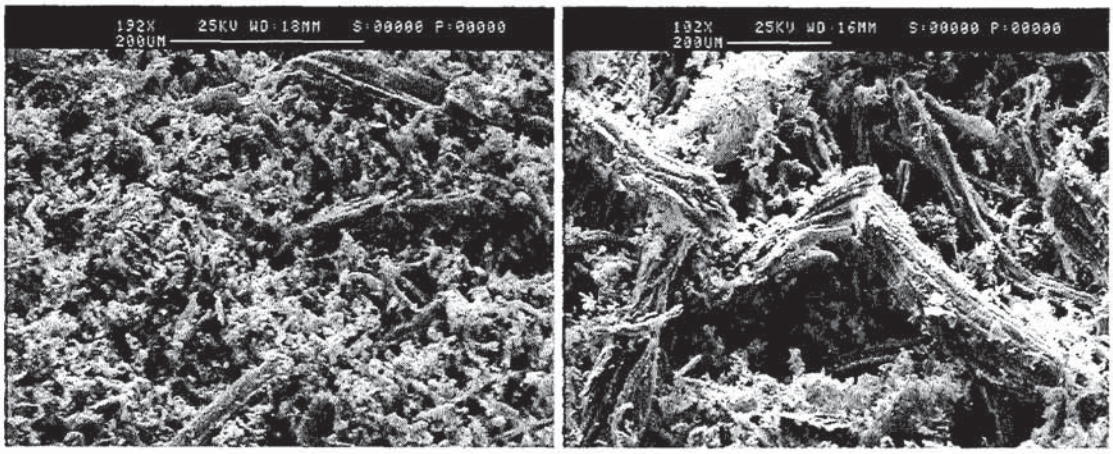

Figure 55: SEM pictures of filter cakes from experiment 157 (left) and experiment 161 (right)

9.2.2 Comparison of resistance to flow

Table 17 shows the resistance to flow of the filter elements (k_F) before the experiments, the resistance to flow of the filter cake (k_c) calculated from the resistance to flow of the filter candle inclusively the filter cake (k_{c+F}) after the experiments. Furthermore, k_c was set in relation to the amount of char collected on the filter element to evaluate the specific resistance of flow.

It can be seen that the resistance to flow for the Tenmat candle and the Inconel candle are in the same order of magnitude. The kc of the Tenmat candle increased slightly from 7.2 to 8.6 $*10^8$1/m from the first Tenmat experiment to the second one what can be due to conditioning of the candle by particles penetrating the filter matrix. The Inconel candle showed values of around 9 $*10^8$ 1/m.

The resistance to flow of the filter cakes increased with the duration of the experiments and with the particle load reaching the filter candle and can give therefore no clear information of the cleaning characteristics. Therefore the kc was set in relation to the amount of char collected and it was found that the Tenmat experiments have half the

value of the Inconel experiment. The kc/char load shows that the remaining filter cakes of the experiments with Tenmat filters (face velocity > 3 cm/s) is higher than with the Inconel experiment (face velocity = 2 cm/s) which indicates that the filter cake with higher face velocity has higher permeability.

The remaining dust layer from the pre-coating experiment has with 10.9 $*10^{14}$1/m the highest value. This high value of the experiment with the totally removed filter cake actually agree with the literature [105], which found that the residual dust layer has a lower permeability than the removed filter cakes. Additionally it is possible that some of the nano-sized Aeroxide® particles penetrated the filter membrane and decreased the permeability

Table 17: Resistance to flow of filter element, filter cake and filter cake per area load char

	Inconel	Tenmat 1	Tenmat 2	Inconel+Pre-coat
k_{Filter} [1/m]	9.5 $*10^{8}$	7.2 $*10^{8}$	8.6 $*10^{8}$	9.2 $*10^{8}$
k_{Cake} [1/m]	6.1 $*10^{8}$	9.2 $*10^{8}$	16.7 $*10^{8}$	5.1 $*10^{8}$
$k_{Cake/Char\ load}$ [1/m]	3.5 $*10^{14}$	1.6 $*10^{14}$	1.5 $*10^{14}$	10.9 $*10^{14}$

The used Tenmat filter candle showed a dark black colour of the fibres, which was found not only on the surface but through the whole diameter of the candle (see Figure 56). Hence various analyses with SEM analysis were done to examine whether secondary cracking of vapours cause serious carbonisation and can cause clogging of the inner structure. Figure 56 gives an example for the SEM analysis pictures. It can be seen that some particles were found which penetrated in the filter matrix but there were no signs that the diameter of the fibres increased significantly due to carbon deposition. Therefore it can be concluded that carbonisation changes the colour of the fibre surface but is only a very thin layer which is not likely to disturb the filtration process.

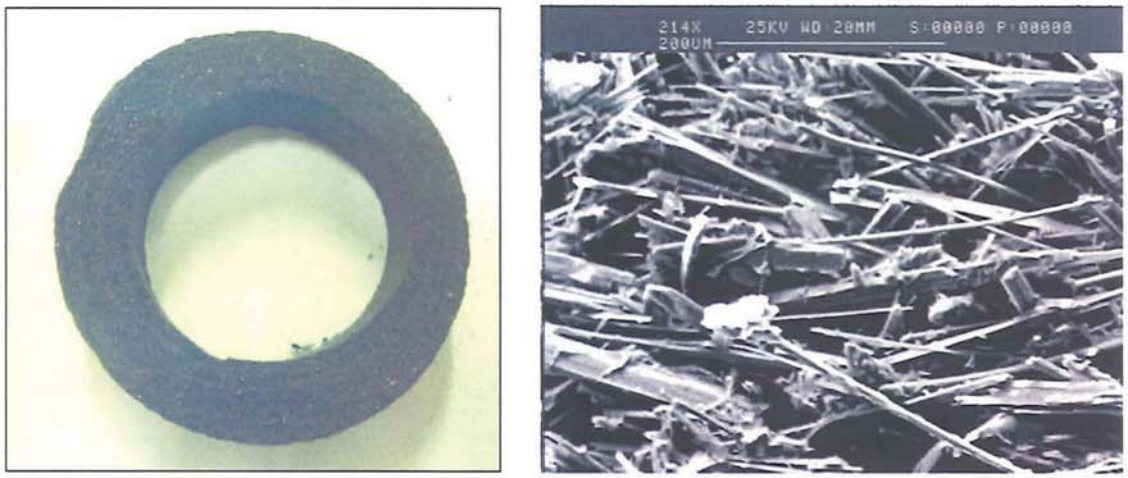

Figure 56: Picture of a slice of used Tenmat candle (left) and SEM-Picture of the same piece (right)

9.2.3 Evaluation of filtration experiments

9.2.3.1 Experiment 157 with Inconel candle

As described earlier the particle load of the gas stream reaching the Inconel candle was lower compared with the Tenmat experiments. The lower face velocity and the lower particle load caused the initial pressure drop and the pressure drop increase to be lower than in the Tenmat experiments. It was possible twice to achieve a reduction in pressure drop by reverse pulsing, however the 3rd and 4th reverse pulse had no impact. The inspection of the filter candle showed patchy cleaning in very small patches of around 2-5 mm.

The very small patches are phenomena which can be attributed to the low resistance to flow of the filter cake in relation to kc of the filter element. The ratio of k_{Filter} to k_{Candle} is reflected in the distribution of the applied cleaning forces during reverse pulsing. This means in this case that 2/3 of the pressure drop developed during the reverse flow is on the filter candle and only 1/3 applies on the filter cake. Therefore, longer experiments would be necessary to know with certainty how the filter cake detachment performs at higher pressure drops on the cake. However, due to the fact that it was not possible to remove the less dense filter cakes from the Tenmat experiments it has to be assumed that the cleaning forces of the jet pulse system applied are not high enough to achieve stable filtration conditions.

9.2.3.2 Experiment 161 and 193, Tenmat candle

The high velocity and char load was the reason that the pressure drop was higher and increased faster than in the experiment before. In both experiments with the Tenmat candle a partial removal of the filter cake was achieved. Compared to Experiment 157 the patches fell off in large chunks of up to 5 cm, resulting in large fully cleaned areas.

In the case of Experiment 193 it was possible to recover the pressure drop 5 times very well until the pressure drop recovery was reduced leading to a steady increase in pressure. The initial pressure drop of the candle was 1.7 kPa and it was possible to keep the pressure drop for 4 hours below 3 kPa. The experiment lasted more than 6 hours and was stopped at a differential pressure of 4 kPa with no further pressure reduction. Hence there is a tendency that the pressure would continue to rise.

Again it would need longer experiments to prove whether the pressure drop will reach stable conditions. However, the large removed patches indicate that it is possible to remove the cake and that the cleaning forces applied are nearly high enough to clean the whole candle.

9.2.3.3 Experiment 191, Inconel candle with pre-coating

For this experiment Aeroxide, a nanosized fumed TiO_2, was introduced prior to each filtration cycle to create a highly dendritic pre-coat on the filter candle. Due to the nano size of the Aeroxide® there will be very little surface contact of the pre-coated particles with the filter candle surface, which will reduce the contact forces and improve cleaning.

The amount of pre-coating material was 50 g resulting in an area load of 9.6 g/dm^2, which caused the initial pressure to double from 0.5 kPa to 1.0 kPa. The start of the pyrolysis process increased it further to 1.1 kPa. During the filtration time of 40 min the pressure rose to 1.5 kPa when the 1st reverse pulse was injected after stopping the feed and the fluidising Nitrogen to avoid a gas stream against the reverse pulse cleaning gas stream. After the cleaning procedure the fluidising gas was started again resulting in a differential pressure of 0.8 kPa. The lower pressure drop indicated successful removal of the filter cake. During the experiment it was possible to demonstrate 2 successful

cleaning cycles with total removal of the filter cake and only a residual dust cake remaining.

The residual dust layer showed a high resistance to flow and the remaining Aeroxide® particles developed a black carbonised surface. As for the other experiments it would be necessary to make longer experiments, but this time to prove the stability of the filter cake removal.

10 Conclusions

A hot gas filtration test unit was designed and build to filter the hot vapour stream of the 1 kg/h fluidising bed reactor. Successful hot filtration of fast pyrolysis vapours with up to 7 hours biomass feeding was demonstrated, with a solid content of the produced oils below 0.01 wt% with the ceramic fibre filter candle. The Bekaert Inconel sintered metal fibre candle showed with 0.15 wt% a quite high solid content, which can be attributed to relatively large fineness of the filter membrane of 20 µm and a relatively short duration of the experiment without enough time for conditioning of the filter candle. Pre-coating of the filter candle with nano-sized Aeroxide improved the filtration efficiency to a solid content of 0.03 wt%. Peukert [106] analysed sintered metal candles and found filtration efficiencies higher than 99.995 %. Hence, it can be assumed that a metal fibre candle with a smaller fineness and additional time for conditioning will achieve an efficiency which reduces the solid content to around 0.01 wt% .

Additional secondary cracking of the vapours on the filter candle and filter cake reduces the amount of organic liquid from an average of 55 wt% down to 45 to 50 wt%. This means a reduction of liquid yield of 10-20 %. The reduction of organic yield increases with increasing filtration time due to increased secondary cracking with developing filter cake. The increase in pressure possibly intensifies the catalytic impact of the mineral matter in the char. As expected the reduction of liquid yield is accompanied by an increase in non-condensable gases and reaction water.

The gas composition of the filtration experiments changes compared to standard experiments and also during the filtration time. This can be attributed to additional catalytic cracking which promotes the formation of gaseous hydrocarbon from larger molecules. Additionally the amount of carbon dioxide decreases and the amount of carbon monoxide of the gas composition increases, which can be due to reduction of carbon dioxide on the carbon of the filter cake.

Analysis of the pyrolysis oils showed significant increase of product quality due to lower viscosities and reduced aging of the hot gas filtered oils. However, it was not

possible to decrease the mean average molecular weight of the high molecular mass compounds. Therefore, the explanation for the increase in quality is more likely caused by the physical reduction of particulates rather than changes in the chemical composition. Furthermore, the removed char particulates will not act as nuclei for further carbonisation during storage. In the framework of this work it was not possible to monitor changes in the chemical structure of the pyrolysis oil. This also relates to the influence of the filter candle material where no changes were found, besides a higher increase in reaction water with the Inconel candle compared to the ceramic one.

Another advantage of the absence of particles after the condensation system is the protection of downstream equipment from blockage. Especially the entrance to the condensation unit is a critical point of the fast pyolysis system. The particles entrained in the vapours agglomerate on the condensed oil and cause an increase of viscosity so that the oil adheres on the wall instead of floating down. With further agglomeration of particles this phenomena can block the condensation unit. For all of the filtration experiment, the pipework after the filter and the quench system was totally clean compared to depositions without filtration. It can be concluded that the general problem of char accumulation in pipework and condensers is focused at the filter vessel were it can be tackled by a good cleaning system. The problem of char accumulation in the pipes would be avoided if the hot filter is placed physically as close to the reactor as possible. Consequently, the ideal constellation is to put the filter candles directly in the freeboard of the pyrolysis reactor.

The filtration experiments showed that it was possible to regenerate the pressure difference via reverse jet-pulse during the first filtration cycles, but subsequent cleaning pulses showed less cleaning effect and consequently no stable cleaning characteristics.

The examination of the filter candles showed patchy cleaning of the filter cake. It was found that the filter cakes produced with higher face velocity (>3 cm/s) produce less dense cakes with high permeability because of a larger particle size distribution of the char. Whereas at a lower velocity (2 cm/s) the particles below 200 µm separate due to gravity without reaching the filter cake.

However, due to the larger particle load on the candle the pressure drop increases more rapidly with higher face velocity (>3 cm/s), which increases the amount of cleaning cycles.

Visual analysis of the remaining filter cake and removed filter cake patches revealed a dry filter cake without any signs of tar condensation.

Reverse pulse cleaning with low pressure drop on the filter cake results in patchy cleaning with many small removed areas around 3-5 mm. Whereas reverse pulses applied at thicker cakes with high pressure drops remove the cake in large patches of 3-5 cm.

It can be concluded that the cleaning forces generated during reverse pulse cleaning are not high enough to detach the filter cake fully, although it was possible to remove large patches of filter cake. The remaining filter cake was easily removable with a spatula after the experiment, which indicates that it would be possible to remove it fully with higher cleaning forces.

Pre-coating the filter candle with nano sized fumed Aeroxide to form an additional layer between filter candle and filter cake resulted in total removal of the filter cake with only a thin residual dust layer remaining. However, the residual dust layer has a comparable large resistance to flow which indicates some penetration of particles into the candle structure and longer experiments are necessary to confirm the promising result.

Finally it has to beard in mind that a small filtration test unit has the disadvantage that it consists of only of one filter candle and therefore less volume of the filter vessel and filter head. Hence the cleaning forces during reverse pulse can be expected to be higher in an industrial filter house, because the large filter head volume increases the amount of gases which entrain additionally with the jet pulse. Furthermore, during the reverse pulse the gas flow builds up pressure on the clean gas side of the filter vessel, causing the differential pressure between raw and clean gas side to decrease.

11 Recommendations

Beside of an increase in process water, it was not possible to monitor changes in the chemical composition of filtered oils compared to the non-filtered oils, although the quality regarding viscosity of the filtered oils improved significantly. As described the analysis of the MMW with GPC is limited, because it detects only compounds with molecular weight above 105 Da. Therefore it is recommended to use GC-MS and/or GC-FID to identify and quantify the low molecular weight organic acids, aldehydes, ketones and alcohols, as an increase in acids and/or alcohols would increase the mutual solubility of the oil compounds. This would give information whether the quality improvement of the filtered oil is only due to physical reasons but also due to some improvement of the chemical composition of the oils.

Regarding the decomposition of the high molecular weight compounds it was found that the additional secondary cracking on the filter cake did not reduce the MMW of the GPC detectable compounds, which is likely due to formation of the high molecular weight compounds during condensation of the oil from the vapour phase. Hence it is recommended to intensify the research on the chemical composition of the vapour phase to gain knowledge about the reaction pathways during condensation. This information would help to find possibilities to influence the condensation reactions catalytically or to find suitable additives for the vapour phase to improve the quality of the later condensed oil.

The number of experiments was limited in the framework of this project, due to the large amount of work associated of running the 1kg/h fast pyrolysis reactor including filtration unit and calculation of an accurate mass balance. However more and especially longer experiments would be necessary to get more information about the stability of the filtration process regarding pressure drop development and cleaning efficiencies of the filter cake. Industrial filtration experiments in advanced coal gasification have shown that up to 100 cleaning cycles were necessary to give a clear statement about the possibility to achieve stable pressure drop conditions. Therefore, I suggest to run a filtration unit on a larger laboratory unit (5 kg/h rig at Aston) or on a process development unit to allow longer duration of the experiments.

Regarding the design of a hot filtration test unit it would be of an advantage to have at least two parallel filter chambers, to allow the process gas stream to flow through a parallel chamber when the reverse pulse is introduced in the other chamber. Furthermore, it should be considered to design a larger volume for the filter head to enable the entrainment of additional gas into the nitrogen reverse pulse stream and hence increase the reverse pulse flow. These measurements would help to increase the cleaning forces and resemble more an industrial application, which can lead to a better pressure drop recovery. Additionally, Mai et al developed an advanced cleaning system by connecting the reverse pulse directly to the filter candle and claim to achieve larger cleaning forces than conventional reverse jet pulse systems.

Reduction of adhesion forces between filter element and filter cake by developing a pre-coat layer on the candle prior filtration showed very promising results. It is recommended to continue this approach and to prove the reliability with longer experiments. In addition the research can be extended by the assessment of pre-coat material with positive catalytic impact on the later oil or one which can act as an absorbent for sulphur and chlorine removal.

Finally it would be important to assess the filtration characteristics of different feedstocks. It can be expected that filter cake properties like density and permeability will be affected by the properties of the parent material i.e. density, amount of volatile matter and ash content. Therefore, filtration characteristics like pressure drop development, adhesion forces between candle and cake or inside the cake itself are influenced by the feedstock with subsequent consequences for the cleaning efficiency of the reverse pulse.

References

1. Bridgwater, A.V., D. Meier, and D. Radlein, *An overview of fast pyrolysis of biomass.* Organic Geochemistry, 1999. 30: p. 1479-1493.

2. Bridgwater, A.V.,D.C. Elliott, L. Fagern, J.S. Gifford, K.L. Mackie, and A.J. Toft, *The Nature and Control of Solid, Liquid and Gaseous Emissions from the Thermochemical Processing of Biomass.* Biomass and Bioenergy, 1995. 9(5): p. 325-341.

3. Czernik, S. and A.V. Bridgwater, *Overview of applications of biomass fast pyrolysis oil.* Energy & Fuels, 2004. 18: p. 590-598.

4. Bridgwater, A.V., A.J. Toft, and J.G. Brammer, *A techno-economic comparison of power production by biomass fast pyrolysis with gasification and combustion.* Renewable and Sustainable Energy Reviews, 2002. 6: p. 181–248.

5. Scahill, J., J.P. Diebold, and C. Feik, *Removal of Residual Char Fines from Pyrolisis Vapors by Hot Gas Filtration.* Developments in Thermochemical Biomass Conversion, ed. A.V. Bridgwater. Vol. 1. 1997, Blacky Academic and Professional: London. 253-266.

6. Agblevor, F.A., S. Besler, and R.J. Evans. *Inorganic Compounds in Biomass Feedstocks: Their Role in Char Formation and Effect on the Quality of Fast Pyrolysis Oils.* in *Biomass Pyrolysis Oil Properties and Combustion Meeting.* 1994. Estes Park, CO: National Renewable Energy Laboratory, Golden, CO, NREL CP-430-7215.

7. Bevan, S., R. Gieger, N. Sobel, and D. Johnson, *Filter Systems for IGCC Applications.* in *Advanced Coal-Based Power and Environmental Systems '97 Conference.* 1997. Pittsburgh, Pennsylvania.

8. Davidson, M., et al. *Power Systems Development Facility: Filter Element Evaluation During Combustion Testing.* in High Temperature Gas Cleaning, E. Schmidt, Editor, 1996, Karlsruhe.

9. Alvin, M.A., *Impact of char and ash fines on porous ceramic filter life.* Fuel Processing Technology, 1998. 56: p. 143–168.

10. Alvin, M.A., T.E. LIppert, E.S. Diay, and E.E. Smeltzer, *Filter Component Assessment.* in *Advanced Coal-Fired Power Systems '96 Review Meeting.* 1996. Morgantown, West Virginia.

11. Alvin, M.A., *Assesment of Metal Media Filters for Advanced Coal-Based Power Generation Applications.*

12. Zevenhoven, R. and P. Kilpinen, *Control of Pollutants in Flue Gases and Fuel Gase, Chapter 5: Particulates*. 2004: Helsinki University of Technology.

13. Pan, W. and G.N. Richards, *Influence of metal ions on volatile products of pyrolysis of wood.* Journal of Analytical and Applied Pyrolysis, 1989(2): p. 117-126.

14. Scott, D.S., P. Majerski, J. Piskorz, and D. Radlein, *A second look at fast pyrolysis of biomass—the RTI process.* Journal of Analytical and Applied Pyrolysis, 1999. 51: p. 23-37.

15. Bridgwater, A.V., *Principles and practice of biomass fast pyrolysis processes for liquids.* Journal of Analytical and Applied Pyrolysis, 1999. 51: p. 3-22.

16. Bridgwater, A.V., *Renewable fuels and chemicals by thermal processing of biomass.* Chemical Engineering Journal 2003. 91: p. 87–102.

17. Meier, D. and O. Faix, *State of the art of applied fast pyrolysis of lignocellulosic materials - a review.* Bioresource Technology, 1999. 68: p. 71-77.

18. Radlein, D., *The production of chemicals from fast pyrolysis bio-oils*, in *Fast Pyrolysis of Biomass: A Handbook*, A.V. Bridgwater, Editor. 1999, CPL Press: Newbury, UK. p. 164-188.

19. Piskorz, J., P. Majerski, D. Radlein, A. Vladars-Usas, and D.S. Scott, *Flash pyrolysis of cellulose for production of anhydro-oligomers.* Journal of Analytical and Applied Pyrolysis, 2000. 56: p. 145-166.

20. Dobele, G., D. Meier, O. Faix, S. Radtke, G. Rossinskaja, and G. Telysheva, *Volatile products of catalytic flash pyrolysis of celluloses.* Journal of Analytical and Applied Pyrolysis, 2001. 58-59: p. 453-463.

21. Lede, J. and J. Mercadier, *Simulation of the thermal cracking of biomass derived vapours, by the model reaction of decomposition of isocyanuric acid.* J. Anal. Appl. Pyrolysis, 2003. 67: p. 295-305.

22. Piskorz, J., P. Majerski, D. Radlein, D.S. Scott, and A.V. Bridgwater, *Fast pyrolysis of sweet sorghum and sweet sorghum bagasse.* Journal of Analytical and Applied Pyrolysis, 1998. 46: p. 15-29.

23. Fahmi, R., A.V. Bridgwater, L.I. Darvell, N.Yates, and S. Thain, *The Effect of Alkali metals on Combustion and Pyrolysis of Lolium and Festuca Grasses, Switchgrass and Willow.* Fuel, 2007. 86(1): p. 1650-1569.

24. Nowakowski, D.J., J.M. Jones, M.D. Brydson, and A.B. Ross, *Potassium catalysis in the pyrolysis behaviour of short rotation willow coppice.* Fuel, 2007. 86: p. 2389-2402.

25. Scott, D.S., L. Paterson, J. Piskorz, and D. Radlein, *Pretreatment of poplar wood for fast pyrolysis: Rate of cation removal.* Journal of Analytical and Applied Pyrolysis, 2000. 57: p. 169-176.

26. Piskorz, J., D. Scott, and S. Czernik, *Liquid products from the fast pyrolysis of wood and cellulose*, in *Research in Thermochemical Biomass Conversion*, A.V. Bridgwater, Editor. 1988, Elsevier Science: London & New York. p. 557-583.

27. Hague, R.A., *The pre-treatment and pyrolysising of biomass for the production of liquids for fuel and speciality chemicals*. 1998, PhD-Thesis, Aston University.

28. Radlein, D., J. Piskorz, and D.S. Scott, *Fast pyrolysis of natural polysaccharides as a potential industrial process.* Journal of Analytical and Applied Pyrolysis, 1991. 19: p. 41-63.

29. Oasmaa, A. and C. Peacocke, *A guide to physical property characterisation of biomass-derived fast pyrolysis liquids*. 2001, Espoo: VTT Publications 450.

30. Oasmaa, A. and D. Meier, *Norms and standards for fast pyrolysis liquids. 1. Round robin test.* Journal of Analytical and Applied Pyrolysis, 2005. 73: p. 323-334.

31. Oasmaa, A. and S. Czernik, *Fuel Oil Quality of Biomass Pyrolysis Oils: State of the Art for the End Users.* Energy & Fuels 1999(13): p. 914-921.

32. Fratini, E., M. Bonini, A. Oasmaa, Y. Solantausta, J. Teixeira, and P. Baglioni, *SANS Analysis of the Microstructural Evolution during the Aging of Pyrolysis Oils from Biomass.* Langmuir 2006. 22: p. 306-312.

33. Oasmaa, A. and E. Kuoppala, *Fast Pyrolysis of Forestry Residue. 3. Storage Stability of Liquid Fuel.* Energy & Fuels, 2003. 17: p. 1075-1084.

34. Oasmaa, A., K. Sipila, Y. Solantausta, and E. Kuoppala, *Quality Improvement of Pyrolysis Liquid: Effect of Light Volatiles on the Stability of Pyrolysis Liquids.* Energy & Fuels 2005, 19, 2556-2561, 2005. 19: p. 2556-2561.

35. Boucher, M.E., A. Chaala, H. Pakdel, and C. Roy, *Bio-oils obtained by vacuum pyrolysis of softwood bark as a liquid fuel for gas turbines. Part II: Stability and ageing of bio-oil and its blends with methanol and a pyrolytic aqueous phase.* Biomass and Bioenergy, 2000. 19: p. 351-361.

36. Boucher, M.E., A. Chaala, and C. Roy, *Bio-oils obtained by vacuum pyrolysis of softwood bark as a liquid fuel for gas turbines. Part I: Properties of bio-oil and its blends with methanol and a pyrolytic aqueous phase.* Biomass and Bioenergy, 2000. 19: p. 337-350.

37. Diebold, J.P. and S. Czernik, *Additives to Lower and Stabilze the Viscosity of Pyrolysis Oils during Storage.* Energy & Fuels, 1997. 11: p. 1081-1091.

38. Milne, T.A., F.A. Agblevor, M. Davis, S. Deutch, and D. Johnson, *A review of the chemical composition of fast pyrolysis oils from biomass*, in *Developments in Thermochemical Biomass Conversion*, A.V. Bridgwater and D.G.B. Boocock, Editors. 1997, Blackie Academic & Professional: London. p. 408-424.

39. Meier, D. and B. Scholze, *Fast pyrolysis liquid characteristics*, in *Biomass Gasification and Pyrolysis - State of the Art and Future Prospects*, M. Kaltschmitt and A.V. Bridgwater, Editors. 1997, CPL-Press: Newbury. p. 431-441.

40. Scholze, B. and D. Meier, *Characterization of the water-insoluble fraction from pyrolysis oil (pyrolytic lignin). Part I. PY–GC/MS, FTIR, and functional groups.* Journal of Analytical and Applied Pyrolysis, 2001. 60: p. 41-54.

41. Oasmaa, A., E. Kuoppala, and Y. Solantausta, *Fast Pyrolysis of Forestry Residue. 2. Physicochemical Composition of Product Liquid.* Energy and Fuels, 2003(17): p. 433-443.

42. Oasmaa, A. and D. Meier, *Analysis, characterisation and test methods of fast pyrolysis liquids.*, in *Fast Pyrolysis of Biomass: A Handbook Volume 2.*, A.V. Bridgwater, Editor. 2002, CPL Press: Newbury. p. 23-35.

43. Sipila, K., E. Kuoppala, L. Fagernas, and A. Oasmaa, *Characterization of Biomass-based Flash Pyrolysis Oils.* in *Biomass and Bioenergy* 1998. 14(2): p. 103-113.

44. Scholze, B., C. Hanser, and D. Meier, *Characterization of the water-insoluble fraction from fast pyrolysis liquids (pyrolytic lignin) Part II. GPC, carbonyl goups, and 13C-NMR.* in *Journal of Analytical and Applied Pyrolysis*, 2001. 58-59: p. 387-400.

45. Bayerbach, R., *Über die Struktur der oligomeren Bestandteile von Flash-Pyrolyseölen aus Biomasse*, in *Wood Chemistry*. 2006, University of Hamburg: Hamburg.

46. Diebold, J.P., S. Cyernik, J.W. Scahill, S.D. Philips, and C.J. Feil, *Hot-Gas Filtration to Remove Char from Pyrolysis Vapors Produced in the Vortex Reactor at NREL.* in *Specialists Workshop on Biomass OIl Properties and Combustion*. 1994. Estes Park, Co.

47. Lede, J., J.P. Diebold, C. Peacoke, and J. Piskorz, *The nature and properties of intermediate and unvaporized biomass pyrolysis materials*, in *Development in Thermochemical Biomass Conversion*, A.V. Bridgwater and D.G.B. Boocock, Editors. 1997, Blacky Academic & Professional. p. 27-42.

48. Evans, R.J. and T.A. Milne, eds. *Molecular-Beam Mass-Spectrometric Studies of Wood Vapor and Model Compounds over HZSM-5 Catalyst.* in *Pyrolysis oils from biomass: produzing, analyzing, and upgrading.*, ed. E.J. Soltes and T.A. Milne. 1988, American Chemical Society: Washington D.C. 123-137.

49. Daugaard, D.E. and R.C. Brown. *The transport phase of pyrolytic oil exiting a fast fluidized bed reactor.* in *6th International Conference on Thermochemical Biomass Conversion.* 2004. Victoria, Canada: CPL Press 2006.

50. Garcia, R., R. French, S. Czernik, and E. Chornet, *Catalytic steam reforming of bio-oils for the production of hydrogen: Effects of catalyst composition.* in *Applied Catalysis A: General*, 2000. 201: p. 225–239.

51. Horne, P.A. and P.T. Williams, *Upgrading of biomass-derived pyrolytic vapours over zeolite ZSM-5 catalyst: effect of catalyst dilution on product yields.* Fuel, 1996. 75(9): p. 1043-1050.

52. Zhang, H., R. Xiao, H. Huang, and G. Xiao, *Comparison of non-catalytic and catalytic fast pyrolysis of corncob in a fluidized bed reactor* in *Bioresource Technology*, 2009. 100: p. 1428-1434.

53. Diebold, J.P. and J. Scahill, *Biomass to Gasoline: Upgrading Pyrolysis Vapours to Aromatic Gasoline with Zeolite Catalysis at Atmospheric Pressure*, in *Pyrolysis Oils from Biomass: Producing, Analyzing, and Upgrading* E. Soltes and T. Milne, Editors. 1988, ACS Symposium Series 376.

54. Salter, E.H., *Catalytic pyrolysis of biomass for improved liquid fuel quality* 2001, PhD-Thesis, Aston University.

55. Nokkosmaki, M.I., A.O.I. Krausea, E.A. Leppamaki, and E.T. Kuoppala, *A novel test method for catalysts in the treatment of biomass pyrolysis oil.* Catalysis Today, 1998. 45: p. 405-409.

56. Nokkosmaki, M.I., E.T. Kuoppala, E.A. Leppamaki, and A.O.I. Krausea, *A novel test method for cracking catalysts* in *Journal of Analytical and Applied Pyrolysis*, 1998. 44: p. 193-204.

57. Diebold, J.P., *The Cracking Kinetics of Depolymerized Biomass Vapors in a Continuous Tubular Reactor.* 1985, Thesis T-3007, Colorado School of Mines.

58. Boroson M.L. J. B. Howard, J.P. Longwell. and W.A. Peters, *Heterogeneous Cracking of Wood Pyrolysis Tars over Fresh Wood Char* in *Energy & Fuels*, 1989. 3: p. 735-740.

59. Pattiya, A., *Catalytic Pyrolysis of Agricultural Residues for Bio-Oil Production.* 2007, PhD-Thesis, Aston University.

60. Guerrero, M., M.P. Ruiz, A. Millera, M.U. Alzueta, and R. Bilbao, *Characterization of Biomass Chars Formed under Different Devolatilization Conditions: Differences between Rice Husk and Eucalyptus.* in *Energy and Fuels*, 2008(22): p. 1275–1284.

61. E. Biagini, P. Narducci, and L. Tognotti, *Size and structural characterization of lignin-cellulosic fuels after the rapid devolatilization.* Fuel, 2008. 87: p. 177-186.

62. Biagini, E., M. Simone, and L. Tognotti, *Characterization of high heating rate chars of biomass fuels.* Proceedings of the Combustion Institute, 2009. 2043-2050.

63. Cetin, E., B. Moghtaderi, R. Gupta, and T.F. Wall, *Influence of pyrolysis conditions on the structure and gasification reactivity of biomass chars.* in *Fuel*, 2004. 83: p. 2139-2150.

64. Sharma, R.K., J.B. Wooten, V.L. Baliga, X. Lin, W.G. Chan, and M.R. Hajaligul, *Characterization of chars from pyrolysis of lignin.* in *Fuel*, 2004. 83: p. 1469-1482.

65. Hoerweg, C., *Catalytic Quality Improvement of Biomass Fast Pyrolysis Liquids by the use of olivine based Catalysts*, in *Institut für Verfahrenstechnik, Umwelttechnik und Technische Biowissenschaften.* 2005, University of Vienna: Vienna.

66. M.S. Skjøth-Rasmussen, P. Glarberg, M. Ostberg, J.T. Johanssen, H. Livbjerg, A.D. Jensen, and T.S. Christensen, *Formation of polycyclic aromatic hydrocarbons and soot in fuel-rich oxidation of methane in a laminar flow reactor.* in *Combustion and Flame* 2004(136): p. 91-128.

67. Li Liu, K.T. Rim, D. Eom, T.F. Heinz, and G.W. Flynn, *Direct Observation of Atomic Scale Graphitic Layer Growth.* in *Nano Letters*, 2008. 8(7): p. 1872-1878.

68. Koziriski, J.A. and R. Saade, *Effect of biomass burning on the formation of soot particles and heavy hydrocarbons. An experimental study.* in *Fuel*, 1998. 71(4): p. 225-231.

69. Morf, P. and P. Hasler, *Mechanisms and kinetics of homogeneous secondary reactions of tar from continuous pyrolysis of wood chips.* Fuel, 2002(81): p. 843-853.

70. Britt, P.F., A.C. Buchanan, M.M. Kidder, C. Owens, J.R. Ammann, J.T. Skeen, and L. Luo, *Mechanistic investigation into the formation of polycyclic aromatic hydrocarbons from the pyrolysis of plant steroids.* in *Fuel*, 2001. 80: p. 1727-1746.

71. Seville, J.P.K., U. Tuzun, and R. Clift, *Processing of Particulate Solids.* 1997, London: Blackie Academic.

72. Berbner, S. and T. Pilz, *Characterization of the filtration and regeneration behaviour of rigid ceramic barrier filters at high temperatures.* Powder Technology, 1996(86): p. 103-111.

73. Berbner, S., *Zur Druckstossregenerierung keramischer Filterelemente bei der Heissgasreinigung*, in *Fakultaet fuer Chemieingenieurwesen.* 1995, Universitaet Karlsruhe: Karlsruhe.

74. Al-Hajeri, M.H., A. Aroussi, K. Simmons, and S.J. Pickering, *A parametric study of filtration through a ceramic candle filter.* in *Proc. IMechE*, 2005. 219.

75. Earnest, G.S., M.G. Gressel, L. Mickelsen, E.S. Mozer, and C.D. Reed, *Guidance for Filtration and Air-Cleaning Systems to Protect Building Environments*. DHHS (NIOSH) Publication No. 2003-136. 2003: NIOSH Publications Dissemination, 4676 Columbia Parkway, Cincinnati, OH 45226-1998.

76. Ito, S., G. Tanaka, and S. Kawamura, *Changes in pressure loss and face velocity of ceramic candle filters caused by reverse cleaning in hot coal gas filtration.* Powder Technology, 1998. 100: p. 32-40.

77. Dockter, B.A., J.P. Hurley, T.A. Watne, K.A. Katrinak, and C.A. O Keefe, *Advanced Coal-Fired Power Systems* in *Advanced Coal-Fired Power Systems '96 Review Meeting*. 1996. Morgantown, West Virginia.

78. Christ, A. and U. Renz, *Numerical Simulation of Filter Cake Build-Up on Surface Filters*, in *High Temperature Gas Cleaning*, E.Schmid, Editor. 1996: Karlsruhe. p. 169-182.

79. Aroussi, A., K. Simmons, and S.J. Pickering, *Particulate deposition on candle Filters.* Fuel, 2001. 80: p. 335-343.

80. Kavouras, A. and G. Krammer, *Deriving cake detachment versus cake area load in a jet pulsed filter by a mechanistic model.* Powder Technology, 2003. 133: p. 134-146.

81. Neiva, A.C.B., L. Goldsein jr, P. Calvo, L.M. Romes, and J. Arouzo, *Modelling of Cake Compressibility on Gas Filters*, in *High Temperature Gas Cleaning 2*, E. Schmid, et al., Editors. 1999: Karlsruhe.

82. Hajek, S. and W. Peukert, *Comparison of Ceramic and Metal Filter Components for High Temperature Filtration*, in *High Temperatuer Gas Cleaning*, E. Schmidt, Editor. 1996: Karlsruhe. p. 219 - 231.

83. Kanaoka, C. and M. Amornkitbamrung, *Effect of filter permeability on the release of captured dust from a rigid ceramic filter surface.* Powder Technology, 2001. 118: p. 113-120.

84. Laux, S., B. Giernoth, H. Bulak, and U. Renz, *Aspects of pulse-jet cleaning of ceramic filter elements, in Gas Cleaning at High Temperatures*, in *Gas Cleaning at High Temperatures*, R. Clift and J.P.K. Seville, Editors. 1993, Blacky Academic and Professional: Glasgow, UK. p. 203-224.

85. Chuah, T.G., C.J. Withers, and J.P.K. Seville, *Prediction and measurements of the pressure and velocity distributions in cylindrical and tapered rigid ceramic filters.* Separation and Purification Technology, 2004. 40(1): p. 47-60.

86. Mai, R., M. Fronhoefer, and H. Leibold, *Flow Characteristics of Filter Candles during Recleaning*, in *High Temperature Gas Cleaning*, E.Schmid, Editor. 1996: Karlsruhe. p. 194 - 206.

87. Schildermans, I., J. Baeyens, and K. Smolders, *Pulse jet cleaning of rigid filters: a literature review and introduction to process modelling.* Filtration & Separation, 2004. 41(5): p. 26-33.

88. Stephen, C.M., S.K. Grannell, and J.P.K. Seville, *Conditioning and Pulse-Cleaning of Rigid Ceramic Filters*, in *High Temperature Gas Cleaning*, E. Schmidt, Editor. 1996: Karlsruhe. p. 208-217.

89. Kanaoka, C., T. Kishima, and M. Furuuchi, *Accumulation and Release of Dust from a Rigid Ceramic Filter Element*, in *High Temperature Gas Cleaning*, E. Schmidt, Editor. 1996: Karlsruhe. p. 183 - 191.

90. Berbner, S., *Zur Druckstossregenerierung keramischer Filterelemente bei der Heissgasreinigung*. 1995, PhD-Thesis, University Fridericiana Karlsruhe.

91. Grannell, S.K. and J.P.K. Seville, *Effect of Venturi Inserts on Pulse Cleaning of Rigid Ceramic Filters*, in *High Temperature Gas Cleaning II*, E.Schmid, et al., Editors. 1999: Karlsruhe. p. 96 - 109.

92. Grannell, S.K., C.M. Stephen, M. Koenigsberger, S. Lehnert-Batar, E.J.C. Beattie, T. Pilz, and J.P.K. Seville, *Investigation into the Behaviour of Particle Compacts and Comparison with Industrial Experience*, in *High Temperature Gas Cleaning*, Schmidt, Editor. 1996: Karlsruhe. p. 145-156.

93. Dittler, A. and G. Kasper, *Simulation of operational behaviour of patchily regenerated, rigid gas cleaning filter media.* Chemical Engineering and Processing, 1999(38): p. 321 - 327.

94. Dittler, A. and G. Kasper, *Influence of Regeneration Behaviour of Rigid Filter Media on their Residual Pressure Drop*, in *High Temperature Gas Cleaning*, E. Schmidt, Editor. 1996: Karlsruhe. p. pp. 119 - 127.

95. Alvin, M.A., *Assessment of Metal Media Filters for Advanced Coal-Based Power Generation Applications.* in *5th International Symposium on Gas Cleaning at High Temperature.* Conference Procedings, September 17 - 20, 2002. Pittsburgh, Pennsylvania.

96. Stankiewicz, E.P., A.J. Sherman, and A.A. Zinn. *Advanced Hot Gas Filter Development.* in *Advanced Coal-Based Power and Environmental Systems '97 Conference*. 1997. Pittsburgh, Pennsylvania.

97. Leibold, H., W. Bundschuh, and R. Mai, *Further Development of Ceramic Hot Gas Filter Media for Long-Term Stable Fine Dust Filtration*, in *High Temperature Gas Cleaning 2*, E. Schmid, et al., Editors. 1999: Karlsruhe.

98. Zimmerlin, B., H. Leibold, and H. Seifert, *Performance of Nano-scaled Ceramic Membranes during Fine and Sticky Dust Filtration*, in *High Temperature Filtration 2*, E.Schmid, T. Pilz, and A. Dittler, Editors. 1999.

99. Solantausta, Y, *Bio Fuel Oil - Upgrading by Hot Filtration and Novel Physics Methods*, in *EU Contract JOR-CT98-0253*. 1998.

100. Wang, X., *BIOMASS FAST PYROLYSIS IN A FLUIDIZED BED - Product cleaning by in-situ filtration*. 2006, PhD-Thesis, University of Twente.

101. Sheng, C. and J.L.T. Azevedo, *Estimating the higher heating value of biomass fuels from basic analysis data.* Biomass and Bioenergy, 2005. 28: p. 499-507.

102. Tenmat, *Material Safety Data Sheet:CS1150-RF1000*. 2004: Tenmat Ltd, Ashburton Road West, Manchester M17 IRU.

103. Tenmat, *Firefly Hot Gas Filters*, in *Product Information Sheet*: Tenmat Ltd, Ashburton Road West, Manchester M17 IRU.

104. Lloyd, B.T. *Experiences of the application of Hot Gas Filtration to Industrial Processes*. in *Advanced Coal-Based Power and Environmental Systems '97 Conference*. 1997. Pittsburgh, Pennsylvania.

105. Dahlin, R.S. and E.C. Landham, *Effects of Dust Characteristics on Hot-Gas Filter Performance in a Transport Reactor System*, in *High Temperature Gas Cleaning II*, E. Schmidt, et al., Editors. 1999: Karlsruhe.

106. Peukert, W., *High Temperature Filtration in the Process Industry.* Filtration and Seperation, June 1998: p. 461-464.

Appendix

Flowsheet of 1kg/h pyrolysis system with filtration unit

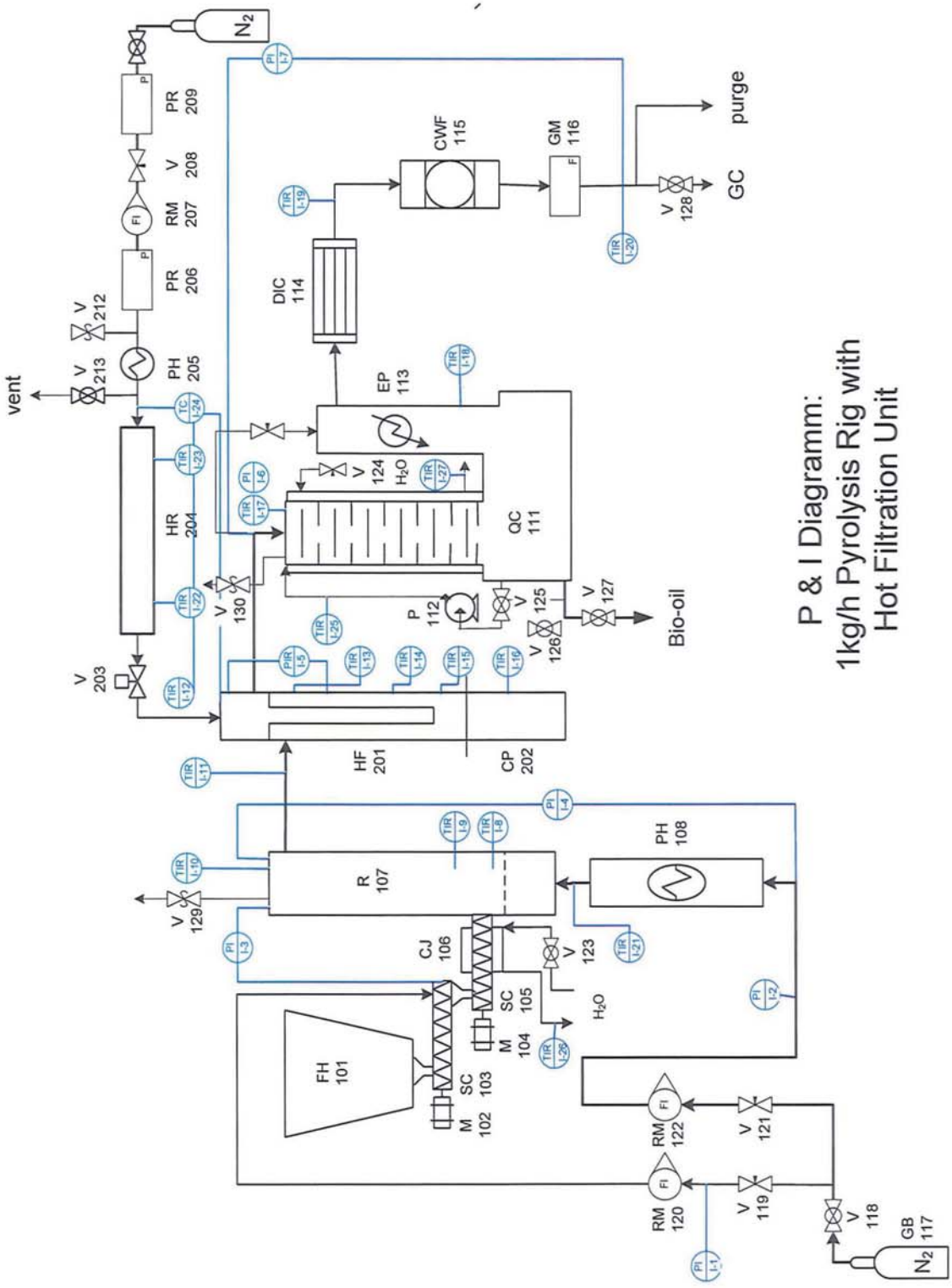

Temperature recordings

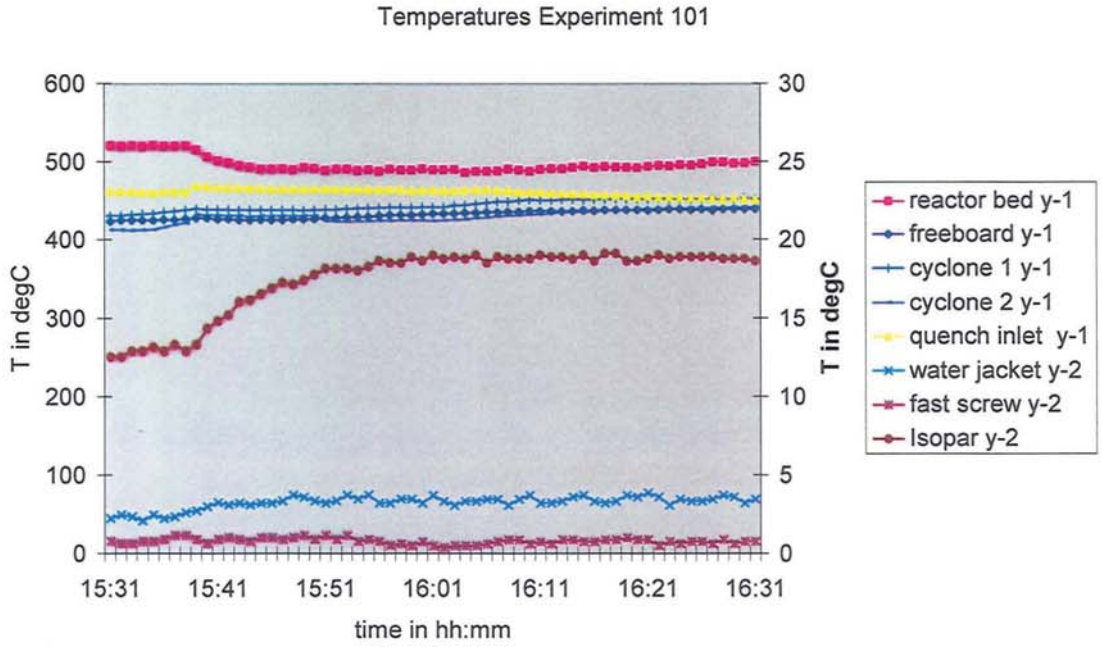

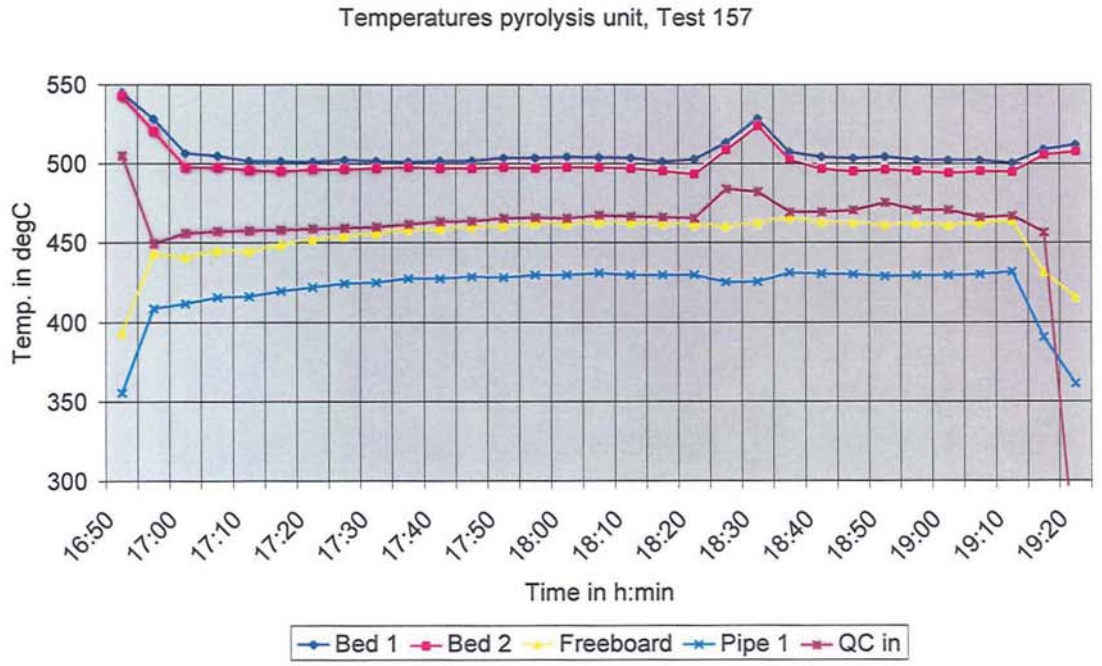

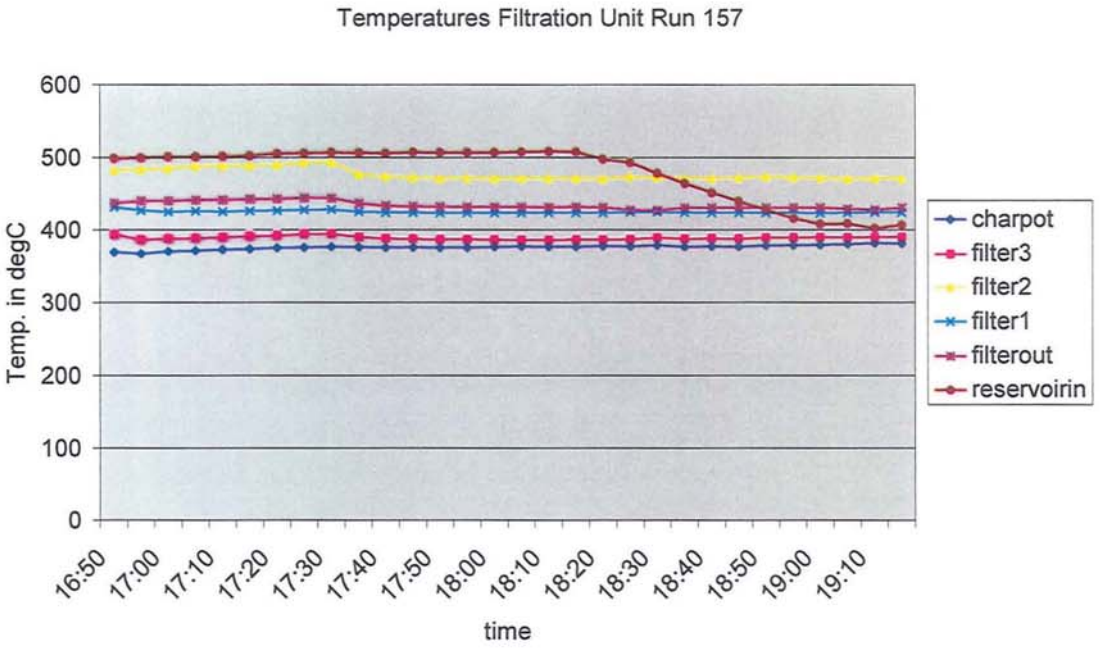

Picture of produced pyrolysis oil, experiment 161

Secondary reactor for preliminary experiments

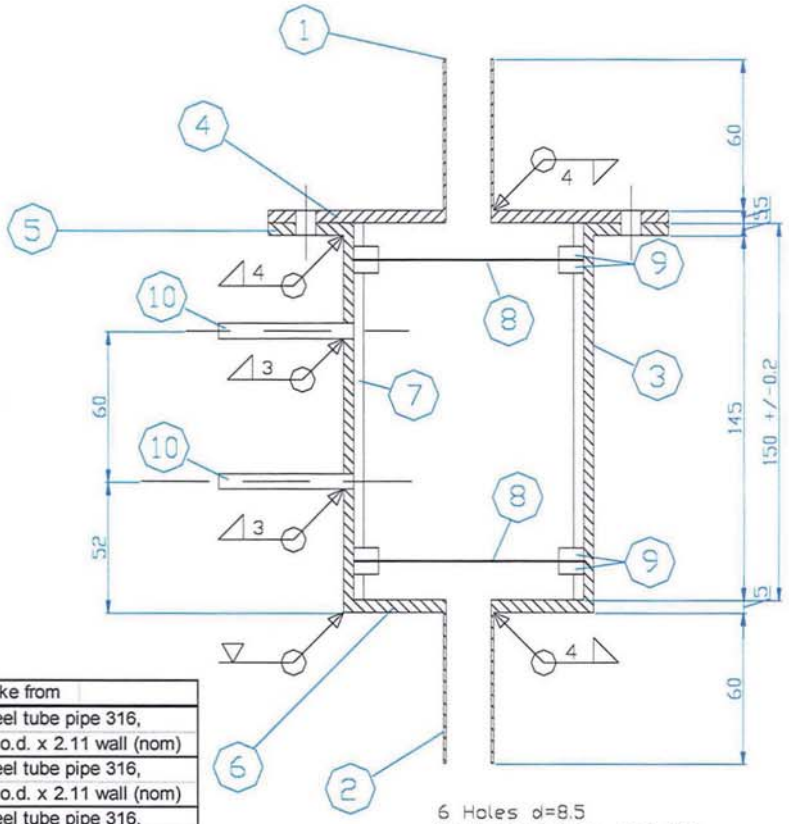

Do Not Scale

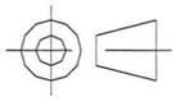

Item	No Off	Description	Make from
1	1	Tube section	S/steel tube pipe 316, 26.7 o.d. x 2.11 wall (nom)
2	1	Tube section	S/steel tube pipe 316, 26.7 o.d. x 2.11 wall (nom)
3	1	Tube section	S/steel tube pipe 316, 100mm o.d. x 4mm (nom)
4	1	Flange	S/steel 316 thickness 5mm
5	1	Flange	S/steel 316 thickness 5mm
6	1	Flange	S/steel 316 thickness 5mm
7	6	Spacer	S/steel 316 see Sh 02
8	2	Mesh	S/steel 316 "Free issue"
9	4	Support Ring	S/steel 316 see Sh 02
10	2	Tube section	S/steel tube pipe 316, 10.3 o.d. x 1.73 wall (nom)

Tolerances:
Linear +/- 0.2 mm
Angular +/- 2° UOS

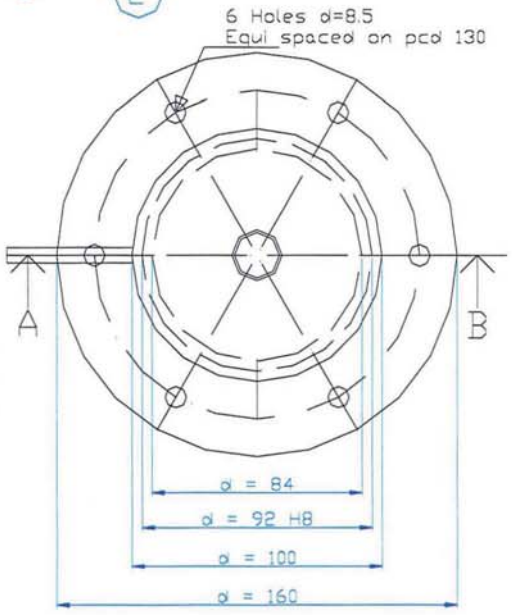

Drg No	JS-04-01	Sh 01 of 02	11.8.2004
Vapour Cracking Device		J. Sitzmann	0121-3593611 ext.4644
Bio-Energy Research Group		sitzmanj@aston.ac.uk	